Shell Model Studies of the Quark-antiquark Excitations in the Nucleon

Thesis submitted to the
Faculty of Science
University of Glasgow

by

SIRAJUDDIN MALIK

for the degree of
Doctor of Philosophy

Department of Physics & Astronomy
University of Glasgow
GLASGOW
G 12 8QQ

October 1989

Contents

ACKNOWLEDGEMENTS

I would like to thank Prof. R. P. Ferrier, the head of Department, for his overall supervision of the research work in the department

I wish to express my sincere gratitude to Dr A. Watt, my supervisor, under whose inspiring and kind guidance, the present research has been conducted. Without his everlasting helpful encouragement and careful concern, this work could never have been completed.

I am indebted to the staff and students of the theory group for their help in various ways. Especially I must thank Prof. R. R. Whitehead and Prof. R. G. Moorhouse for their encouraging efforts and keen interest in connection with the theoretical research going on in this department. My thanks are extended to the computing staff for their help during my research and printing of this thesis.

I also wish to thank my friends for many happy and unforgettable moments that we all shared together in Glasgow. I gratefully acknowledge S. G. Haq and S. H. Shah for their sincere support and encouragement at difficult times when I faced some financial problems.

I am extremely grateful to the Government of Pakistan for financial support during the period of my study.

Last but not least, my warmest thanks go to my parents, brothers, sisters, wife and children for their constant patience, support and ecouragement during my stay in Glasgow (Scotland).

ABSTRACT

The calculation of the nucleon-nucleon interaction from quantum chromodynamics is a problem which has been received a great deal of attention in recent years. Many studies have been made on the assumption that nucleons are composed of exactly three quarks bound in colourless triplets and that the N-N interaction arises from the exchange of gluons between quarks in different nucleons. It is now clear that this model can not account for the long range attractive part of the interaction which is responsible for nuclear binding and these long range forces arise from the exchange of colourless mesons, namely quark-antiquark pairs.

As a first step we have extended the simple 3q-model of the nucleon to include the presence of quark-antiquark pairs. Antiquarks are viewed in our model, as excitations from a filled sea of quarks. The numerous interactions between particles are handled by a version of the Glasgow nuclear shell model with colour and intrinsic parity added.

We first obtain values of the model parameters which reproduce the observed mass of the nucleon and give a quite reasonable value of the N-Δ mass-difference in the present extended quark model. We then calculate the magnetic moment, root mean squared mass and charge radii and charge density of the proton and neutron.

The present model predicts that the components of the internal wavefunction of the nucleon with configuration $(q^4\bar{q})$ contribute 13-14 % and 4.1-5.3 % to the total values of the magnetic moment and root mean squared radii of the nucleon respectively. The charge density of the neutron calculated in the present model predicts the charge mean square radius of the neutron to be negative.

CHAPTER 1

INTRODUCTION

The study of nuclear structure has been the subject of many experimental and theoretical investigations since the discovery of the atomic nucleus by Rutherford [1] in 1911. With the discovery of neutron [2] in 1932, nuclei were known to consist of protons and neutrons. Protons and neutrons are collectively called nucleons. The nucleus is, therefore, treated as a system of many nucleons which are bound together by the strong interaction.

To study the observed properties of the nucleus many nuclear models have been suggested. Two types of nuclear models [3] namely microscopic models and collective models have been widely used in theoretical investigations. In microscopic models the nucleons are assumed to be inert, rigid and structureless particles moving in specified orbits. But the collective models ignore the nucleons entirely and describe the overall shape of the nucleus. Since the microscopic models could explain some aspects of nuclear structure successfully, for a long time it was thought that the nucleons are inert and structureless particles. But some experimental data of nuclear structure can not be explained on the assumption that the nucleons are elementary structureless particles.

The field of nuclear structure is strongly connected with the nuclear forces because the structure-characteristics of a nucleus should be understood in terms of basic interactions between pairs of nucleons.

In a nucleus, since the neutron is uncharged and the protons having alike charge repel each other, there must be some special interactions between nucleons, so-called "nuclear forces" which keep the nucleons together within the nucleus. Scattering experiments show that these interactions are strong interactions which are repulsive at short range ($r \leq 0.6$ fm) and attractive at medium and long ranges ($r \leq 2$ fm).

In 1935 Yukawa proposed a theory [4], the so-called meson theory, according to which he assumed a meson field as the mediating field for nuclear forces and postulated a new particle " the pion (π-meson)" as a carrier of the nuclear force. The pion was discovered experimentally by Powell and co-workers [5]. Since Yukawa's meson theory in 1935, meson exchange has been accepted as one of the mechanisms giving rise to the nucleon-nucleon interaction.

In some ways, the nuclear force resembles the chemical force between atoms and like the chemical force, it is not the fundamental force but it is a resultant and relatively complicated manifestation of more fundamental forces acting within the nucleon and connected with its internal structure.

The discovery of the short-lived excited states of the nucleon e.g. Δ–states, and the scattering of electrons by nucleons provided evidence for the sub-structure of the nucleon.

In 1964 Gell-Mann [6] and Zweig independently proposed that hadrons are composite particles with quarks as their constituents. Quarks are spin-1/2 fermions and their wavefunction is specified by the usual degrees of freedom such as spin, flavour (analogous to isospin) with an additional degree of freedom "the colour charge"

which has been assigned to the quark to allow the Pauli exclusion principle to be satisfied. Quarks are assumed to be coloured particles with red, green or blue colour charge. Quarks can never exist in an isolated state although baryons and mesons can. All observed hadrons exist in colour singlet state i.e. in colourless state. The hadrons, strongly interacting particles, split into particles of different spin types, half integral spin particles called baryons and integral spin mesons. The baryon and meson are composed of three quarks and quark-antiquark pair respectively [7]. This model of hadron's structure is referred as the quark model. Soon the quark model assumption was supported by the analysis of data obtained from high energy inelastic electron -proton scattering experiment [8] which revealed that protons are composite particles.

In the simple quark model the nucleon is constructed from three quarks, i.e proton and neutron have uud and ddu quark-structure respectively [7]. Since quarks are fermions, the overall wavefunction of the nucleon must be antisymmetric. Therefore the nucleon if it is to exist in a colour singlet state should have antisymmetric colour wavefunction and symmetric spatial-spin-isospin wavefunction to obtain an overall antisymmetric wavefunction.

Deep inelastic scattering of leptons by nuclei or nucleons [7-9] and the EMC effect [10] confirm that the nucleons are composite particles and they can no more be considered structureless rigid elementary particles.Their structure and the forces between them can be studied in terms of interactions between their constituent quarks on the basis of a theory, the so-called Quantum

chromodynamics (QCD) [7,11]. QCD, a non-abelian gauge theory built on SU(3) colour symmetry is a theory of colour forces between quarks. The force between quarks is thought to be transmitted by the family of eight massless vector bosons, called gluons described by the eight λ^a of SU(3) [7]. Their role is analogous to the role of photons in Quantum-electrodynamics (QED) [12]. Since quarks are constituents of hadrons, the QCD which binds quarks in hadrons is believed at present to be a theory of strong interactions. Many attempts have been made to understand the single baryon's properties [13-20] and baryon -baryon interaction [21-40] mainly in terms of QCD motivated phenomenology.

It may be expected that the internal structure of the nucleon plays an important role in connection with the nuclear force and specially in its short range part when the two nucleons overlap with each other. Therefore a good model of the internal structure of a nucleon is the prerequisite for achieving a proper understanding of the nucleon-nucleon interaction.

A number of models have been proposed to describe the internal structure of a nucleon, among them we have potential models [13], the bag models (such as MIT bag model [14], soliton bag model [15] and hybrid chiral bag models [16] i.e. cloudy bag model [16a]) and Skyrme's model [17] and its versions with vector mesons [18].
The 3q-potential model studies of the single nucleon's structure has been fairly successful. The (3q)-(3q)- potential models of the NN-scattering can describe only the extreme short range part of the nuclear force [20-36] and fail to explain the other parts because of the lack of mesonic character responsible for the

medium and long range attractive parts of the NN-interaction.

The most successful type of the bag models is the MIT bag model. In its simple version, the MIT bag model [14] treats the baryon as three non-interacting relativistic quarks confined in a static spherical cavity. It gives generally good results (but not close to the observed values) for energies, charge radii and magnetic moments. A serious drawback of the MIT bag model is that it does not allow the pion's emission and absorption by a nucleon and hence can not provide any one pion exchange potential between two nucleons which is important as has been pointed out by the extensive analysis of NN-interaction. Pionic effects must be considered for the explanation of the long range potential between the nucleons.

In the cloudy bag model [16a] the quarks in the MIT bag model are surrounded by a cloud of pions. The values of charge radii and magnetic moments predicted by this model are better than the values predicted by the MIT bag model. Its predicted values are in good agreement with the experimental values.

Similarly all the models, in which the internal quarks of the nucleon are coupled with external meson fields, provide good description of the single nucleon' structure but the description of NN-interaction is not complete.

A detailed review of the studies of the single nucleon's structure and NN-interaction in terms of the above models has been given in references [19,20].

Since the nuclear force i.e the nucleon-nucleon interaction is one of the most fundamental subjects of nuclear physics, it has been studied exhaustively. Many investigations have been carried

out to study the nucleon-nucleon interaction in terms of the nucleon's internal structure models mentioned above among which the potential models [22-30] and the bag models [20] are very common.These models are successful in producing quite reasonable values of the nucleon's properties such as masses, charge radii and magnetic moments but could not explain the nucleon-nucleon interaction precisely. In most of these studies the short range part of the NN-interaction has been studied [21-33]. The short range repulsion of the nuclear force can be described as a quark-exchange force with appropriate qq-interactions. In fact the range of quark-exchange interaction is determined by the size of the nucleon because the exchange-process demands that the quark wavefunctions of the two nucleons overlap with each other. The size of the nucleon is of the same order as the range of the two-pion exchange that is most important for the nuclear binding and is larger than the short range of the nuclear force.

The confinement property of QCD suggests that the colour is strongly confined in a small region typically within ≤ 1 fm. The gluon, being a coloured quantum, is also confined in colourless system and therefore gluon exchange among valence quarks would not be able to explain a long range nuclear force. It means that the meson exchange potential should necessarily be introduced to explain the medium and long range of the nucleon-nucleon interaction.

In previous quark model studies either the mesonic degree of freedom is entirely neglected [13-14] or the quarks and the mesonic fields are treated as separate entities [16]. These models are rather unsatisfactory as the mesons and nucleons are treated

in different ways. It is very desirable to develop a unified model in which the quark-structure of the meson is treated on the same basis as the structure of the nucleon.

Soon after the present work was begun, an attempt for proposing more convincing quark model of the hadron's structure, was made by Fujiwara and Hecht [37-40] with a philosophy that a model in which baryons and mesons are described in terms of their common constituents (i.e. quarks and antiquarks) should be preferred. They extended a simple 3q-model of the single nucleon by incorporating the quark-antiquark excitations generated by quark-gluon interaction directly into the model space and obtained an improved single nucleon wavefunction including $(3q)(q\bar{q})$ -components in addition to the dominant (3q)-components given [38] by

$$\Psi = a_{\underset{\sim}{0}}\psi_{\underset{\sim}{0}}(3q) + \sum_{\alpha \neq 0} a_\alpha \psi_\alpha \left((3q)(q\bar{q})\right) \qquad (1.1)$$

Their extended quark model uses quark-quark interaction which is a combination of quark confinement potential (quadratic type) and one gluon exchange potential through the colour analog of the Fermi-Breit interaction. The full Breit quark-gluon interaction [37] includes the five types of terms shown below.

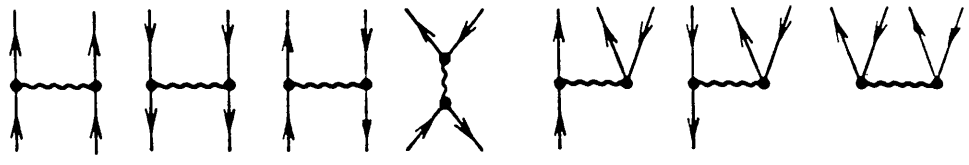

Fig. 1.1 **The full Breit interaction hamiltonian.**

The qq-interaction includes tensor and spin-orbit terms [27,28] but these terms have been omitted in ref. [37] mainly for simplicity and also because their investigation is restricted to S-wave scattering.

The qq-interaction used by Fujiwara and Hecht [37] is given by

$H_{qq} = \sum_{i<j} V_{ij}$ where the two body interaction V_{ij} is

$$V_{ij} = \alpha_s \hbar c \frac{1}{4} (\lambda_i . \lambda_j) \left\{ \frac{1}{r_{ij}} - \frac{\pi \hbar^2}{m^2 c^2} \delta(r_{ij}) \left[1 + \frac{2}{3} (\sigma_i \cdot \sigma_j) \right] \right\} - (\lambda_i . \lambda_j) a_c r_{ij}^2 \qquad (1.2)$$

Here, and in all following work, the $\lambda^{(a)}$ are the eight generators of SU(3) colour, σ denotes the Pauli spin matrices and $\mathbf{r}_{ij} = \mathbf{r}_i - \mathbf{r}_j$ when the position of particles i and j are $\mathbf{r}_i$ and $\mathbf{r}_j$ respectively. α_s is the coupling constant of the gluon-exchange interaction, m is the mass of a quark, $\hbar$ is planck's constant and c is the speed of the light. The last term is a phenomenological confining potential.

The $(3q)(q\bar{q})$-components of the single nucleon wavefunction (1.1) is generated by the $(q\bar{q})$-pair creation interaction (type (4a) of quark-gluon interaction shown in fig. 1.1) namely, the transition potential which has been discussed in connection with baryon -meson coupling constants by Yu and Zhang [41]. In non-relativistic approximation, having ignored the terms involving $1/c^2$, the transition potential is

$$V_{q \to qq\bar{q}}(1,2) = \frac{i}{2\pi} \alpha_s \frac{1}{4} (\lambda_1 . \lambda_2) \left\{ \frac{\pi}{2mc} \left(\frac{2}{r^2} (\sigma_1 . \mathbf{n}) + \frac{i}{r^2} (\sigma_1 \times \sigma_2) . \mathbf{n} + \frac{2i}{r} (\sigma_1 . \mathbf{p}_2) \right) \right. \qquad (1.3)$$

Here " 1 " denotes a sea quark, "2" denotes a valence quark. The unit vector (i.e. the direction vector) is given by

$$\mathbf{n} = \frac{\mathbf{r}}{r} = \frac{\mathbf{r}_1 - \mathbf{r}_2}{|\mathbf{r}_1 - \mathbf{r}_2|} \qquad (1.4)$$

The extended quark model of Fujiwara and Hecht [37-40] uses the same set of parameters as usually used in quark models, the oscillator length parameter b, the quark-gluon coupling constant (QCD analog of the fine structure) α_s and the strength constant of phenomenological confinement potential a_c. The choice of the parameters has been made consistent with the single nucleon's physical properties.

Fujiwara and Hecht studied the effects of $(q^4\bar{q})$-configurations on the nucleon-nucleon interaction and the ground state of a nucleon within the framework of the resonating group method [37]. In this study, as a first step they included only $q\bar{q}$-excitations into the model and ignored $q^2\bar{q}^2$ and other higher excitations for simplicity. The results of their calculations are quite encouraging. The model predicts that the repulsive core heights predicted by (3q)-(3q) models of NN-scattering are largely reduced and the $q\bar{q}$-excitations produce effective potentials with weaker attractive part in 0.8-1.5 fm range. The nucleon's charge radii and magnetic moments predicted by the extended quark model [37] are quite reasonable . Their values include relativistic corrections.

Fujiwara also applied the extended quark model to the octet baryon (B_8) and B_8-B_8 interaction [38]. The parameters were reevaluated and for $m_s=m_u=m_d$ the common value 928 Mev was obtained for the B_8 energies. In spite of smaller amplitude of (3q)$(q\bar{q})$-components in the nucleon's internal wavefunction, their contributions to the single nucleon's properties and also to the NN-interaction are significant. They contribute 40-45 % of the total magnetic moments of the octet baryons [38].

In a second step towards their goal, Hecht and Fujiwara further improved the single nucleon's wavefunction in which the dominant (3q)-components are augmented by (3q)($q\bar{q}$)-components generated by interactions of type (4a) as well as (3q)($q^2\bar{q}^2$)-components generated by the interactions of type (5) of the quark-gluon interaction shown in fig 1.1. With this improved wavefunction of the single nucleon, they studied the NN-interaction within the framework of resonating group method [39]. These studies provide improved information about the nuclear force. The main characteristics and the features of the nucleon-nucleon interaction in terms of the extended quark model are summarized in table 2 of reference [39b].

Having given a brief review of the quark-structure models of the single nucleon in general and of the extended quark model [37-40] of a nucleon's structure and the NN-interaction in particular, we shall now talk about the important features of the present investigations.

Our present study is motivated mostly by the encouraging results of the extended quark model of a nucleon [37-40] proposed by Fujiwara and Hecht. The description of our model used in the present work is as follows.

We extended a simple (3q)-model of the single nucleon with 3 valence quarks in 0S shell by assuming three filled shells $0\bar{S}_{1/2}$, $0\bar{P}_{1/2}$ and $0\bar{P}_{3/2}$ occupied by 48 ghost quarks below the lowest positive energy state (with E=0 i.e. Fermi level) forming a sea of ghost quarks analogous to the Fermi-Dirac vacuum of negative energy states all filled with fictitious electrons. It should be noted that ghost quarks are assigned negative intrinsic parity. The

real space also expands to include all 36 single-quark states of 0P shells in addition to 12 states of 0S shell. But all states are empty except 3 occupied in 0S shell. Overall 96 single-particle basis states compose our model space. Here the single-particle state is specified by the set of usual quantum numbers n, l, j, m, f, c [36] with one extra quantum number of intrinsic parity (designated by "h" for real quark and "g" for ghost quark) for distinguishing real quarks from ghost quarks.

To study the wavefunction of a nucleon we consider three quarks (i.e. two u-quarks and one d-quark in case of proton and two d-quarks one u-quark in case of a neutron) in the $0S_{1/2}$ real shell and the sea shells all to be filled at the beginning. In an assumed sea, there are equal number of u-quarks and d-quarks with equal numbers of each colour.

To include the mesonic character into the internal wavefunction of a nucleon we generate quark-antiquark excitations into the wavefunction. These excitations are generated by exciting quarks from filled-shell sea of ghost quarks into the real space. This can be done by applying $q\bar{q}$-pair creation interaction (type (4a) of fig 1.1) namely the transition potential $V_{q\rightarrow qq\bar{q}}$ (given in equation1.3) between pairs of quarks, derived from O.G.E theory [42]. Quark-antiquark excitations inherent in the quark-gluon interaction can be understood as a result of sea quark effects [41] in which a quark-antiquark pair is produced by one gluon exchange as shown in fig. 1.2(a). The mechanism (a.1,2) of fig 1.2 has been used in the model to create $q\bar{q}$-terms in the quark-structure of a nucleon.

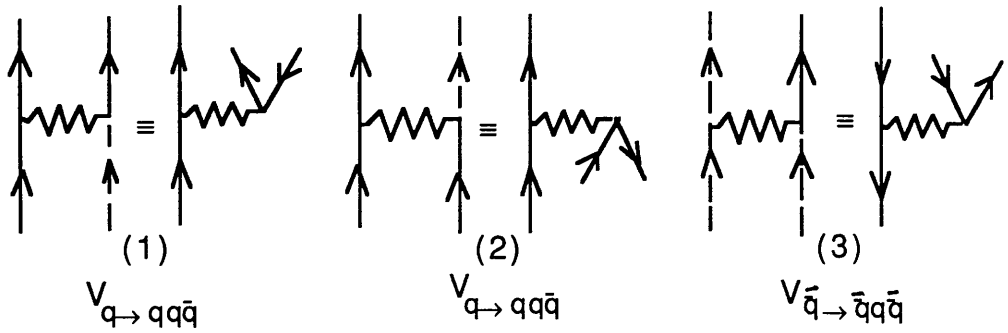

a) $(q\bar{q})$-pair creation interaction.

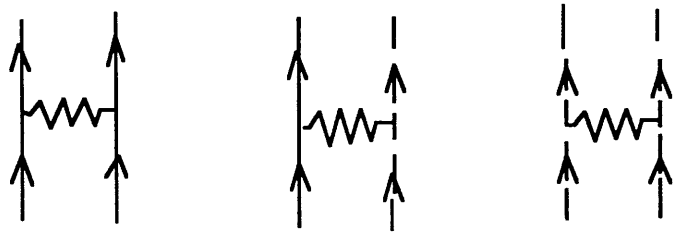

b) qq-interactions.

Fig. 1.2) Interactions between quarks. In these diagram, a continuous line represents a real quark and a broken line represents a ghost quark.

As a result of the transition potential acting between a real quark and a ghost quark when a ghost quark gets excited to occupy a positive energy state available in a real shell, a hole is created due to an absence of quark in that particular sea shell. This is obvious from interactions of type a(1) of fig. 1.2. The transition potential changes the nature of ghost quark and converts it into real quark and so increasing the number of real quarks in the valence shell. Conversely it may also happens that the transition potential acting between two real quarks de-excite one real quark to occupy a negative energy state if available empty in the sea as

clear from interaction of type a(2) of fig.1.2. This decreases the total number of quarks in the valence shells. In order to conserve parity, it must be remembered that in our model, valence and sea quarks have opposite intrinsic parities and so the excitations of quark from $0\bar{S}$ sea shell can take place to 0P real shell and the quark from $0\bar{P}$ sea shell to 0S real shell. These excitations give rise to $(0S)^3(0P)(0\bar{S})$ and $(0S)^4(0\bar{P})$ types of shell model $(q^4\bar{q})$-configurations which introduce $(3q+q\bar{q})$-components into the internal wavefunction of the single nucleon in addition to the (3q)-components.

A number of excitations of types $q\bar{q}$, $q^2\bar{q}^2$, $q^3\bar{q}^3$, . . . $q^n\bar{q}^n$ can take place. These excitations also include the excitations due to self polarisation of the filled-shell sea of ghost quarks analogous to the Dirac's vacuum self-polarisation. If we allow all the excitations then it will be impossible to manage such a large number of states and the calculation will be too big to handle.

To avoid such problems, we have switched off the interactions of type a(3) of fig 1.2 between ghost quarks in the sea and allowed the interactions of type a(1) between a real quark and a ghost quark and interaction of type a(2) between two real quarks. Quark-quark interactions of types (b) of fig 1.2 are used to act between every pair of quarks whether both are real, one real and the other ghost or both of them are ghost quarks. We have used the same qq-interaction as used in ref. [37] and shown in equation (1.2).

For simplification we also managed to generate only $q\bar{q}$-excitations and did not incorporate $q^2\bar{q}^2$ and other higher excitations into the quark model of the single nucleon.

In our model of the present investigations, we considered a nucleon as a purely many-quark system of 51 quarks with at least 3 quarks in 0S valence shell and at least 47 ghost quarks in assumed sea representing a filled-shell core with one quark missing. The single nucleon's wavefunction , therefore, contains (3q)-components obtained from shell-occupancies with 3 valence quarks in 0S shell plus filled core and $(3q+q\bar{q})$-components obtained from the shell-occupancies with 4 quarks in real shells, at least 3 in 0S shell plus core with one quark missing. We obtained the improved wavefunction of the single nucleon of the form as given (1.1). We have not included the intrinsic quantum numbers of the antiquark directly into the nucleon's internal wavefunction but have used the hole representing the absence of one quark in an assumed filled-shell core which represents an antiquark in 51-quark system. Our model represents a nucleon as a many-quark system with mesonic character as clear from the above discussion of our model.

In the present study we have incorporated the quark-antiquark excitations into the simple (3q)-model of the single nucleon to study the effects of such excitations on nucleon's structure and static properties using Glasgow shell model techniques.

The plan of the thesis is as follows:

In the current chapter 1 we give a brief review of the previous studies of the nucleon's structure and the nuclear force and describe the model used in the present study of nucleon's structure. Since we have performed our calculations in terms of the extended quark model of the single nucleon (described above) in conjunction with the Glasgow shell model programme, we

discussed the shell model computational techniques [45] in chapter 2. A short review of the shell model is given at the beginning of the chapter. We describe the basis states of the model. To store and locate the single particle occupied states in the computer memory we have introduced a colour code technique instead of using bit mapping because bits in the computer word are insufficient to accommodate large number of single quark states in the present calculations. The locations of the single quarks in a many-quark state are constrained by the colour codes condition $R \leq G \leq B$. This constraint almost removes nearly all the coloured states. The hamiltonian used in the present many-quark system is given in table 4.3. To obtain eigenvectors and eigenvalues of the energy matrix element, we used the Lanczos iterative method of tri-diagonalisation. The Lanczos algorithm is described in section (2.6). Dealing with many-quark system, the shell model calculations come across the problems of spurious centre-of-mass states and coloured states. We talk about these problems in sections 2.5.2 and 2.5.3. The last section of chapter 2 includes the procedures of computation of the electromagnetic properties such as magnetic moments, charge radii and charge density of the single nucleon.

Since the shell model requires all the information about the hamiltonian in terms of pre-calculated two body matrix elements, we evaluated the required matrix elements by the procedures described in chapter 3 and appendices A and B. In chapter 3 we discuss the procedure of evaluating matrix elements of the transition potential (1.3) in accordance with the scheme given in fig 3.1 and in appendix A we calculate the orbital matrix elements

and reduced matrix elements using generating function, properties of the binomial theorem, gamma function and associated Laguerre polynomials and theory of angular momentum. Reduced matrix elements of the pauli spin operators appearing in evaluation of matrix elements of the potential (chapter 3) are evaluated in appendix B.

In chapter 4 we first discuss the procedure used to work out the single-particle energies for different shells and energy of the core and then describe the choice and selection of model parameters. The results of the present calculations and their discussions are the main contents of chapter 4.

The present work has been concluded with recommendations for future work in chapter 5.

Some of the present work has already been reported in Nuclear Physics Conference at Manchester [43].

CHAPTER 2

GLASGOW SHELL MODEL TECHNIQUES

2.1 INTRODUCTION.

There have been significant conceptual and technical developments in the nuclear shell theory. A number of theoretical approaches to the shell model calculations have been developed by the nuclear theoretical physicists.The shell model calculations are conceptually very simple, just construct the hamiltonian matrix and diagonalise it to obtain the eigenvalues and eigenvectors. The complexity, of course, arises when there are many active particles or active orbits and the number of states becomes so large that the calculation gets too big to be handled. To avoid this problem one has to keep the restriction of the configuration space to a manageable size by making approximations in the form of basis truncations. But if we make the truncations then it is difficult for us to know whether the inevitable discrepancies between calculation and observation are due to the interaction being used or due to the truncations. Therefore, it is always desired to do calculations which are as free of approximations as possible to try to separate the effects of the force from those of the basis. A new numerical approach different from the conventional shell model approaches was advocated by Whitehead [44] which, in many

cases, permits one to do very large calculations and removes some of these difficulties. Our Glasgow shell model programme is based on this approach. The unconventional shell model techniques embodied in the Glasgow shell model programme [45] do away with the traditional shell model formalism of group theory [46], angular momentum algebra and method of fractional parentage [47] and replace all these with the elementary operations of second quantisation. The basis states are taken as Slater determinants and are sometimes represented in the computer by assigning a single particle state to each position in the computer word, a 1-bit representing an occupied state and 0-bit an unoccupied one. Bit manipulation is then easily encoded.

The programme requires the information about the hamiltonian in the form of pre-calculated two body matrix elements and diagonalises the hamiltonian by the Lanczos method to obtain the energy eigenvalues and eigenvectors.

In nuclear physics and even in the nuclear shell model calculations we are interested in a few lowest energy eigenstates and in the present case, in particular, we are mostly interested in the ground state energy of the nucleon. Since the dimension of the configuration space considered may be large, it would be preferred not to have to diagonalise the complete and large energy matrix if only a few lowest eigenvalues are desired. Most procedures that are in use, e.g, Householder method [48] need a complete diagonalisation of the full matrix. But the Lanczos iterative method of tri-diagonalisation is the only procedure which allows one to obtain some eigenvalues and eigenvectors quite accurately

from only part of the full matrix.

The principles of the method are given in ref. [49] whereas the essential features of the algorithm relevant to our approach have been discussed at length in ref. [45]. we will give a brief description of the method in section (2.6).

The Glasgow code is the most powerful computing technique by which many of the large full basis calculations for sd-shell nuclei have been fruitfully performed [50,51]. A few years ago, it was modified [36] to a new version and was used to do calculations for six quarks system. We have further modified the programme and have studied the effects of quark-antiquark excitations on the structure of the nucleon. Our results will be presented in chapter 4 . In the last section of this chapter, we would talk about the ways to setup the wavefunction of the system of 51 quarks comprising the structure of the nucleon. We shall also describe the procedures for evaluating the root mean square radii of mass (and of the charge), magnetic moment and the charge density of the system. These properties can be measured very accurately and provide a good test of the wavefunction of the nucleon resulting from numerical calculations.

2.2 OCCUPATION NUMBER REPRESENTATION

The formalism that is based on the elementary operations of creation and annihilation operators is called second quantisation [52]. Second quantisation is extensively used in a theory of the nuclear spectroscopy and specially in cases where one deals with

many particles distributed over many active single particle orbitals for proper antisymmetrisation and the evaluation of matrix elements.

For identical fermions in a single particle model, the indistinguishability of the particles makes it meaningless to determine which particle is in which single particle state and therefore the particle indices seem to be inapplicable . Here we need to use the states labels because one wants to know only which states are occupied. Since it emphasises the fact that for a completely antisymmetric wavefunction of many identical fermions only the knowledge of occupation numbers of the various single particle states is the relevant information, the formalism of fermion creation and annihilation operators is also referred to as the occupation number representation. In this formalism we are introduced to the very basic definitions like,

$$a_\alpha\dagger \mid 0 > = \mid \alpha > \; ; \quad a_\alpha\dagger \mid \alpha > = 0 \qquad (2.2.1)$$

and

$$a_\alpha \mid \alpha > = \mid 0 > \; ; \quad a_\alpha \mid 0 > = 0 \qquad (2.2.2)$$

where $|0>$ is called the vacuum state (ie the state with no particles) and the operators $a_\alpha\dagger$ (and a_a) creates and annihilates a particle in a quantum state α which is characterised by a set of certain quantum numbers as discussed in section 2.4.1.

2.2.1 WAVEFUNCTION OF MANY-FERMION SYSTEM

We know that a normalised antisymmetric wavefunction for A independent fermions is defined by the Slater determinant [53],

$$\Psi = \frac{1}{\sqrt{A!}} \begin{vmatrix} \Phi_{\alpha_1}(1) & \Phi_{\alpha_2}(1) & \ldots & \Phi_{\alpha_A}(1) \\ \Phi_{\alpha_1}(2) & \Phi_{\alpha_2}(2) & \ldots & \Phi_{\alpha_A}(2) \\ \cdot & \cdot & & \cdot \\ \cdot & \cdot & & \cdot \\ \Phi_{\alpha_1}(A) & \Phi_{\alpha_2}(A) & \ldots & \Phi_{\alpha_A}(A) \end{vmatrix}$$

$$\equiv \frac{1}{\sqrt{A!}} \det\{\alpha_1, \alpha_2, \ldots \alpha_A\} \qquad (2.2.1.1)$$

In second quantised notation, we write the wavefunction for A fermions in different states as the product of A creation operators applied to the vacuum state $|0>$, i.e.

$$a^\dagger_{\alpha_1} \ldots a^\dagger_{\alpha_i} a^\dagger_{\alpha_j} \ldots a^\dagger_{\alpha_A} | 0 > = | \alpha_1 \ldots \alpha_i \alpha_j \ldots \alpha_A > \qquad (2.2.1.2)$$

Since we can write

$$a^\dagger_{\alpha_1} \ldots a^\dagger_{\alpha_i} a^\dagger_{\alpha_j} \ldots a^\dagger_{\alpha_A} | 0 > = \frac{1}{\sqrt{A!}} \det \{ \alpha_1 \ldots \alpha_i \alpha_j \ldots \alpha_A \}$$

$$= - \frac{1}{\sqrt{A!}} \det\{ \alpha_1 \ldots \alpha_j \alpha_i \ldots \alpha_A \}$$

$$= - a^\dagger_{\alpha_1} \ldots a^\dagger_{\alpha_j} a^\dagger_{\alpha_i} \ldots a^\dagger_{\alpha_A} | 0 > \qquad (2.2.1.3)$$

it implies that

$$a^\dagger_{\alpha_i} a^\dagger_{\alpha_j} = - a^\dagger_{\alpha_j} a^\dagger_{\alpha_i}$$

or $$a^\dagger_{\alpha_i} a^\dagger_{\alpha_j} + a^\dagger_{\alpha_j} a^\dagger_{\alpha_i} = \left\{ a^\dagger_{\alpha_i}, a^\dagger_{\alpha_j} \right\} = 0 \qquad (2.2.1.4)$$

i.e the interchange of labels of the states i and j introduces a minus sign. The expressions (2.2.1.3) and (2.2.1.4) show that the antisymmetry of the many-fermion wavefunction (2.2.1.2) is guaranteed by the requirement that the creation operators anticommute. The following anticommutation relations are also satisfied by the creation and annihilation operators.

$$\left\{ a_{\alpha_i} , a_{\alpha_j} \right\} = 0$$

and $$\left\{ a^{\dagger}_{\alpha_i} , a_{\alpha_j} \right\} = \delta_{ij}$$ it introduces $\delta_{ij} = 1$ if $\alpha_i = \alpha_j$

2.2.2 WAVEFUNCTION OF CLOSED-SHELL CORE

A closed shell is one in which all possible substates allowed by the Pauli exclusion principle are occupied. we, therefore, write a core-state comprising more than one closed shell in occupation number formalism as

$$| c > = \Pi_i \, a^{\dagger}_i | 0 > \qquad (2.2.2.1)$$

The above definition (2.2.2.1) can be extended to the case of more than one closed shells by writing the wavefunction of the core (in angular momentum formalism) as

$$| c > = \Pi_{\substack{i = 1, 2, \ldots F \\ m_i = -j_i , -j_i +1, \ldots, +j_i}} a^{\dagger}_i | 0 >$$

In our present model, the wavefunction of the core comprising $0\bar{S}_{1/2}$, $0\bar{P}_{1/2}$ and $0\bar{P}_{3/2}$ shells with a total of 48 occupied single -quark states (allowed by the Pauli exclusion principle) will be represented explicitly by an expression,

$$| c > = \prod_{i=1}^{48} a^{\dagger}_{\bar{\alpha}_i} | 0 > \qquad (2.2.2.2)$$

where $\bar{\alpha}$ represents the set of necessary quantum numbers defining a single particle state of the core.

2.2.3 OPERATORS

In the occupation number representation, we define a one -body operator by

$$O^{(1)} = \sum_{ij} < \alpha_i | O | \alpha_j > a^{\dagger}_{\alpha_i} a_{\alpha_j} \qquad (2.2.3.1)$$

where the summation runs over all possible single particle states under consideration.

The two body operator such as the interaction

$$O^{(2)} = \sum_{i<j} v(i,j)$$

which is symmetric with respect to interchange of particle indices i and j may be written in second quantised form as

$$O^{(2)} = \frac{1}{4} \sum_{ijkl} (\alpha_i, \alpha_j \mid v \mid \alpha_k, \alpha_l) a^{\dagger}_{\alpha_i} a^{\dagger}_{\alpha_j} a_{\alpha_l} a_{\alpha_k}$$

$$= \frac{1}{4} \sum_{ijkl} V_{ijkl} a^{\dagger}_{\alpha_i} a^{\dagger}_{\alpha_j} a_{\alpha_l} a_{\alpha_k} \qquad (2.2.3.2)$$

Here the summation runs over the complete set with state labels $i \neq j$ and $k \neq l$. V_{ijkl} is a two body antisymmetrised matrix element. The order of the creation and annihilation operators should be noted.

The occupation number representation has been used as a basic language and a fundamental tool in the Glasgow shell model computational techniques [45] because it is well suited to the bit structure of the computer word. The many-particle basis states (i.e the Slater determinants) are represented in the computer by assigning an α value (representing a s.p. state) to each position in the computer word and then 1 or 0 at each position depending on whether the single particle state is occupied or not.

2.3 PARTICLES AND HOLES

A closed shell with one particle missing is expected to behave like a particle with some opposite properties. The vacancy created due to the absence of a particle in a closed shell core is referred

as a hole which behaves like an antiparticle. If a particle is missing from a state |j,-m> in the core then the hole created will correspond to a state with angular momentum j equal to that of a missing particle but with projection +m equal and opposite to that of a missing particle. It suggests that a hole-state $|h>_{jm}$ is equivalent to the state of closed-shell core with one particle missing. Mathematically we may express this statement, in angular momentum formalism as

$$|h>_{jm} = \frac{1}{\sqrt{2j!}} \det\{(j,-j)(j,-j+1) \ . \ . \ (j,-m-1)(j,-m+1) \ . \ . \ (j,+j)\}$$

$$= a_{j,-m}\left\{a^{\dagger}_{j,+j}\, a^{\dagger}_{j,j-1} \cdots a^{\dagger}_{j,-m+1} a^{\dagger}_{j,-m-1} \cdots a^{\dagger}_{j,-j}\right\}|0> \qquad (2.3.1)$$

In general it can be written in terms of a hole creation operator $b\dagger_{j\,m}$ (applied to the core state |c >),

$$|h>_{j_i m_i} = b^{\dagger}_{j_i m_i}|C>$$

$$= a_{\widetilde{(j_i m_i)}}|C> \qquad (2.3.2)$$

where $|\widetilde{j_i m_i}>$ is a time reversed state equals $(-1)^{j_i+m_i}|j_i,-m_i>$

Therefore we have

$$|h>_{j_i m_i} = b^{\dagger}_{j_i m_i}|C> = (-1)^{j_i+m_i} a_{j_i,-m_i}|C> \qquad (2.3.3)$$

it implies that

$$b^{\dagger}_{j_i m_i} = (-1)^{j_i+m_i} a_{j_i,-m_i}$$

i.e the hole creation operator equals a specific particle annihilation operator multiplied by the relevant phase-factor.

In the present model, by analogy with the Fermi electron sea we have assumed a sea of quarks (i.e closed-shell core defined in (2.2.2.2) below the Fermi surface comprised of $0\bar{S}$, $0\bar{P}$ shells accommodating 48 quarks (called ghost quarks), in accordance

with the Pauli exclusion principle, in singly occupied single particle states. If a quark is excited and removed from an occupied state

$$|\bar{\alpha}\rangle = |n, l, j, -m, t_3, c, g\rangle$$

in the sea to the real shell above the Fermi level and is placed in an unoccupied state $|\alpha\rangle$, it will give rise to a hole in the core and adds one quark to the real quarks. The hole created will correspond to a state represented by

$$|\alpha_h\rangle = |n, l, j, m, \bar{f}, \bar{c}, g\rangle$$

In occupation number representation, we may express this in terms of a hole creation operator.

$|\alpha_h\rangle = b^{\dagger}_{\alpha_h}|C\rangle$ where $|C\rangle$ is a closed-shell core defined in (2.2.2.2). This expression can be written in terms of a particle annihilation operator analogous to one shown in (2.3.3).

$$|\alpha_h\rangle = F \times a_{\bar{\alpha}, -m}|C\rangle$$

where F is a phase-factor as defined in ref. [37] and for the present case we have $F = (-1)^{j+m_j+1/2+ m_t+ \phi(v)}$. All these quantum numbers come for the hole state. The colour phase-factor has been defined in reference [37].

The Elliott SU(3) notation is used for the colour degree of freedom. The colour triplet has $(\lambda\mu)=(10)$: and the colour phase factor $\phi(v)$ is defined by the $3\times\bar{3}\rightarrow 1$ SU(3) Wigner coefficient

$$\sqrt{3}\langle(10)\upsilon;\ (01)\nu^c|(00)\rangle = (-1)^{\phi(v)}$$

The process, in which a quark is lifted out of the occupied negative energy state (in Fermi filled sea of ghost quarks) and placed in an unoccupied positive energy state of a real shell causing a hole (that represents an antiquark) in the core and

increasing the number of real quarks by one, in this nomenclature is referred as a quark-antiquark excitations. Other excitations such as q^2q^{-2}, q^3q^{-3} and q^nq^{-n} can be constructed by exciting 2 quarks, 3 quarks and n quarks respectively from the core to the real shells above the Fermi surface in a similar way. These states are expected to lie at energies substantially higher than 1p1h states (i.e $q\bar{q}$ states) and consequently will not mix with them. They are therefore left out of the basis space (Tamm Dancoff Approximation [54]). If we consider all such excitations then the expected wavefunction of the nucleon will be of the following form

$$|\Psi_N> \equiv 3q+(3q+q\bar{q})+(3q+q^2\bar{q}^{\,2})+(3q+q^3\bar{q}^{\,3})+ \ldots .$$

and we would not be able to manage to do such a big calculation. We, therefore, confine our calculation only to $(q\bar{q})$-excitations. This can be done by fixing the occupancies of the sea shells to keep atleast 47 ghost quarks in the sea. We choose to define our zero of energy with respect to the filled sea. We calculate the total energy of the core (i.e of filled sea),

$$E_{core} = \sum_k \varepsilon_k$$

where the summation runs over all the occupied single particle states within the filled core.

Analogous to the Fermi electron sea, we have assumed the core filled with ghost quarks as vacuum. To define the core as a new vacuum state $|\Phi_0>$ which is a filled Fermi sea of quarks, we make its energy equal to zero by subtracting the calculated core- energy from all other energies worked out. According to Fermi Dirac's theory a vacuum is considered as a sea of electrons in which

virtual pairs of electron-positron are created and then annihilated. This phenomenon of virtual creation and then annihilation of electron-positron pairs is called vacuum polarisation effect [55]. Analogously we may also expect a similar effect giving rise to quark-antiquark excitations.Therefore quark-antiquark excitations caused due to interactions between the sea quarks also include the excitations due to self polarisation of vacuum (the sea of ghost quarks). It means that if we include the excitations due to vacuum polarisation

$$|\Phi_0> = 0+q\bar{q} + q^2\bar{q}^2 + q^3\bar{q}^3 + . \ . \ . \ .$$

also in the model space to construct the wave function of the nucleon then the problem becomes more complicated and can not be tackled at present. If vacuum polarisation is included, the state $q^4\bar{q}$ could arise in the nucleon wavefunction from vacuum polarisation. To include all $q\bar{q}$-pairs arising from the presence of quarks in the nucleon, we would therefore have to include q^5q^{-2} terms, but they could arise from q^2q^{-2} terms in the vacuum and so on. There are only two consistent approaches. One is to include all terms $q^{3+n}q^{-n}$ but that is too difficult. The other is to allow no vacuum polarisation at all, and this is the truncation which we adopt in this work. These constraints mentioned above allow us to do calculation for constructing the wavefunction of the nucleon with the components 3q and $3q+q\bar{q}$.

2.4 MODEL BASIS STATES

To specify the model space we have to define the model basis states. In this section we describe the specification of single-particle and many- particle basis states.

2.4.1 SINGLE-PARTICLE BASIS STATES

In nuclear shell model, a single-particle state is defined by a set of quantum numbers n, l, j, m and t_3 i.e the principal quantum number (number of nodes of the radial wavefunction), orbital angular momentum, total angular momentum, the projection of j along the Z-axis and isospin projection respectively [56]. To do shell model calculations with quarks, then a colour quantum number "c" must be included in the set of quantum numbers describing a single-particle state [36]. In the present case since we are dealing with real quarks and ghost quarks, the set of quantum numbers is further extended to include another quantum number called intrinsic parity quantum number distinguishing real quarks from ghost quarks. The intrinsic parity quantum number is either designated by "h" which comes for even intrinsic parity to represent a real quark or by "g" which stands for odd intrinsic parity to represent a ghost quark.

In the present model we are dealing with two kinds of particles i.e. real quarks, ghost quarks and also with a hole, therefore, we have to define three types of single-particle basis states. Usually a state is given by displaying all quantum numbers necessary for its complete specification.

The specification of the spherical basis states is given as follows:

Nature of particle	State notation	Set of quantum numbers
Real quark	$\|\alpha\rangle$	(n, l, j, m, f, c, h)
Ghost quark	$\|\bar{\alpha}\rangle$	(n, l, j, m, f, c, g)
Antiquark (hole)	$\|\alpha_h\rangle$	(n, l, j, m, $\bar{f}$, $\bar{c}$, g)

2.4.2 MANY-PARTICLE BASIS STATES

We have chosen to use the Slater determinants as many-particle basis states in our shell model programme because of their suitability to represent the antisymmetric wave function of a many-particle system. The Slater determinants are constructed from a selection of single-particle spherical basis states. There are a number of ways for selecting single-particle states to construct Slater determinants. We write a Slater determinant in the occupation number representation as the product of creation operators applied to the vacuum as shown in (2.2.1.2).

For the present system, Slater determinants are constructed by putting 51 quarks into single-particle orbits out of the 96 available orbits of 0S, 0P real and ghost shells such that there are at least 47 quarks in the core, at least 3 quarks in the 0S shell. In general we can represent a many-particle state for a system of 51 quarks by a Slater determinant (as defined in 2.2.1.1) defining an antisymmetric wave function of the system as

$$\Psi = \frac{1}{\sqrt{(51)!}} \begin{vmatrix} |\alpha_1>_1 \ldots |\alpha_4>_1 |\bar{\alpha}_5>_1 |\bar{\alpha}_6>_1 \ldots |\bar{\alpha}_{51}>_1 \\ |\alpha_1>_2 \ldots |\alpha_4>_2 |\bar{\alpha}_5>_2 |\bar{\alpha}_6>_2 \ldots |\bar{\alpha}_{51}>_2 \\ \cdot \quad \cdot \quad \cdot \quad \cdot \quad \cdot \\ \cdot \quad \cdot \quad \cdot \quad \cdot \quad \cdot \\ \cdot \quad \cdot \quad \cdot \\ |\alpha_1>_{51} \ldots |\alpha_4>_{51} |\bar{\alpha}_5>_{51} \ldots |\bar{\alpha}_{51}>_{51} \end{vmatrix}$$

$$= \frac{1}{\sqrt{(51)!}} \det \left\{ |\alpha_1> \ldots |\alpha_4> |\bar{\alpha}_5> |\bar{\alpha}_6> \ldots |\bar{\alpha}_{51}> \right\} \qquad (2.4.2.1)$$

These many-particle states are of course antisymmetric and have definite values of $M = \Sigma_i m_i$ and $T_3 = \Sigma_i t_{3i}$ but not necessarily having definite total angular momentum and isospin.

A complete set of many-particle states (Slater determinants) with the desired number of u-quarks and d-quarks, parity, M and occupancies of real and ghost shells is set up at the start of the calculation. A single bit of the computer word may be used to represent a single-particle orbital and the values 0 or 1 are used to indicate whether the orbital is empty or filled. It means that an A-particle state i.e a Slater determinant for A particles in n-dimensional model space is represented by a string of bits containing A 1-bits. A typical determinant such as mentioned above is shown below.

$\Psi_A(2,3,5, \ldots n-1)$

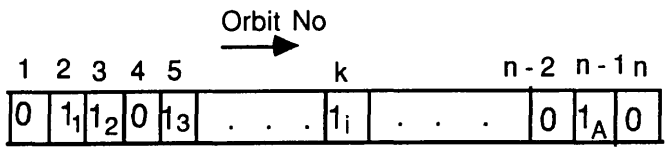

$$= \qquad (2.4.2.2)$$

One can obtain a new determinant by applying the creation and annihilation operators , for example $a_1^\dagger a_4^\dagger a_5 a_2$ to the determinant (2.4.2.2) as

$$\Psi'_A(1,3,4,\ .\ .\ n\text{-}1) \equiv a_1^\dagger a_4^\dagger a_5 a_2\ (\Psi_A(2,3,5,\ .\ .\ n\text{-}1)$$

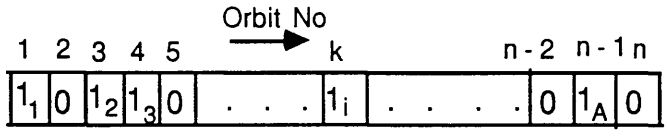

(2.4.2.3)

According to the Pauli exclusion principle, no two positions in the representation can have the same set of quantum numbers and each box has assigned the m-value such that the same particles may be put in boxes with different m-values.That is why the given scheme of basis representation is called m-scheme [3].

The computer representation of the Slater determinants and a number of other practical and computational aspects of shell model manipulations with Slater determinants have been described in quite detail in reference [45].

In the present calculation the bit-mapped representation of the occupied single-particle states and many-particle states is inadequate because 96 single quark orbits do not fit in a 32-bit computer word as n quarks in N orbits require N bits.

An alternate representation, namely codes-representation has been introduced to locate and store the occupied states in a computer memory. A single-particle orbit m occupied by ith quark is represented by a code calculated from a binomial coefficient as given below,

Code = $m_i C_i$

Fig.2.1

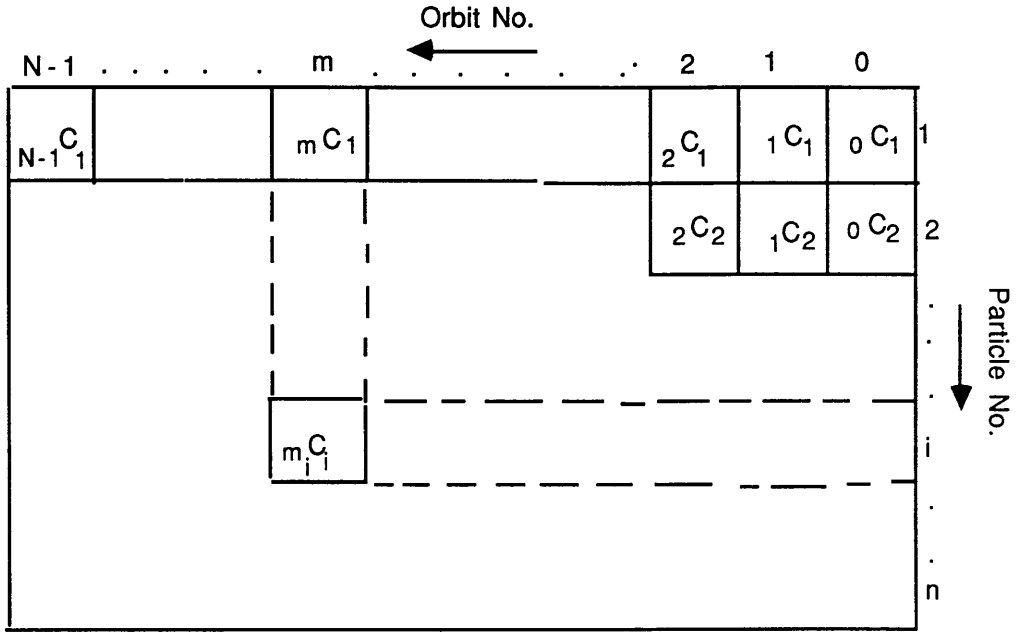

The arrays of codes for different orbits occupied by various particles are shown in fig. 2.1. It is convenient to have a rectangular array of coefficients and we define $^{p}C_{q}=0$ if p<q.

The sum of codes of the occupied orbits in a certain many-particle state gives the code of that state. For example, the codes of many-particle states shown in expressions (2.4.2.2) and (2.4.2.3) will be given by

$$C_{total} = {}_2C_1 + {}_3C_2 + {}_5C_3 + \ldots + {}_kC_i + \ldots + {}_{n-1}C_A \quad \text{and}$$

$$C'_{total} = {}_1C_1 + {}_3C_2 + {}_4C_3 + \ldots + {}_kC_i + \ldots + {}_{n-1}C_A \quad \text{respectively.}$$

The bit mapping is an inefficient method of storage and it is inadequate for large number of single-particle orbits requiring the number of bits equal to total number of orbits. For example, in this case n particles in N orbits require N bits whereas the representation of codes calculated from binomial coefficients is

much more compact as it needs only $\log_2({}^{N}C_n)$ bits.

2.5 SHELL MODEL APPROACH TO THE MANY-BODY PROBLEM

According to our model, a nucleon has been considered as a system of many quarks. The treatment of the motion of the quarks in a nucleon can be considered as an example of the many-body problem. Since the shell model takes into account the individual particles and provides the microscopic description of the system, it may be only an approximation of the exact many-body problem. In its most elementary form of the shell model, it is assumed that the motion of a particle under the influence of all the others is approximated by its motion in a self-consistent field of force. There is enough empirical information on nuclear structure to justify the use of this assumption in many cases. We may use it as a basis for more elaborate theories of the many-body problem. A full description of a microscopic theory of the many-body system is given by the solution of a many-body Schrodinger equation

$$H\Psi^{(A)} = \left\{ \sum_{i=1}^{A} \frac{\mathbf{P}_i^2}{2m} + \sum_{i<j}^{A} V_{ij} \right\} \Psi^{(A)}(1,2,3, \ldots A) = E\Psi^{(A)}(1,2,3, \ldots A) \quad \ldots\ldots (2.5.1)$$

where $\Psi^{(A)}$ (in case of fermions)is an antisymmetric wavefunction of A-particle system defined in (2.2.1.1) and 'i' is the particle index.

With the assumption of a self-consistent field, the above equation (2.5.1) reduces to the much simpler equation

$$H_0\Psi^{(A)} = \left\{ \sum_{i=1}^{A} h_i \right\} \Psi^{(A)} = \sum_{i=1}^{A} \left\{ \frac{\mathbf{P}_i^2}{2m} + V(i) \right\} \Psi^{(A)} = E\Psi^{(A)} \qquad (2.5.2)$$

In occupation number representation, the shell model Hamiltonian H_0 is given by

$$H_0 = \sum_i \varepsilon_i \, a_i^\dagger a_i \qquad (2.5.3)$$

and $$E = \sum_{i=1}^{A} \varepsilon_i \qquad (2.5.4)$$

The solutions $\Psi^{(A)}$ of equation (2.5.2) are antisymmetrised products of single particle wave functions Φ_i, which are eigenfunctions of the single particle hamiltonian h_i .

i.e $$h_i \Phi_i = \varepsilon_i \Phi_i \qquad (2.5.5)$$

where ε_i represents single particle energy eigenvalue.

The eigenfunctions Φ_i form a complete set of orthonormal basis states. i.e

$$< \Phi_{\alpha_i} \mid \Phi_{\alpha_j} > = \delta_{\alpha_i \, \alpha_j}$$

where α_i and α_j represent the sets of quantum numbers defining the single particle states i and j respectively. Similarly the many-particle wavefunction $\Psi^{(A)}$ also form an orthonormal complete set of basis.

i.e $$< \Psi_k^{(A)} \mid \Psi_l^{(A)} > = \delta_{kl}$$

2.5.1 MANY BODY HAMILTONIAN

For a system of A particles, the Hamiltonian is written as a sum of single particle kinetic energies and two body interactions [54] .

i.e $$H = \sum_{i=1}^{A} T_i + \sum_{i<j}^{A} V(i,j) \qquad (2.5.1.1)$$

where the two-body potential (interaction) V_{ij} represents the realistic force between two particles.

Since we use the Slater determinants as many particle basis states represented in occupation number representation, it will be pretty fair to use an appropriate form for the model Hamiltonian. The many body Hamiltonian (2.5.1.1) is a sum of one-body and two-body parts that can be written in a second quantised version by expressing it in terms of one-body and two-body operators defined in (2.2.3.1) and (2.2.3.2) respectively. i.e

$$H = \sum_{i\,j} < i \mid T \mid j > a_i^+ a_j + \frac{1}{4} \sum_{i\,j\,k\,l} (ij \mid V \mid kl) a_i^+ a_j^+ a_l a_k \qquad (2.5.1.2)$$

where T is the kinetic energy and V is the interaction between two particles.

In the problem at hand, the interaction V includes;

i) the interaction V_{qq} between two quarks whether in real shells or in ghost shells, ii) the interaction V_{qQ} between a real quark and a ghost quark. The interaction (i) and (ii) can be related by an expression $V_{qQ} = -V_{qq}$ in the same sense as there exists a relation [57] between qq-interaction and quark-antiquark interaction.

iii) The interaction $V_{q\text{-}qq\bar{q}}$, between a real quark and a ghost quark or between two real quarks, that gives rise to the particle-hole excitations. In occupation number representation we can express the transition potential as

$$H_{q\to qq\bar{q}} = \sum_{\alpha\beta\gamma\delta} <\Psi_\gamma(1)\Psi_\delta(2) \mid V(1,2) \mid \Psi_\alpha(1)\Psi_{\bar{\beta}}(2)> a_\gamma^\dagger a_\delta^\dagger b_\beta^\dagger a_\alpha$$

where $b_\beta\dagger$ is a hole creation operator.

In general, we can write the hamiltonian H as

$$H = \sum_{i\,j} H_{ij}^{(1)} a_i^\dagger a_j + \frac{1}{4} \sum_{ijkl} H_{ijkl}^{(2)} a_i^\dagger a_j^\dagger a_l a_k \qquad (2.5.1.3)$$

where $H_{ij}^{(1)}$ and $H_{ijkl}^{(2)}$ are the matrix elements of one-body and two-body hamiltonian respectively.

i.e $H_{ij}^{(1)} = < i \mid H^{(1)} \mid j >$ and $H_{ijkl}^{(2)} = (ij \mid H^{(2)} \mid kl)$.

$H^{(1)}$ is usually,but not necessarily diagonal. But if it is diagonal then $H_{ij}^{(1)} = H_i^{(1)} \delta_{ij}$.

In the shell model programme, the Hamiltonian (as a whole) could be treated as a two-body operator as described in reference [45]. For computational shell model manipulations we have selected the occupation number representation as a basic language of the programme, therefore it will be more convenient to use the matrix elements of two-body hamiltonian between uncoupled two -particle states. The two-body matrix elements in an uncoupled angular momentum (and isospin) representation can be written using the standard vector coupling result as

$$H_{ijkl}^{(2)} = < j_i\ m_i \tfrac{1}{2}\ t_{3i}\ ,\ j_j\ m_j \tfrac{1}{2}\ t_{3j}\ ; \mid H^{(2)} \mid j_k\ m_k \tfrac{1}{2}\ t_{3k},\ j_l\ m_l\ \tfrac{1}{2}\ t_{3l} >$$

$$= \sum_{\substack{JM \\ TM_T}} (j_i m_i, j_j m_j | JM)(j_k m_k, j_l m_l | JM)(\tfrac{1}{2}\ t_{3i},\ \tfrac{1}{2}\ t_{3j} | TM_T)(\tfrac{1}{2}\ t_{3k},\ \tfrac{1}{2}\ t_{3l} | TM_T)$$

$$\times\ < j_i, j_j\ ;\ JMTM_T \mid H^{(2)} \mid j_k, j_l\ ;\ JMTM_T >$$

$$= \sum_{\substack{JM \\ TM_T}} (-1)^{j_i + j_k - j_j - j_l} \begin{pmatrix} j_i & j_j & J \\ m_i & m_j & -M \end{pmatrix} \begin{pmatrix} j_k & j_l & J \\ m_k & m_l & -M \end{pmatrix} \begin{pmatrix} \frac{1}{2} & \frac{1}{2} & T \\ t_{3i} & t_{3j} & -M_T \end{pmatrix} \begin{pmatrix} \frac{1}{2} & \frac{1}{2} & T \\ t_{3k} & t_{3l} & -M_T \end{pmatrix}$$

$$\times\ (2J+1)(2T+1) < j_i, j_j\ ;\ JMTM_T \mid H^{(2)} \mid j_k, j_l\ ;\ JMTM_T > \qquad (2.5.1.4)$$

The programme requires all the information about the hamiltonian in terms of pre-calculated one-body and two-body matrix elements. The procedures of evaluating the matrix elements have been described in chapter 3 and appendix A.

2.5.2 THE CENTRE-OF-MASS PROBLEM

In the shell model approach , the inter-particle potential is expressed as the sum of the single particle potentials $\Sigma U(r_i)$ fixed in space and the residual interaction [3].

To represent the single particle potential one chooses to use either the Harmonic oscillator potential or Saxon-Wood potential. The resulting hamiltonian is no longer translationally invariant and consequently the model wavefunction may contain unphysical components. In the model, since the centre of potential is fixed (at the origin) not the centre-of-mass of the system, it may gives rise to the unphysical states associated with the centre-of-mass oscillations about the origin. In conventional terms, the states in which the centre-of-mass oscillation is in 0S ground state are called nonspurious states and those with excited centre-of-mass motion are known as spurious or redundant states. In the shell model, the wavefunctions for A-particle system are described by 3A particle co-ordinates. Out of which, 3 describe the motion of centre-of-mass of the system and the remaining 3(A-1) describe the relative positions of the particles i.e the internal structure of the system.

If we choose to use the Harmonic oscillator wave functions and the active orbits include all the levels in a single major oscillator shell, the shell model states will have the same centre-of-mass motion but differ only in internal structure as normally desired. Otherwise the states with different centre-of-mass motion will contribute unphysical effects to the energy calculation and distort the calculated spectrum. It has been found [58] that all the shell

model wavefunctions with the lowest energies allowed by the Pauli's exclusion principle in the harmonic oscillator potential would correspond to the nonspurious states and all of the states with excited centre-of-mass of the system generated in the model space consisting of two or more major oscillator shells are spurious.

The operators (usually used in shell model calculations) that do not depend purely on the relative co-ordinates of the particles will mix spurious and nonspurious states.Therefore it is important to be sure that there is no mixing of physical and unphysical states. A number of ways have been advocated e.g [59-61] to achieve this aim. The problem can be solved only in case when one could separate out centre-of-mass motion from the internal motion. There is no solution to the problem of spuriousity due to centre-of-mass motion in non-separable case.

The single-particle hamiltonian for the harmonic oscillator potential can be written as a sum of the hamiltonian for translationally invariant relative motion (H_{rel}) and centre-of -mass hamiltonian ($H_{C.M}$) .

$$\text{i.e} \quad H_{S.P} = \frac{1}{2m}\sum_{i=1}^{A} \mathbf{P}_i^2 + \frac{1}{2} mw^2 \sum_{i=1}^{A} \mathbf{r}_i^{\,2} \qquad (2.5.2.1)$$

$$= H_{rel} + H_{C.M}$$

where

$$H_{rel} = \frac{1}{2m}\sum_{i=1}^{A} \left(\mathbf{p}_i - \frac{\mathbf{P}}{A}\right)^2 + \frac{1}{2} mw^2 \sum_{i=1}^{A} \left(\mathbf{r}_i - \mathbf{R}\right)^2 \qquad (2.5.2.2)$$

and $$H_{C.M} = \frac{\mathbf{P}^2}{2M} + \frac{1}{2} Mw^2 \mathbf{R}^2 \qquad (2.5.2.3)$$

Here M (=mA) and m denote the mass of the system and mass of

the particle respectively. The vectors **R** and **p** are defined as

$$\mathbf{R} = \frac{1}{A}\sum_{i=1}^{A} \mathbf{r}_i \qquad \text{and} \qquad \mathbf{P} = \sum_{i=1}^{A} \mathbf{p}_i \qquad (2.5.2.4)$$

In computational shell model manipulations the hamiltonian is treated as a purely two-body operator. Therefore we write the hamiltonian for the centre-of-mass oscillator

$$H_{osc} = \frac{\mathbf{p}^2}{2mA} + \frac{1}{2} mw^2 A\mathbf{R}^2$$

$$= \frac{1}{A}\left[\frac{A}{2m}\left\{\frac{1}{A-1}\sum_{i<j}\frac{(\mathbf{p}_i + \mathbf{p}_j)^2}{2} - \frac{A-2}{A(A-1)}\sum_{i<j}\frac{(\mathbf{p}_i - \mathbf{p}_j)^2}{2}\right\}\right.$$

$$\left. + \frac{1}{2} mw^2 A\left\{\frac{1}{A-1}\sum_{i<j}\frac{(\mathbf{r}_i + \mathbf{r}_j)^2}{2} - \frac{A-2}{A(A-1)}\sum_{i<j}\frac{(\mathbf{r}_i - \mathbf{r}_j)^2}{2}\right\}\right]$$

$$H_{osc} = \frac{1}{A-1}\sum_{i<j} H_{C.M}(ij) - \frac{A-2}{A(A-1)}\sum_{i<j} H_{rel}(ij) \qquad (2.5.2.5)$$

The best approach in dealing with the centre-of-mass spuriosity problem appears to be to calculate the expectation value $<H_{osc}>$ for the final eigenstates and check to verify that the states are nonspurious with respect to centre-of-mass excitations.

For a nonspurious state we have $< H_{osc}> = \frac{3}{2}\hbar w$ and for spurious states $< H_{osc}>$ takes on the values $\frac{5}{2}\hbar w$, $\frac{7}{2}\hbar w$, . . . [36].

To make the system more physical, the kinetic energy associated with the centre-of-mass oscillation

$$\frac{\mathbf{P}^2}{2M} = \frac{1}{2mA}\left(\sum_{i=1}^{A} \mathbf{p}_i\right)^2$$

would be subtracted off the kinetic energy term and we get the kinetic operator T in (2.5.1.1) as

$$T = \frac{1}{2m}\left\{\sum_i \mathbf{p}_i^2 - \frac{1}{A}\left(\sum_i \mathbf{p}_i\right)^2\right\}$$

$$= \frac{1}{A}\sum_{i<j} \frac{(\mathbf{p}_i - \mathbf{p}_j)^2}{2m} \qquad (2.5.2.6)$$

The expression (2.5.2.6) shows that the kinetic energy operator can be treated as two-body operator.

2.5.3 COLOURED STATES PROBLEM

In the quark model [7], the baryons and the mesons are defined as the bound states of three quarks and a quark-antiquark pairs respectively. According to the colour confining property of QCD, hadrons must exist as colourless states because no coloured states are ever seen.

In the present case as we are dealing with many-quark system we should be sure that the state,to be a physical one, is colourless. Therefore to obtain the colourless states and to avoid the coloured states possibly formed by the combination of coloured quarks, we make sure that the Slater determinants which appear in the basis for the many-quark system have equal number of quarks of the three different colours red, blue and green. In addition we constrained the colour codes such that $R \leq G \leq B$ in our shell model code, where R,G and B denote the codes for the red, green and blue quarks respectively. These codes are used to locate the positions of the quarks in the computer memory as discussed in section (2.4.2). This constraint helps to truncate the model space by removing unphysical coloured states. It does not remove all coloured states and it does not remove any colourless states.

Since the constraint is not enough to ensure colourless eigenstates, we evaluate the expectation value of the Casmir's operator for colour $<c^2>$,

$$< C^2 > = (\sum \lambda_i)^2 = \sum_i \lambda_i^2 + \sum_{i<j} \{ (\lambda_i + \lambda_j)^2 - \lambda_i^2 - \lambda_j^2 \}$$

to decide if a state is colourless and physical or coloured and unphysical. The expectation value $<c^2>$ is zero for colourless state [7(a)].

The centre-of-mass operator H_{osc} and colour casmir's operator c^2 are used at the end of the calculation for evaluating their expectation values to distinguish spurious states from nonspurious and coloured states from colourless states.

2.6 THE LANCZOS ALGORITHM

The central feature of the Glasgow shell model programme [45] is the use of Lanczos Algorithm for the construction and tri-diagonalisation of the energy matrix. A full treatment of the method as a numerical tool [48] is not required for the shell model application. The important features of the method relevant to our work have been discussed at length in references [44,45]. some description of the method is given below.

We start with any normalised vector v_1 arbitrarily chosen in a N-dimensional space and operate on it with the hermitian operator H, the hamiltonian to obtain a new vector v_2 (orthogonal to v_1).

$$Hv_1 = \alpha_1 v_1 + \beta_1 v_2$$

Similarly a third vector v_3 (orthogonal to v_1 and v_2) is generated by operating with H on v_2. i.e

$$Hv_2 = \beta_1 v_1 + \alpha_2 v_2 + \beta_2 v_3$$

In a similar way a complete set of orthonormal vectors v_i is generated by the repeated operations with H. For a configuration space of dimension N, one finds

$$Hv_1 = \alpha_1 v_1 + \beta_1 v_2$$

$$Hv_2 = \beta_1 v_1 + \alpha_2 v_2 + \beta_2 v_3$$

$$Hv_3 = \beta_2 v_2 + \alpha_3 v_3 + \beta_3 v_4$$

. . . . . .

. . . . . .

$$Hv_{n-1} = \beta_{n-2} v_{n-2} + \alpha_{n-1} v_{n-1} + \beta_{n-1} v_n$$

$$Hv_n = \beta_{n-1} v_{n-1} + \alpha_n v_n + \beta_n v_{n+1}$$

. . . . . .

. . . . . .

The process of iterations terminates automatically with vector v_N since the space is spanned. For the Nth step we have

$$Hv_N = \beta_{N-1} v_{N-1} + \alpha_N v_N \quad \ldots . \quad (2.6.1)$$

because there can not be any more vector orthogonal to $v_1, v_2, v_3, \ldots v_N$, that is the new vector v_{N+1} must be zero.

The co-efficients α_i and β_i defined by

$$\alpha_i = \langle v_i | H | v_i \rangle$$

and $$\beta_i = \langle v_i | H | v_{i+1} \rangle = \langle v_{i+1} | H | v_i \rangle$$

are the matrix elements of the hamiltonian H in the basis $v_1, v_2, v_3, \ldots v_N$ whereas all other matrix elements of H vanish.

i.e $$\langle v_i | H | v_j \rangle = \langle v_j | H | v_i \rangle = 0 \quad \text{for } |i-j| \geq 2.$$

From the above sequence of iterations (2.6.1), it is clear that the matrix representation of H in the orthonormal basis formed by vectors $v_1, v_2, v_3, \ldots v_N$ (which are called Lanczos vectors) is a real

symmetric tri-diagonal matrix.

$$\hat{H}_{Tri} \equiv \begin{pmatrix} \alpha_1 & \beta_1 & \cdots & \cdots & 0 \\ \beta_1 & \alpha_2 & \beta_2 & \cdots & \\ 0 & \beta_2 & \alpha_3 & \beta_3 & \cdots \\ & \cdots & \cdots & \cdots & \\ & & \cdots & & \\ & & & \cdots & \\ 0 & \cdots & \cdots & \cdots & \alpha_N \end{pmatrix}$$

To obtain eigenvalues and eigenvectors, the tri-diagonal matrix $\hat{H}_{Tri}$ can be diagonalised by the standard methods of bisection and inverse iteration [49].

Unfortunately if one uses inexact arithmetic, the process of iteration does not really terminate at the Nth step because round off errors prevent v_{N+1} from being exactly zero.Continuing the process with such a small vector, the same eigenvalues will be reproduced again and again. This exotic effect also disrupts the orthogonalisation of the basis vectors and practically the vector v_N will be no more orthogonal to the previous vectors v_i. Therefore re-orthogonalisation will be needed. That is why in shell model programme [45] the re-orthogonalised version of the method has been used.

The important property of the method is that the extreme eigenvalues of $\hat{H}_{Tri}$ converge rapidly as N increases. In the shell model work we are often interested only in a few lowest energy states, so it is sufficient to get convergence of nearly 10 eigenvalues which can be obtained by the order of 100 iterations

as it is clear from the some convergence curves given in reference [44,45].

For rapid convergence, it is advantageous to start with an initial vector v_1 that contains relatively large components of the lowest eigenvectors. This can be achieved by operating a few times with H on an arbitrary vector v_0. i.e

$$v_1 = H^n v_0$$

For n=5, the rate of convergence of the low lying eigenstates get improved [45] in some cases. The eigenvalue is only accepted as converged if it does not change at all in the sixth decimal place. The complete convergence of any eigenvalue is ensured by calculating the J and T values for each eigenstate in question.

To find J and T values of a certain state we have to compute the expectation value of J^2 and T^2. This can be done by applying the Lanczos procedure itself to the eigenvectors, with H in sequence (2.6.1) replaced by J^2 and T^2 or by using the formula connecting the lowering and raising operators with J^2 or T^2. i.e

$$J^2 = J_- J_+ + (J_Z)^2 + J_Z$$

Or $$T^2 = T_- T_+ + (T_Z)^2 + T_Z$$

The sharp values (i.e integral or half integral values) of J and T indicate complete convergence of the eigenvalues.

The eigenvectors Ψ_i of the original H are related to those of the tri-diagonal matrix $H^{\wedge}_{Tri}$ by

$$\Psi_i = \sum_{\kappa=1}^{N} \psi_k^{(i)} \, v_k \qquad (2.6.3)$$

where v_k are the Lanczos basis vectors that are represented as the linear combination of the Slater determinants

$$v_k = \sum_i a_{ki} \psi_i$$

and $\Psi^{(i)}$ are the eigenvectors of the tri-diagonal matrix $H^{\wedge}_{Tri}$.

The Glasgow shell model computational code [45] based on the Lanczos method used for the m-scheme uncoupled representation has been the most powerful technique in existence for carrying out the shell model calculations in a large space. The Lanczos method is also useful for coupled representation [62] but that is not practically more successful.

2.7 DETERMINATION OF STATIC AND ELECTROMAGNETIC PROPERTIES OF THE NUCLEON

In accordance with the basic assumption of the present model, the nucleon is supposed to be a system of 51 quarks (as discussed in chapter 1) described by the wavefunction 2.4.2.1.

In order to achieve a proper understanding about the size and structure of the nucleon, we have to study its static and electromagnetic properties. We, therefore, determine the root mean square radii of mass and charge, the charge density and the magnetic moment of the nucleon. The knowledge of the magnetic moment of a nucleon provides information on its internal structure.

2.7.1 MAGNETIC MOMENT

In the single particle model, the magnetic moment of the system is given by the expectation value (in the ground state) of the vector sum of the z-components of the magnetic moment operators of the individual particles. Therefore in the present case we express the magnetic moment of the nucleon as [63]

$$\mu = < \Psi_0 \mid \sum_i \mu_z(i) \mid \Psi_0 > \qquad (2.7.1.1)$$

where Ψ_0 represents the ground state wavefunction of the nucleon. The magnetic moment of a single-particle is expressed as the sum of magnetic moments contributed by its orbital angular momentum and spin angular momentum. i.e

$$\mu = \mu_l + \mu_s \qquad (2.7.1.2)$$

In non-relativistic limit, the orbital magnetic moment μ_l is defined by

$$\mu_l = \frac{e_q}{2m_q} \mathbf{l} \qquad (2.7.1.3)$$

where e_q and m_q are the charge and mass of the quark respectively. $\mathbf{l}$ is the orbital angular momentum of the quark. The charge possessed by u-quark and d-quark is

$e_u = +\frac{2}{3} e_p$ and $e_d = -\frac{1}{3} e_p$ respectively, where e_p is the charge possessed by the proton.

In analogy with the electron's spin magnetic moment, the quark to be considered a point like fermion would be expected to have the spin magnetic moment μ_s of the form [64]

$$\mu_s = g\frac{e_q}{2m_q}\sigma$$

$$= g\frac{e_q}{m_q}\mathbf{s} \qquad (2.7.1.4)$$

where $\mathbf{s}$ is a quark's spin angular momentum and factor g (analogous to Land'e g-factor) has value equal to 2 [64].

Therefore we write the expression (2.7.1.2) as

$$\mu = \frac{e_q}{e_p}\left(\frac{M}{2m_q}\right)\mathbf{l} + 2\frac{e_q}{e_p}\left(\frac{M}{m_q}\right)\mathbf{s}$$

$$= g_l\mathbf{l} + 2g_s\mathbf{s}$$

or $$= \mu_N\mathbf{l} + 4\mu_N\mathbf{s} \qquad (2.7.1.5)$$

where $\mu_N \left(= \frac{e_q}{e_p}\frac{M}{2m_q}\right)$ is a unit called the nuclear magneton. M is the mass of a nucleon. We assumed that the mass of a u-quark is equal to the mass of a d-quark, i.e $m_u = m_d = m_q$. g_l and g_s are gyromagnetic

ratio due to orbital angular momentum and spin angular momentum respectively.

In the occupation number representation, we therefore express equation (2.7.1.1) as

$$\mu = \sum_{ij} \langle i |\mu_z| j\rangle\langle\Psi_0|a_i^\dagger a_j|\Psi_0\rangle + \sum_{\bar{i}\bar{j}} \langle \bar{i} |\mu_z| \bar{j} \rangle\langle\Psi_0|a_{\bar{i}}^\dagger a_{\bar{j}}|\Psi_0\rangle$$

or $$\mu = \sum_{ij} \langle \mu_z \rangle_{ij}\ \rho_{ij} + \sum_{\bar{i}\bar{j}} \langle \mu_z \rangle_{\bar{i}\bar{j}}\ \rho_{\bar{i}\bar{j}} \qquad (2.7.1.6)$$

In this section, i and j represent u-quark single particle orbits and $\bar{i}$, $\bar{j}$ come for d-quark single particle orbits. where $\langle\mu\rangle_{ij}$ represents the matrix element of μ_z i.e.

$$\langle\mu_z\rangle_{ij} = \langle i |\mu_z| j \rangle$$

and ρ_{ij}, the single particle density matrix element is defined by

$$\rho_{ij} = \langle\Psi_0 | a_i^\dagger a_j | \Psi_0\rangle$$

Using a definition of the reduced matrix element, we can rewrite the equation (2.7.1.6) as

$$\mu = \sum_{ij}\left[(-1)^{j'-m}\begin{pmatrix} j' & 1 & j \\ -m & 0 & m\end{pmatrix}\left\{g_l\langle n'j'||\mathbf{l}||nj\rangle + 2\,g_s\langle n'j'||\mathbf{s}||nj\rangle\right\}\delta_{\gamma\gamma'}\,\rho_{ij}\right]$$

$$+\sum_{\bar{i}\bar{j}}\left[(-1)^{j'-m}\begin{pmatrix} j' & 1 & j \\ -m & 0 & m\end{pmatrix}\left\{g_l\langle n'j'||\mathbf{l}||nj\rangle + 2g_s\langle n'j'||\mathbf{s}||nj\rangle\right\}\delta_{\gamma\gamma'}\,\rho_{\bar{i}\bar{j}}\right]$$

or

$$= \sum_{ij}\left[\frac{e_u}{e_p}\left(\frac{M}{2m_q}\right)(-1)^{j'-m}\begin{pmatrix} j' & 1 & j \\ -m & 0 & m\end{pmatrix}\left\{\langle n'j'||\mathbf{l}||nj\rangle + 4\langle n'j'||\mathbf{s}||nj\rangle\right\}\delta_{\gamma\gamma'}\,\rho_{ij}\right]$$

$$+\sum_{\bar{i}\bar{j}}\left[\frac{e_d}{e_p}\left(\frac{M}{2m_q}\right)(-1)^{j'-m}\begin{pmatrix} j' & 1 & j \\ -m & 0 & m\end{pmatrix}\left\{\langle n'j'||\mathbf{l}||nj\rangle + 4\langle n'j'||\mathbf{s}||nj\rangle\right\}\delta_{\gamma\gamma'}\,\rho_{\bar{i}\bar{j}}\right] \qquad \ldots (2.7.1.7)$$

Here γ includes c, f and h or g quantum numbers.

The reduced matrix element of the operator l can be written as

$$\langle n'j' \,||\, l \,||\, n\,j\rangle = \langle n'\ (l\,s')\,j' \,||\, l \,||\, n\ (l\,s)j\rangle$$

Since the operator operates on the first part of the combination, we obtain [65]

$$\langle n' j' \| \mathbf{l} \| nj \rangle = (-1)^{l'+s'+j+1} \sqrt{(2j'+1)(2j+1)} \begin{Bmatrix} l' & j' & s' \\ j & l & k \end{Bmatrix} \langle n' l' \| \mathbf{l} \| nl \rangle \quad \ldots . \quad (2.7.1.8)$$

Similarly we may write

$$\langle n' j' \| \mathbf{s} \| n j \rangle = \langle n' (l s') j' \| \mathbf{s} \| n (ls) j \rangle$$

and therefore we get

$$\langle n' (l's') j' \| \mathbf{s} \| n (ls) j \rangle = (-1)^{l+s+j'+1} \sqrt{(2j'+1)(2j+1)} \begin{Bmatrix} s' & j' & l \\ j & s & k \end{Bmatrix} \times \langle \frac{1}{2} \| \mathbf{s} \| \frac{1}{2} \rangle \delta_{n n'} \delta_{l l'} \quad (2.7.1.9)$$

The reduced matrix elements of the $\mathbf{l}$ and $\mathbf{s}$ have the values [52]

$$\langle n' l' \| \mathbf{l} \| nl \rangle = \sqrt{l(l+1)(2l+1)}\ \delta_{n n'} \delta_{l l'} \quad (2.7.1.10)$$

and

$$\langle \frac{1}{2} \| \mathbf{s} \| \frac{1}{2} \rangle = \sqrt{\frac{3}{2}} \quad (2.7.1.11)$$

The expression (2.7.1.7) for the magnetic moment of the nucleon can be written concisely as

$$\mu = \sum_{i\,j} \left[\frac{e_u}{e_p} \left(\frac{M}{2m_q}\right) \left\{ \langle \mathbf{l}_z \rangle_{ij} + 4 \langle \mathbf{s}_z \rangle_{ij} \right\} \rho_{ij} \right] + \sum_{\bar{i}\,\bar{j}} \left[\frac{e_d}{e_p} \left(\frac{M}{2m_q}\right) \left\{ \langle \mathbf{l}_z \rangle_{\bar{i}\,\bar{j}} + 4 \langle \mathbf{s}_z \rangle_{\bar{i}\,\bar{j}} \right\} \rho_{\bar{i}\,\bar{j}} \right] \quad (2.7.1.12)$$

The calculated values of the matrix elements $\langle \mathbf{l}_z \rangle$ and $\langle \mathbf{s}_z \rangle$ between the single quark states for the u-quarks and d-quarks are given in table 4.10. The quantum numbers for specification of the orbits and their evaluated density matrix elements are given in table 4.6 and table 4.9 respectively.

Using the data given in table 4.9 and 4.10 with the help of an expression (2.7.1.12), we can evaluate the magnetic moment of the nucleon.

2.7.2 ROOT MEAN SQUARE RADIUS OF MASS

Considering the nucleon as a system of many quarks (contain -ing u-quarks and d-quarks), its mean square radius would be expressed as

$$\overline{r^2} = \frac{1}{M}\sum_{i=1}^{A} m_q(i)\, r_i^2 = \frac{1}{A}\sum_{i}^{A} r_i^2 \qquad (2.7.2.1)$$

because we take $m_u = m_d = m_q$ and $M = Am_q$, where A is the total number of quarks.

If Ψ_0 represents the ground state wavefunction of the nucleon then the mean square radius of the nucleon will be expressed in the occupation number representation as

$$\langle r^2 \rangle = \frac{1}{A} \langle \Psi_0 | \Sigma r_i^2 | \Psi_0 \rangle$$

$$= \frac{1}{A}\sum_{ij} \langle r^2 \rangle_{ij}\, \rho_{ij} \qquad (2.7.2.2)$$

where $\langle r^2 \rangle_{ij}$ represents the matrix element of r^2 between single particle states i and j.

i.e. $$\langle r^2 \rangle_{ij} = \langle i | r^2 | j \rangle \delta_{ij} \qquad (2.7.2.3)$$

The operator r^2 also has non-zero matrix elements between oscillator shells differing in energy by $2\hbar\omega$ but this does not occur in our case and we have [52]

$$\langle r^2 \rangle_i = \langle nl | r^2 | nl \rangle$$

$$= (N_i + \frac{3}{2})\, b^2 \qquad (2.7.2.4)$$

where $N(=2n+l)$ is an oscillator quantum number and b is an oscillator length parameter.

Therefore from an equation (2.7.2.4), we get

$$\langle r^2 \rangle_{0s} = \frac{3}{2} b^2 \qquad (2.7.2.5)$$

and $$\langle r^2 \rangle_{0p} = \frac{5}{2} b^2 \qquad (2.7.2.6)$$

The diagonal matrix element of the single particle density matrix is given by

$$\rho_i = \langle \Psi_0 \mid a_i \dagger a_i \mid \Psi_0 \rangle \qquad (2.7.2.7)$$

defines the probability that the single particle orbit 'i' is occupied in the ground state of the nucleon Ψ_0.

The physical situation of the present system defining a nucleon is equivalent to a system comprised of 4 quarks and one hole (in a core under consideration), where a hole is treated as an anti-particle i.e an anti-quark. Keeping this idea in mind, using equation (2.7.2.2) we may express the root mean square radius of the nucleon as given by

$$\langle r^2 \rangle^{\frac{1}{2}} = \left[\frac{1}{A} \left\{ \sum_i \langle r^2 \rangle_i \rho_i + \sum_{\bar{i}} \langle r^2 \rangle_{\bar{i}} (3-\rho_{\bar{i}}) \right\} \right]^{\frac{1}{2}} \qquad (2.7.2.8)$$

where i stands for real single particle orbit and $\bar{i}$ comes for sea (ghost) single particle orbit. A will be defined as

$$A = \sum_i \rho_i + \sum_{\bar{i}} (3- \rho_{\bar{i}}) \qquad (2.7.2.9)$$

The density matrix element of filled sea orbit is 3 because of three colours and therefore the density matrix element of the hole-state will be 3 minus density of that particular orbit.

2.7.3 ROOT MEAN SQUARE CHARGE RADIUS

We define the mean square charge radius of the nucleon by an expression

$$\langle r^2 \rangle_{ch} = \frac{1}{e}\left[\sum_k e_q(k) \langle r^2 \rangle_k \rho_k\right] \qquad (2.7.31)$$

where k runs over all single particle diagonal matrix elements. Here e represents the total charge contained in the nucleon and e_q is the charge of the quark. The total charge 'e' held by the nucleon is defined as

$$e = \sum_k e_q\,(k)$$

$$= \sum_i (e_u^{(i)} \rho_i + e_d^{(i)} \rho_i) + \sum_{i^-} \left\{(3-\rho_{\bar{i}})e_{\bar{u}}^{(\bar{i})} + (3-\rho_{\bar{i}})e_{\bar{d}}^{(\bar{i})}\right\} \qquad (2.7.3.2)$$

The expression (2.7.3.1) for the mean square charge radius of the nucleon will be written elaborately as

$$\langle r^2 \rangle_{ch} = \frac{1}{e}\left\{\sum_i \left\{ e_u^{(i)} \rho_i \langle r^2 \rangle_i + e_d^{(i)} \rho_i \langle r^2 \rangle_i\right\}\right\}$$

$$+ \frac{1}{e}\left\{\sum_{\bar{i}} \left\{(3-\rho_{\bar{i}})e_{\bar{u}}^{(\bar{i})} \langle r^2 \rangle_{\bar{i}} + (3-\rho_{\bar{i}})e_{\bar{d}}^{(\bar{i})} \langle r^2 \rangle_{\bar{i}}\right\}\right\} \qquad (2.7.3.3)$$

2.7.4 CHARGE DENSITY AS A FUNCTION OF RADIAL DISTANCE

We work out the charge density of the nucleon using the expression

$$\rho_{ch}(r) = \sum_i e_q(i)\, \rho_i\, |\, \Phi_i\, |^2 \qquad (2.7.4.1)$$

where Φ_i is a normalised space-spin wavefunction of a quark

defined by the expression.

$$\Phi_{nljm}(r,\theta,\phi) = R_{nl}(r)\sum Y_{l\,m_l}(\theta,\phi)\,\chi_{s\,m_s}\langle l m_l\, s\, m_s | j m\rangle \qquad (2.7.4.2)$$

Here R_{nl} is a normalised radial wavefunction and $Y_{lm}(\theta,\phi)$ is a normalised angular wavefunction called the spherical harmonics. $\chi_{s\,m_s}$ is the spin wavefunction of the quark.

Since the possible values of j are $l \mp \frac{1}{2}$, the corresponding eigenfunction may be written as [66]

$$\Phi_{nlj=l+\frac{1}{2},\,m} = R_{nl}(r)\left\{\left(\frac{l+m+\frac{1}{2}}{2l+1}\right)^{\frac{1}{2}} Y_{l\,m-\frac{1}{2}}\chi_{\frac{1}{2}\,\frac{1}{2}} + \left(\frac{l-m+\frac{1}{2}}{2l+1}\right)^{\frac{1}{2}} Y_{l\,m+\frac{1}{2}}\chi_{\frac{1}{2}\,-\frac{1}{2}}\right\} \qquad (2.7.4.3)$$

$$\Phi_{nlj=l-\frac{1}{2},\,m} = R_{nl}(r)\left\{-\left(\frac{l-m+\frac{1}{2}}{2l+1}\right)^{\frac{1}{2}} Y_{l\,m-\frac{1}{2}}\chi_{\frac{1}{2}\,\frac{1}{2}} + \left(\frac{l+m+\frac{1}{2}}{2l+1}\right)^{\frac{1}{2}} Y_{l\,m+\frac{1}{2}}\chi_{\frac{1}{2}\,-\frac{1}{2}}\right\} \qquad (2.7.4.4)$$

We know that the normalised radial wavefunction of a particle in 0S shell is given by

$$R_{00}(r) = \frac{2}{\sqrt{\sqrt{\pi}\,b^3}}\; e^{-\frac{r^2}{2b^2}} \qquad (2.7.4.5)$$

and the normalised radial wavefunction of a particle in a 0p shell will be given by

$$R_{01}(r) = 2\sqrt{\frac{2}{3\sqrt{\pi}\,b^5}}\; r\; e^{-\frac{r^2}{2b^2}} \qquad (2.7.4.6)$$

The corresponding normalised angular wavefunctions (i.e the spherical harmonics) expressed in Cartesian co-ordinates representation [52]

are as follows;

$$Y_{00}(\hat{r}) = \frac{1}{\sqrt{4\pi}} \tag{2.7.4.7}$$

$$Y_{10}(\hat{r}) = \sqrt{\frac{3}{4\pi}}\ \frac{z}{r} \tag{2.7.4.8}$$

$$Y_{1\pm1}(\hat{r}) = \mp\sqrt{\frac{3}{8\pi}}\ \frac{x \pm iy}{r} \tag{2.7.4.9}$$

If we denote the spin wavefunction χ_{sm_s} that describe a state with spin angular mpmentum $s = \frac{1}{2}$ with z-component $+\frac{1}{2}$ and $-\frac{1}{2}$ by eigenvectors $\begin{pmatrix}1\\0\end{pmatrix}$ and $\begin{pmatrix}0\\1\end{pmatrix}$ respectively,then using equations (2.7.4.5) and (2.7.4.7) for $\Phi_{00\,\frac{1}{2}+\frac{1}{2}}$ in expression (2.7.4.3), we obtain

$$\Phi_{00\,\frac{1}{2}+\frac{1}{2}} = \frac{1}{\sqrt{(\sqrt{\pi}\,b)^3}}\ e^{-\frac{r^2}{2b^2}}\ \begin{pmatrix}1\\0\end{pmatrix} \tag{2.7.4.10}$$

$$\Phi_{00\,\frac{1}{2}-\frac{1}{2}} = \frac{1}{\sqrt{(\sqrt{\pi}\,b)^3}}\ e^{-\frac{r^2}{2b^2}}\ \begin{pmatrix}0\\1\end{pmatrix} \tag{2.7.4.11}$$

Therefore we get

$$\left|\Phi_{00\,\frac{1}{2}+\frac{1}{2}}\right|^2 = \frac{1}{(\sqrt{\pi}\,b)^3}\ e^{-\frac{r^2}{b^2}} \tag{2.7.4.12.a}$$

$$\left|\Phi_{00\,\frac{1}{2}-\frac{1}{2}}\right|^2 = \frac{1}{(\sqrt{\pi}\,b)^3}\ e^{-\frac{r^2}{b^2}} \tag{2.7.4.12.b}$$

Using expression (2.7.4.6) and (2.7.4.8) for $\Phi_{01\,\frac{1}{2}\pm\frac{1}{2}}$ in expression (2.7.4.4) we get

$$\Phi_{01\frac{1}{2}+\frac{1}{2}} = -\sqrt{\frac{2}{3\sqrt{\Pi^3}\,b^5}}\ e^{-\frac{r^2}{2b^2}}\left\{z\begin{pmatrix}1\\0\end{pmatrix} + (x+iy)\begin{pmatrix}0\\1\end{pmatrix}\right\} \tag{2.7.4.13}$$

$$\Phi_{01\frac{1}{2}-\frac{1}{2}} = -\sqrt{\frac{2}{3\sqrt{\Pi^3}\,b^5}}\ e^{-\frac{r^2}{2b^2}}\left\{(x-iy)\begin{pmatrix}1\\0\end{pmatrix} - z\begin{pmatrix}0\\1\end{pmatrix}\right\} \tag{2.7.4.14}$$

The corresponding modulus square of the wavefunction (single

particle probability density) will be given by

$$\left|\Phi_{01\,\frac{1}{2}+\frac{1}{2}}\right|^2 = \frac{2}{3\sqrt{\pi^3}\,b^5}\; r^2\; e^{-\frac{r^2}{b^2}} \qquad (2.7.4.15.a)$$

$$\left|\Phi_{01\,\frac{1}{2}-\frac{1}{2}}\right|^2 = \frac{2}{3\sqrt{\pi^3}\,b^5}\; r^2\; e^{-\frac{r^2}{b^2}} \qquad (2.7.4.15.b)$$

The normalized wavefunction $\Phi_{01\frac{3}{2}\pm\frac{3}{2}}$ can be calculated by using expression (2.7.4.6) and (2.7.4.8,9) in expression (2.7.4.3) and we get

$$\Phi_{01\frac{3}{2}+\frac{3}{2}} = -\frac{1}{\sqrt{b^5\sqrt{\pi^3}}}\;(x+iy)\; e^{-\frac{r^2}{2b^2}} \begin{pmatrix}1\\0\end{pmatrix} \qquad (2.7.4.16.a)$$

$$\Phi_{01\frac{3}{2}+\frac{1}{2}} = \frac{2}{\sqrt{3\sqrt{\pi^3}\;b^5}}\; e^{-\frac{r^2}{2b^2}} \left\{ z\begin{pmatrix}1\\0\end{pmatrix} - \frac{1}{2}(x+iy)\begin{pmatrix}0\\1\end{pmatrix} \right\} \qquad (2.7.4.16.b)$$

$$\Phi_{01\frac{3}{2}-\frac{1}{2}} = \frac{2}{\sqrt{3\sqrt{\pi^3}\;b^5}}\; e^{-\frac{r^2}{2b^2}} \left\{ \frac{1}{2}(x-iy)\begin{pmatrix}1\\0\end{pmatrix} + z\begin{pmatrix}0\\1\end{pmatrix} \right\} \qquad (2.7.4.16.c)$$

$$\Phi_{01\frac{3}{2}-\frac{3}{2}} = \frac{1}{\sqrt{b^5\sqrt{\pi^3}}}\;(x-iy)\; e^{-\frac{r^2}{2b^2}} \begin{pmatrix}0\\1\end{pmatrix} \qquad (2.7.4.16.d)$$

From the above expressions (2.7.4.16.a,b,c,d), we obtain

$$\left|\Phi_{01\,\frac{3}{2}+\frac{3}{2}}\right|^2 = \frac{1}{b^5\sqrt{\pi^3}}\;(r^2 - z^2)\; e^{-\frac{r^2}{b^2}} \qquad (2.7.4.17.a)$$

$$\left|\Phi_{01\,\frac{3}{2}+\frac{1}{2}}\right|^2 = \frac{1}{3\sqrt{\pi^3}\;b^5}\;(r^2 + 3z^2)\; e^{-\frac{r^2}{b^2}} \qquad (2.7.4.17.b)$$

$$\left|\Phi_{01\,\frac{3}{2}-\frac{1}{2}}\right|^2 = \frac{1}{3\sqrt{\pi^3}\;b^5}\;(r^2 + 3z^2)\; e^{-\frac{r^2}{b^2}} \qquad (2.7.4.17.c)$$

$$\left| \Phi_{01\,\frac{3}{2}-\frac{3}{2}} \right|^2 = \frac{1}{b^5\sqrt{\pi^3}} \left(r^2 - z^2 \right) e^{-\frac{r^2}{b^2}} \qquad (2.7.4.17.d)$$

The calculated single-particle probability density of the real states and ghost (sea) states are given in tables 4.13. Making use of expression (2.7.4.1), the charge density of the proton and of the neutron calculated with parameters set 3 are represented graphically by the plots shown in the fig. 4.6 and fig. 4.7 respectively. For comparison, the charge density of the nucleon has been calculated using different sets of parameters. The charge density of a proton and of a neutron for three given sets of parameters are shown in figures 4.8 and 4.9 respectively.

CHAPTER 3

EVALUATION OF THE MATRIX ELEMENTS OF THE TRANSITION POTENTIAL

3.1 INTRODUCTION

The Glasgow shell model programme [45] requires all the information about a hamiltonian in the form of pre-calculated two body matrix elements. Since the 'interaction' is one of the parts of the nuclear hamiltonian, we have to compute the matrix elements of the interaction between pairs of the quarks.

To work out the interaction between quarks, we will have to calculate the two body matrix elements of the transition potential. We add an operator H_1 to the potential 1.2 which switches intrinsic parity for distinguishing ghost quarks from real quarks. We, therefore, rewrite the transition potential 1.2 in the following form.

$$V_{q\to qq\bar{q}}(1,2)= K(\lambda_1.\lambda_2)\left[(\sigma_1.\frac{\mathbf{r}_{12}}{r^3}) + \frac{i}{2}(\sigma_1\times\sigma_2).\frac{\mathbf{r}_{12}}{r^3} + \frac{\sqrt{2}}{r}i(\sigma_1.\mathbf{P}_2)\right].H_1 \quad \ldots\ (3.1.1)$$

where K is a strength-constant of the potential, its values calculated with different parameters are given in table 4.3 and $\mathbf{r}_{12}$, the position vector, is given by

$$\mathbf{r}_{12} = \frac{1}{\sqrt{2}}(\mathbf{r}_1 - \mathbf{r}_2)$$

The given transition potential changes the nature of particle 1. The particle 2 will remain unchanged. For example, if we start with one real quark and one ghost quark then this potential will convert a ghost quark into a real quark, i.e an excitation of a quark from a sea to a real shell will take place. But if we initially have two real quarks then the transition potential will convert one real quark into a ghost quark, i.e a de-excitation of a quark from a real shell to the sea will take place provided there is a hole in a sea shell. Here we ignore the interactions between the quarks within the sea because the excitations due to such interactions are also associated with the excitations due to self polarisation of the vacuum which makes the situation more complicated as discussed in chapter 2.

It is clear from the above discussion that one state in a two body matrix element expression (3.3.2) must be different from the other three, i.e if one represents a sea quark, the other three must represent real quarks.

3.2 SINGLE PARTICLE WAVEFUNCTION

In the shell model, a single quark state is defined by a vector state $|\alpha>$ described in terms of quantum numbers as

$$|\alpha> = |n, l, j, m, f, c> \qquad (3.2.1)$$

In the present model, the single particle wavefunction (as described in chapter 2) will be given by

$$|\alpha> = |n, l, j, m, f, c, h> \qquad (3.2.2)$$

for a ghost quark ' h' is replaced by 'g'.

3.3 MATRIX ELEMENTS TO BE EVALUATED

The wavefunction of two-particle system with one particle in an orbit $|\alpha_1\rangle$ and the other in an orbit $|\alpha_2\rangle$ coupled to a total angular momentum J and isospin T is represented by

$$|\alpha_1, \alpha_2; JT\rangle \tag{3.3.1}$$

Therefore we write the two-body matrix element as given by

$$\langle \alpha_1, \alpha_2; JT | V | \alpha_3, \alpha_4; JT\rangle \tag{3.3.2}$$

We know that the nuclear hamiltonians may always be specified by their two body matrix elements in an angular momentum and isospin coupled representation. In this case the two quark states could also be coupled to a definite colour but we leave the colour uncoupled. Since we are dealing with quarks which are fermions, their two particles states $|\alpha_1, \alpha_2 ; JT\rangle$ and $|\alpha_3, \alpha_4; JT\rangle$ must be antisymmetrised and normalised. Therefore the general form of the matrix element M (to be evaluated) will be given by

$$M = (\alpha_1 , \alpha_2; JT|V_{q\to qq\bar{q}}(1,2)|\alpha_3, \alpha_4; JT) \tag{3.3.3}$$

where the interaction operator $V_{q\to qq\bar{q}}$ is a transition potential given in equation (3.1.1).

Here for our convenience i) we have adopted the convention (for identifying the particles) that in the two-particle state the set of quantum numbers written to the left represents the particle 1 and the one written to the right will represent the particle 2, ii) we have replaced bra and ket notations by round brackets on both ends of the matrix element to indicate the normalised and antisymmetrised two quark wavefunctions. We follow the notations of M.K.Pal [63] in which an antisymmetric two body state is represented by a ket with a round bracket $|\ )$ and an

unsymmetrised state is represented by a ket with an angle bracket | >. The symmetric state is supposed to be represented by a ket with a curly bracket | } .

The transition potential has the following three parts.

$$1) \quad V_1(1,2) = \left\{ (\sigma_1 . \frac{\mathbf{r}_{12}}{r^3}) . H_1 \right\} (\lambda_1 . \lambda_2) \tag{3.3.4}$$

$$2) \quad V_2(1,2) = \left\{ (\frac{i}{2} (\sigma_1 \times \sigma_2) . \frac{\mathbf{r}_{12}}{r^3}) . H_1 \right\} (\lambda_1 . \lambda_2) \tag{3.3.5}$$

$$3) \quad V_3(1,2) = \left\{ \frac{\sqrt{2}}{r} i (\sigma_1 . \mathbf{p}_2)) . H_1 \right\} (\lambda_1 . \lambda_2) \tag{3.3.6}$$

We will evaluate the matrix element of each part separately. Therefore the following matrix elements are required to be evaluated.

$$M_1 = (\alpha_1, \alpha_2; JT| V_1(1,2) |\alpha_3, \alpha_4; JT) \tag{3.3.7}$$

$$M_2 = (\alpha_1, \alpha_2; JT| V_2(1,2) |\alpha_3, \alpha_4; JT) \tag{33.8}$$

$$M_3 = (\alpha_1, \alpha_2; JT| V_3(1,2) |\alpha_3, \alpha_4; JT) \tag{3.3.9}$$

These correspond to the relation

$$M = K (M_1 + M_2 + M_3) \tag{3.3.10}$$

In these investigations we are considering three real shells $0S_{1/2}$, $0P_{1/2}$, $0P_{3/2}$ and three ghost shells (i.e sea shells) $0\bar{S}_{1/2}$, $0\bar{P}_{1/2}$ and $0\bar{P}_{3/2}$. Corresponding to these six shells, we require 1280 matrix elements altogether. We have evaluated the matrix elements according to the procedure as discussed below and summarised in figure (3.1).

3.3.a EVALUATION OF MATRIX ELEMENT M_1

We have the matrix element

$$M_1 = (\alpha_1, \alpha_2; JT|\ V_1|\alpha_3, \alpha_4; JT) \qquad (3.3.a.1)$$

where the operator V_1 given in equation (3.3.4) is

$$V_1(1,2) = \left\{(\sigma_1 . \frac{r_{12}}{r^3}).H_1\right\}(\lambda_1 . \lambda_2)$$

3.3.a.1 SYMMETRISATION OF THE OPERATOR

The operator V_1 is not symmetric with respect to an exchange of particle-labels $1 \leftrightarrow 2$. We make it symmetric with respect to an interchange of labels of the particles by rewriting it as,

$$V_1(1,2) = \left\{(\sigma_1 . \frac{r_{12}}{r^3}).H_1\right\}(\lambda_1 . \lambda_2) + \left\{(\sigma_2 . \frac{r_{21}}{r^3}).H_2\right\}(\lambda_2 . \lambda_1)$$

$$= \left\{(\sigma_1 . \frac{r_{12}}{r^3}).H_1 - (\sigma_2 . \frac{r_{12}}{r^3}).H_2\right\}(\lambda_1 . \lambda_2)$$

$$= \frac{1}{2}\left\{(H_1+H_2)(\sigma_1 - \sigma_2) . \frac{r_{12}}{r^3} + (H_1-H_2)(\sigma_1 + \sigma_2) . \frac{r_{12}}{r^3}\right\}(\lambda_1 . \lambda_2)$$

. . . . (3.3.a.1.1)

If we write

$$V_1 = \frac{1}{2}(A + B) \qquad (3.3.a.1.2)$$

then $$A = \left\{(H_1+H_2)(\sigma_1 - \sigma_2) . \frac{r_{12}}{r^3}\right\}(\lambda_1 . \lambda_2)$$

or $$A = O_1(\lambda_1 . \lambda_2) \qquad (3.3.a.1.3)$$

and $$B = \left\{(H_1-H_2)(\sigma_1 + \sigma_2) . \frac{r_{12}}{r^3}\right\}(\lambda_1 . \lambda_2)$$

or $$B = O'_1(\lambda_1 . \lambda_2) \qquad (3.3.a.1.4)$$

where O_1 and O'_1 are given by

$$O_1 = \left\{(H_1+H_2)(\sigma_1 - \sigma_2) . \frac{r_{12}}{r^3}\right\} \qquad (3.3.a.1.5)$$

and $$O_1' = \left\{ (H_1 - H_2)(\sigma_1 + \sigma_2).\frac{r_{12}}{r^3} \right\} \qquad (3.3.a.1.6)$$

Again for simplicity, we evaluate the matrix elements of operators A and B separately. If M_1' and M_1'' be the matrix elements of the operators A and B respectively, then we have

$$M_1 = \frac{1}{2}(M_1' + M_1'') \qquad (3.3.a.1.7)$$

We can evaluate M_1 after having evaluated the following matrix elements.

$$M_1' = (\alpha_1, \alpha_2; JT|\ A\ |\ \alpha_3, \alpha_4; JT) \qquad (3.3.a.1.8)$$

$$M_1'' = (\alpha_1, \alpha_2; JT|\ B\ |\ \alpha_3, \alpha_4; JT) \qquad (3.3.a.1.9)$$

The various steps of the procedure of their evaluation can be fairly understood from a schematic diagram shown in fig: 3.1.

As is clear from the diagram that first of all we separate the colour factor of the wavefunction from the other factors and evaluate it immediately. The matrix elements of the Intrinsic parity operator H are isolated in the same way and are calculated separately. At the next step, making use of the property of recoupling of four angular momenta we decompose the total angular momentum J into the orbital angular momentum L and spin angular momentum S. The transition potential does not contain an isospin operator and so the isospin can not change.. With the help of formulae obtained from the theory of angular momentum we express the matrix element in terms of reduced matrix elements of orbital and spin operators.

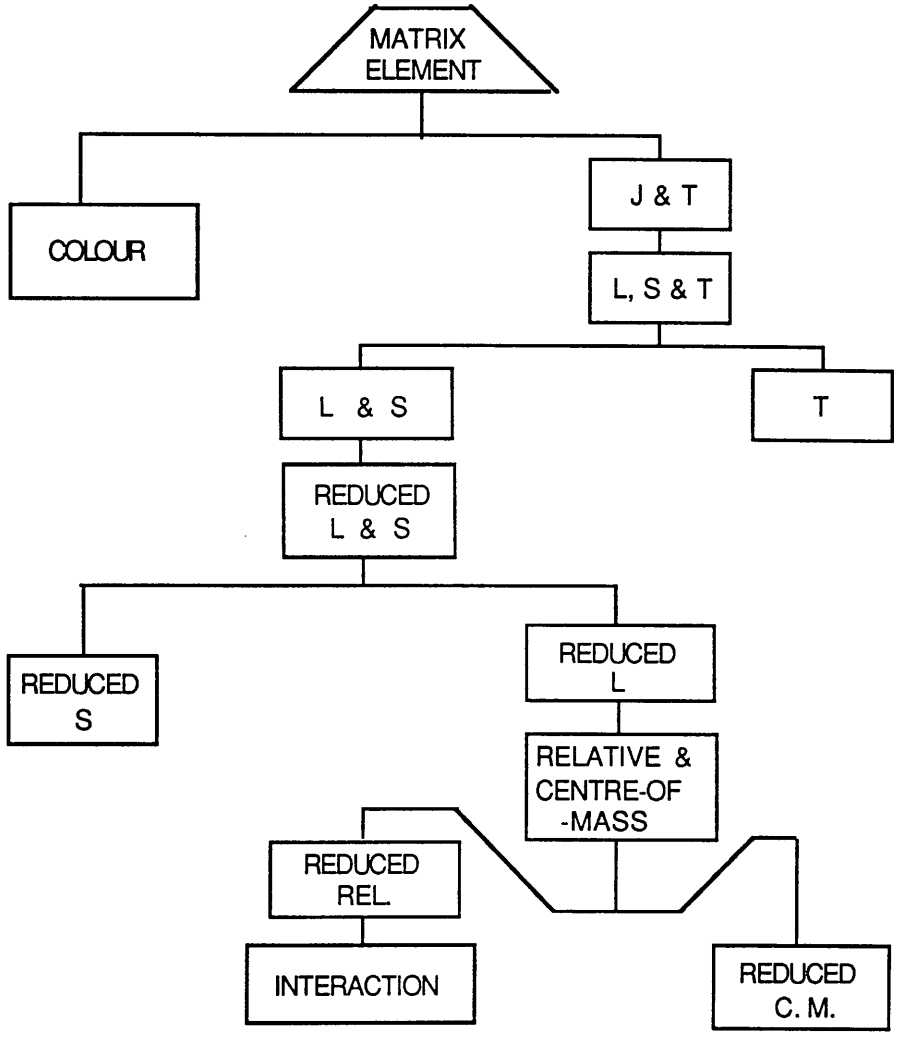

Fig. 3.1) Various steps of the procedure of evaluating matrix elements have been followed according to a scheme shown in the above diagram.

The orbital factor of the matrix element is further factorised by transforming the orbital co-ordinates into relative and centre-of-mass co-ordinates by making use of Moshinsky transformation brackets. The relative and centre-of-mass orbital momenta are then expressed in terms of their reduced matrix elements which are evaluated by using the relevant expressions derived in appendices A and B.

3.3.a.2 SEPARATION OF COLOUR WAVEFUNCTION

As each quark has spin of 1/2 and isospin of 1/2, so the wavefunction of the two quarks may be written with separated orbital and colour parts as,

$$|\alpha_1, \alpha_2; JT> = |\beta_1 c_1, \beta_2 c_2; JT >$$

where β includes all necessary quantum numbers describing a single particle state except colour. The matrix element M_1' will therefore be written as,

$$M_1' = (\beta_1 c_1, \beta_2 c_2; JT| A | \beta_3 c_3, \beta_4 c_4; JT) \qquad (3.3.a.2.1)$$

We know that the normalised antisymmetric wavefunction of the two quarks can be expressed in terms of orbital and colour wavefunctons.

i.e

$$|\beta_1 c_1, \beta_2 c_2; JT) = \frac{1}{\sqrt{2}}\Big[|\beta_1, \beta_2; JT)\ |c_1, c_2\}+ |\beta_1, \beta_2; JT\}\ |c_1, c_2)\Big] \qquad (3.3.a.2.2)$$

Making use of (3.3.a.2.2), we express M_1',the matrix element (3.3.a.2.1) as shown below.

$$(\beta_1 c_1, \beta_2 c_2; JT| A | \beta_3 c_3, \beta_4 c_4; JT) = \frac{1}{2}\Big[(\beta_1, \beta_2; JT|O_1|\beta_3, \beta_4; JT)\{c_1, c_2|\lambda_1.\lambda_2|c_3, c_4\}$$
$$+ (\beta_1, \beta_2; JT|O_1|\beta_3, \beta_4; JT\}\ \{c_1, c_2|\ \lambda_1.\ \lambda_2|c_3, c_4)$$

$$+ \{\beta_1, \beta_2;\ JT|O_1|\beta_3, \beta_4;\ JT)\ (c_1, c_2|\ \lambda_1.\ \lambda_2|c_3, c_4\}$$

$$+ \{\beta_1, \beta_2;\ JT|O_1|\beta_3, \beta_4;\ JT\}\ (c_1, c_2|\lambda_1.\ \lambda_2|c_3, c_4)\Big] \quad \ldots\ (3.3.a.2.3)$$

Since the SU(3) colour operator $(\lambda_1.\lambda_2)$ is symmetric, we have

$$\{c_1, c_2|\ \lambda_1.\ \lambda_2|c_3, c_4) = (c_1, c_2\ |\ \lambda_1.\lambda_2|c_3, c_4\} = 0$$

Hence the expression (3.3.a.2.3) reduces to,

$$M_1' = \frac{1}{2}\Big[(\beta_1, \beta_2;\ JT|O_1|\beta_3, \beta_4;\ JT)\ \{c_1, c_2|\lambda_1.\ \lambda_2\ |c_3, c_4\}$$

$$+ \{\beta_1, \beta_2;\ JT|O_1|\beta_3, \beta_4;\ JT\}\ (c_1, c_2|\lambda_1.\ \lambda_2|c_3, c_4)\Big] \quad \ldots\ (3.3.a.2.4)$$

provided $\beta_1 \neq \beta_2$, $\beta_3 \neq \beta_4$ and $c_1 \neq c_2$, $c_3 \neq c_4$.

At this stage,for simplicity we consider only the colour matrix elements to be normalised and symmetrised. The normalised and symmetrised colour wavefunctions of the two quarks are given by

$$|c_1, c_2) = \frac{1}{\sqrt{2}}\Big[|c_1, c_2> - |c_2, c_1>\Big] \quad \text{if } c_1 \neq c_2$$

$$= 0 \qquad \text{if } c_1 = c_2$$

and $$|c_1, c_2\} = \frac{1}{\sqrt{2}}\Big[|c_1, c_2> + |c_2, c_1>\Big] \qquad \text{if } c_1 \neq c_2$$

$$= |c_1, c_2> \quad \text{if } c_1 = c_2$$

The colours of the two quarks may either be the same or they may be different. If we have $c_1 = c_2$ or $c_3 = c_4$, then $(c_1,c_2|\lambda_1.\lambda_2|c_3,c_4)$ becomes zero and we are left with only the 1st term of the (3.3.a.2.4).

i.e $$M_1' = \frac{1}{2}\Big[(\beta_1,\beta_2;\ JT|O_1|\beta_3,\beta_4;\ JT)\ \{c_1,c_2|\lambda_1.\ \lambda_2|c_3,c_4\}\Big] \qquad (3.3.a.2.5)$$

Generally we consider the following possibilities of the colour combinations in the matrix elements,

i) $<c_i, c_i\ |\ V_c\ |\ c_j, c_j> = 0 \qquad \text{if } i \neq j$

and ii) $<c_i, c_j|\ V_c|\ c_i, c_j> = <c_j, c_k|\ V_c|c_j, c_k> = <c_i, c_k|\ V_c|c_i, c_k>$

for $\{i,j,k\} = \{1,2,3\}$, where $V_c = \sum_{i<j} (\lambda_i . \lambda_j)$. The SU(3) colour operators λ_i^{α} (α = 1,2,3 . . . 8) are normalised such that $(\lambda_i . \lambda_i) = \sum_{\alpha=1}^{8} \lambda_i^{\alpha} . \lambda_i^{\alpha}$. We have made use of Casmir's operator F^2 ($F_i = \frac{1}{2}\lambda_i$) to obtain the expectation value $<(\lambda_1 . \lambda_2)>$ from the expression,

$$\lambda_1 . \lambda_2 = \frac{1}{2}\left\{(\lambda_1 + \lambda_2)^2 - \lambda_1^2 - \lambda_2^2\right\} \qquad (3.3.a.2.6)$$

The magnitudes of Casmir's operators F^2 for some common SU(3) representations are given in ref. [7(a)].

Usually the entire matrix element is just multiplied by the expectation value,

$<(\lambda_1 . \lambda_2)>_{(\lambda\mu)} = -\frac{2}{3}$ for colour antisymmetric pairs of $(\lambda\mu) = (01)$ and $<(\lambda_1 . \lambda_2)>_{(\lambda\mu)} = +\frac{1}{3}$ for the symmetric pairs of $(\lambda\mu) = (20)$.

According to our assumption, we are considering the matrix elements $(\beta_1,\beta_2;JT|O_1|\beta_3,\beta_4;JT)$ with two-quark wavefunctions containing either one ghost-quark state and three real-quark states or three ghost-quark states and one real-quark state.i.e If β_1 represents the state of a ghost quark then β_2, β_3 and β_4 must represent the states of real quarks and if $\beta_1$represents the state of real quark then β_2, β_3 and β_4 must represent the states of ghost quarks. But for simplicity, we have ignored the second possibility and therefore now we are left with the matrix element between quark states $|\beta'_1 g, \beta'_2 h; JT)$ and $|\beta'_3 h, \beta'_4 h; JT)$ only.

3.3.a.3 SEPARATION OF INTRINSIC PARITY WAVEFUNCTION

Using expression similar to expression (3.3.a.2.2) for intrinsic parity, we obtain

$$(\beta'_1 g,\ \beta'_2 h;\ JT|O_1|\beta'_3 h,\beta'_4 h;\ JT)=\frac{1}{2}\Big[(\beta'_1,\beta'_2;\ JT|Op|\beta'_3,\beta'_4;\ JT)\ \{gh|H_1+H_2|hh\}$$
$$+\ (\beta'_1,\beta'_2;\ JT|Op|\beta'_3,\beta'_4;\ JT\}\ \{gh|H_1+H_2|hh)$$
$$+\ \{\beta'_1,\beta'_2;\ JT|Op|\beta'_3,\beta'_4;\ JT)\ (gh|H_1+H_2|hh\}$$
$$+\ \{\beta'_1,\beta'_2;\ JT|Op|\beta'_3,\beta'_4;\ JT\}\ (gh|H_1+H_2|hh)\Big]$$

. . . . (3.3.a.3.1)

where β' includes the quantum numbers required to define a single particle state (as given in expression 3.2.2) except colour and intrinsic parity..

By definition we have ,

$$H|\ h>=g \quad \text{and} \quad H|\ g>=-h \qquad (3.3.a.3.2.i)$$

$$<h\ |\ h>=<g\ |\ g>=1 \qquad (3.3.a.3.2.ii)$$

$$<h\ |\ g>=<g\ |\ h>=0 \qquad (3.3.a.3.2.iii)$$

Using the above properties one finds

$$(g\ h\ |(H_1+H_2)|\ h\ h\}=0$$
$$\{g\ h\ |(H_1+H_2)|\ h\ h\}=\sqrt{2}$$
$$(g\ h\ |(H_1-H_2)|\ h\ h\}=\sqrt{2}$$
$$\{g\ h\ |(H_1-H_2)|\ h\ h\}=0$$

Since the antisymmetric wavefunction | h h) also yields zero value, we obtain the matrix element (3.3.a.3.1) with 1st term left only, i.e.

$$(\beta'_1 g,\ \beta'_2 h;\ JT|O_1|\beta'_3 h,\ \beta'_4 h;\ JT)=\frac{1}{2}\Big[(\beta'_1,\ \beta'_2;\ JT|Op|\beta'_3,\ \beta'_4;\ JT)\times\sqrt{2}\Big]$$
$$=\frac{1}{\sqrt{2}}(\beta'_1,\ \beta'_2;\ JT|Op|\beta'_3,\ \beta'_4;\ JT)$$

. . . . (3.3.a.3.3)

where $Op=(\sigma_1-\sigma_2)\cdot\frac{r_{12}}{r^3}$.

3.3.a.4 NORMALISATION AND ANTISYMMETRISATION OF WAVEFUNCTIONS

We know that the shell model needs properly normalised and antisymmetrised wavefunction of 2-body coupled states defined by [63],

$$|\beta'_1, \beta'_2; JT\rangle = \left[2(1+\delta_{\beta'_1\beta'_2})\right]^{-\frac{1}{2}} \left[|\beta'_1, \beta'_2; JT\rangle - (-1)^{j_1+j_2-J+1-T} |\beta'_2, \beta'_1; JT\rangle\right] \quad \ldots . \text{(3.3.a.4.1)}$$

$$|\beta'_1, \beta'_2; JT\} = \left[2(1+\delta_{\beta'_1\beta'_2})\right]^{-\frac{1}{2}} \left[|\beta'_1, \beta'_2; JT\rangle + (-1)^{j_1+j_2-J+1-T} |\beta'_2, \beta'_1; JT\rangle\right] \quad \ldots . \text{(3.3.a.4.2)}$$

where the numerical factor $\left[2(1+\delta_{\beta'_1\beta'_2})\right]^{-\frac{1}{2}}$ is the normalisation constant. The phase factor $(-1)^{j_1+j_2-J+1-T}$ comes from the symmetry properties of the Clebsch Gordan Coefficients;

$$\langle j_1 m_1, j_2 m_2 \mid JM\rangle = (-1)^{j_1+j_2-J} \langle j_2 m_2, j_1 m_1 \mid JM\rangle$$

$$\langle T_1 t_{31}, T_2 t_{32} \mid TM_T\rangle = (-1)^{T_1+T_2-T} \langle T_2 t_{32}, T_1 t_{31} \mid TM_T\rangle$$

Therefore the matrix element between the two normalised antisymmetric states of two quarks is given by,

$$\begin{aligned}(\beta'_1, \beta'_2; JT|Op|\beta'_3, \beta'_4; JT) = \frac{1}{2}\Big[\Big\{(1+\delta_{\beta'_1\beta'_2})(1+\delta_{\beta'_3\beta'_4})\Big\}^{-\frac{1}{2}} \Big\{&\langle\beta'_1, \beta'_2; JT|Op|\beta'_3, \beta'_4; JT\rangle \\ &+ (-1)^{j_3+j_4-J-T} \langle\beta'_1, \beta'_2; JT|\, Op|\beta'_4, \beta'_3; JT\rangle \\ &+ (-1)^{j_1+j_2-J-T} \langle\beta'_2, \beta'_1; JT|\, Op|\beta'_3, \beta'_4; JT\rangle \\ &+ (-1)^{j_1+j_2+j_3+j_4} \langle\beta'_2, \beta'_1; JT|\, Op|\beta'_4, \beta'_3; JT\rangle\Big\}\Big]\end{aligned} \quad \ldots \text{(3.3.a.4.3)}$$

It may be noted that, in (3.3.a.4.3) the first matrix element corresponds to a transition of the first quark from $\beta'_3 \rightarrow \beta'_1$ and that of the second quark from $\beta'_4 \rightarrow \beta'_2$. It may also be observed that, in the last matrix element of (3.3.a.4.3) the second quark goes from $\beta'_3 \rightarrow \beta'_1$ and the first quark from $\beta'_4 \rightarrow \beta'_2$.It should be remembered that the set of quantum numbers written in the first location in the two- particle state comes for particle 1 and the one written in the second place comes for particle 2. We can re-label the quarks by exchanging $1 \leftrightarrow 2$. The operator Op is not affected by the exchange because it is symmetric with respect to the particle-labels,whereas the two-particle states get changed.If we reverse the order of the coupling in the states $|\beta'_4, \beta'_3; JT\rangle$ and $|\beta'_2, \beta'_1; JT\rangle$ of the last matrix element in (3.3.a.4.3), they change to the new states $|\beta'_3, \beta'_4; JT\rangle$ and $|\beta'_1, \beta'_2; JT\rangle$ with phase factors $(-1)^{j_3+j_4-J+1-T}$ and $(-1)^{j_1+j_2-J+1-T}$ respectively. The phase factors cancel out with $(-1)^{j_1+j_2+j_3+j_4}$ already contained in the last term and the matrix element between the new states is obviously the same as the matrix element in the first term. Similarly we can get the matrix elements in the second and third terms of (3.3.a.4.3) to be equal with same phase factor. Now if the equal terms are added up, the factor 1/2 at the beginning gets cancelled and finally we get,

$$(\beta'_1, \beta'_2; JT|\, Op|\beta'_3, \beta'_4; JT) = \left\{ (1+\delta_{\beta'_1\beta'_2})(1+\delta_{\beta'_3\beta'_4}) \right\}^{-\frac{1}{2}} \Big[\langle \beta'_1, \beta'_2; JT|Op|\beta'_3, \beta'_4; JT\rangle + (-1)^{j_3+j_4-J-T} \langle \beta'_1, \beta'_2; JT|\, Op'|\beta'_4, \beta'_3; JT\rangle \Big] \quad \ldots . \text{(3.3.a.4.4)}$$

The first term of (3.3.a.4.4) is usually called the direct term and the second term the exchange term. It shows that the matrix

element of the two-body potential between antisymmetric states is the combination of direct and exchange terms.

To evaluate the matrix element of Op between two antisymmetric states (shown in 3.3.a.4.4), we shall compute its two terms separately. In (3.3.a.4.4) the numerical factor say N is given by

$$N = \left\{(1+\delta_{\beta'_1\beta'_2})(1+\delta_{\beta'_3\beta'_4})\right\}^{-\frac{1}{2}}$$

where $\delta_{\beta'_1\beta'_2} = \delta_{n_1n_2}\,\delta_{l_1l_2}\,\delta_{j_1j_2}$

Therefore
$$N = 1 \quad \text{if } \beta'_1 \neq \beta'_2 \text{ and } \beta'_3 \neq \beta'_4$$
$$= \frac{1}{\sqrt{2}} \quad \text{if either } \beta'_1 = \beta'_2 \text{ and } \beta'_3 \neq \beta_4$$
$$\text{or} \quad \beta'_1 \neq \beta'_2 \text{ and } \beta'_3 = \beta'_4$$
$$= \frac{1}{2} \quad \text{if } \beta'_1 = \beta'_2 \text{ and } \beta'_3 = \beta'_4$$

The given operator $Op = (\sigma_1 - \sigma_2).\frac{\mathbf{r}_{12}}{r_3}$ is a scalar and it does not change the total angular momentum J. Therefore we can only have the nonvanishing matrix elements between states with the same value of J and M.

3.3.a.5 CONFIGURATIONS

As we know that the shell model single-particle level is specified by quantum numbers (nljm). The quantum number m is usually not shown because all states with the same value of nlj but different values of m (m=-j,-j+1,-j+2, . . ,j-1,j) are degenerate (i.e the set of degenerate (2j+1) states |nljm> is referred as a level (nlj). Therefore the matrix element given in the

first term of (3.3.a.4.4), say $(ME)'_1$ will be written as

$(ME)'_1 = \langle \beta'_1, \beta'_2; JT | Op | \beta'_3, \beta'_4; JT \rangle$

$$= \langle n_1 l_1 j_1 t_{31}, n_2 l_2 j_2 t_{32}; JMTM_T | (\sigma_1 - \sigma_2) . \frac{r_{12}}{r^3} | n_3 l_3 j_3 t_{33}, n_4 l_4 j_4 t_{34}; JMTM_T \rangle$$

. . . . (3.3.a.5.1)

If the same level is occupied by k particles, then the shorthand notation $(nlj)^K$ is used to represent that particular configuration instead of writing quantum numbers (nlj) k times repeatedly.

Since the configuration is denoted by its occupied levels, the two-particle coupled state, when i) both of them are in the same orbit, will be denoted by $|(nlj)^2; JT\rangle$ and ii) when each of them has occupied a different orbit, will be denoted by $|(nlj)(n'l'j'); JT\rangle$.

3.3.a.6 TOTAL ANGULAR MOMENTUM AND ISOSPIN (J,T) COMBINATIONS

For particles in the same configuration (i.e in the same orbit), the Pauli exclusion principle restricts the set of J,T that may occur. For example; we have two particles in the same orbit say 0S,each one characterised by j=1/2 and t=1/2. The values of the total angular momentum J and isospin T will be obtained from the vector addition $J=j_1+j_2$ and $T=t_1+t_2$, and we get J=0 or 1 and T=0 or 1. Therefore the 4 possible values of (J,T) combinations for the two-particle system under consideration will be (0,0), (0,1),(1,0) and (1,1).

In order to get a complete wavefunction of two particles to be antisymmetric under the exchange of all co-ordinates of the two particles, we have to combine a symmetric space-spin

wavefunction with an antisymmetric isospin function or vice versa. Therefore only the (J,T) combinations (0,1) and (1,0) are allowed. From the above discussion we conclude that one can obtain the allowed two-particle antisymmetric states $|(nlj)^2;JT>$ only for J plus T equal to odd. But a two-particle state, with two particles in different orbits can always be antisymmetrised for any combination of the total J and T values.

As a consequence of the Pauli exclusion principle, the allowed values of (J,T) combinations for two particles in the S-shell and p-shells have been given in a Table(3.1) given below.

TABLE 3.1

ALLOWED COMBINATIONS OF J AND T.

Configuration	Allowed (J,T)-combinations
$(0S_{1/2})^2$	(0,1) and (1,0)
$(0P_{1/2})^2$	(0,1) and (1,0)
$(0P_{3/2})^2$	(0,1), (2,1), (1,0) and (3,0)
$(0S_{1/2}, 0P_{1/2})$	(0,1) and (1,0)
$(0P_{1/2}, 0P_{3/2})$	(1,1), (2,1), (1,0) and (2,0)

3.3.a.7 SEPARATING J AND T

Since the operator is independent of isospin, the isospin quantum number of the states may be ignored at this stage and we write the matrix element (3.3.a.5.1) as

$$(ME)'_1 = \langle n_1 l_1 j_1 , n_2 l_2 j_2; JM | (\sigma_1 - \sigma_2).\frac{r_{12}}{r^3} | n_3 l_3 j_3, n_4 l_4 j_4 ; JM\rangle \qquad (3.3.a.7.1)$$

3.3.a.8 TRANSFORMATION OF JJ-COUPLING INTO LS-COUPLING

In matrix element (3.3.a.7.1) the four angular momenta have been coupled as follows;

$$l_1 + s_1 = j_1 \ , \ l_2 + s_2 = j_2 \quad \text{and then} \quad j_1 + j_2 = J \qquad (3.3.a.8.1)$$

This scheme is known as jj- coupling scheme.

To obtain J,the total angular momentum of a two-particle system, we can also couple them according to the following scheme, called LS-coupling scheme.

$$l_1 + l_2 = \Lambda \ , \ s_1 + s_2 = S \quad \text{and then} \quad \Lambda + S = J \qquad (3.3.a.8.2)$$

There exists a unitary transformation that transforms from the set of functions $|(n_1 n_2), \{(l_1 s_1)j_1, (l_2 s_2)j_2\}; JM\rangle$ to the set of functions $|(n_1 n_2),\{(l_1 l_2)\Lambda,(s_1 s_2)S\};JM\rangle$. The transformation coefficients between jj-coupling scheme and LS-coupling scheme is given [67] by,

$$\langle (n_1 n_2), \{(l_1 l_2)\ \Lambda, (s_1 s_2)S\ \}; J \mid (n_1\ n_2), \{(l_1 s_1)j_1\ ,(l_2\ s_2\ )j_2\}; J\rangle$$

$$= \left[(2\Lambda+1)(2S+1)(2j_1+1)(2j_2+1)\right]^{\frac{1}{2}} \begin{Bmatrix} l_1 & l_2 & \Lambda \\ s_1 & s_2 & S \\ j_1 & j_2 & J \end{Bmatrix} \qquad (3.3.a.8.3)$$

where curly bracketed factor is called Wigner's 9j symbol.

Therefore we can express jj-coupled state of two quarks in terms of LS-coupled state of two quarks by recoupling four angular momenta using the Wigner's 9j symbol as follows;

$$|(n_1 n_2)\{(l_1 s_1) j_1, (l_2 s_2) j_2\}; JM> = \sum_{\Lambda S} \Big[\big[(2\Lambda+1)(2S+1)(2j_1+1)(2j_2+1)\big]^{\frac{1}{2}} \times \begin{Bmatrix} l_1 & l_2 & \Lambda \\ s_1 & s_2 & S \\ j_1 & j_2 & J \end{Bmatrix} |(n_1 n_2), \{(l_1 l_2)\Lambda, (s_1 s_2)S\}; JM> \Big]$$

. . . . (3.3.a.8.4)

The given matrix element $(ME)'_1$ will be written between the LS-coupled states of two quarks as shown below.

$$(ME)'_1 = \sum_{\substack{\Lambda S \\ \Lambda' S'}} \Big[\Big[\{(2\Lambda'+1)(2S'+1)(2j_3+1)(2j_4+1)\}\{(2\Lambda+1)(2S+1)(2j_1+1)(2j_2+1)\} \Big]^{\frac{1}{2}} \times \begin{Bmatrix} l_3 & l_4 & \Lambda' \\ s_3 & s_4 & S' \\ j_3 & j_4 & J \end{Bmatrix} \begin{Bmatrix} l_1 & l_2 & \Lambda \\ s_1 & s_2 & S \\ j_1 & j_2 & J \end{Bmatrix}$$

$$\times <(n_1 n_2), \{(l_1 l_2)\Lambda, (s_1 s_2)S\}; JM \left| (\sigma_1 - \sigma_2).\frac{r_{12}}{r^3} \right| (n_3 n_4), \{(l_3 l_4)\Lambda', (s_1 s_2)S'\}; JM> \Big]$$

. . . (3.3.a.8.5)

Where for the present case we have S'= 0,1 and S= 0,1. The values of Λ' and Λ depend upon the configurations (i.e location of the quarks in the orbits). The orbital angular momentum l is 0 and 1 for s-shell and p-shell respectively. Therefore the values of Λ' and Λ, the total orbital angular momenta of two quarks will be 0,1,2. The possible values of J has already been given in Table 3.1. The formulae and expressions used for evaluating Wigner's 9j-symbol have been given in refs. [52,65,67].

3.3.a.9 TRANSFORMATION OF THE MATRIX ELEMENT INTO L AND S REDUCED MATRIX ELEMENTS

We know that the matrix element (3.3.a.8.5) of a scalar product of two tensors $(\sigma_1 - \sigma_2).\frac{\mathbf{r}_{12}}{r^3}$ between LS-coupled states is given [65] by

$$\langle (n_1 n_2), \{\Lambda\ S\};\ JM \left| (\sigma_1 - \sigma_2).\frac{\mathbf{r}_{12}}{r^3} \right| (n_3 n_4), \{\Lambda'\ S'\};\ JM \rangle$$

$$= (-1)^{\Lambda' + S + J} \begin{Bmatrix} J & S & \Lambda \\ 1 & \Lambda' & S' \end{Bmatrix} \langle S \,||(\sigma_1 - \sigma_2)||\, S' \rangle$$

$$\times \langle (n_1 n_2)\Lambda \,||\, \frac{\mathbf{r}_{12}}{r^3} \,||\, (n_3 n_4)\Lambda' \rangle \qquad (3.3.a.9.1)$$

Here the double-bar matrix elements are called reduced matrix elements which are independent of magnetic quantum number.The matrix element $\langle S \,||(\sigma_1 - \sigma_2)||\, S' \rangle$ has been evaluated in the appendix B. Here the curly bracketed factor are called Wigner's 6j-symbols. They have been tabulated in reference [52].

Now we evaluate the radial and orbital part of the matrix element (3.3.a.9.1), which is given by

$$(ME)_{orb.} = \langle (n_1 n_2)\Lambda \,||\, \frac{\mathbf{r}_{12}}{r^3} \,||\, (n_3 n_4)\Lambda' \rangle$$

$$= \langle (n_1 l_1),\ (n_2 l_2);\ \Lambda \,||\, \mathbf{r}_{12}/r^3 \,||\, (n_3 l_3),\ (n_4 l_4);\ \Lambda' \rangle \qquad (3.3.a.9.2)$$

3.3.a.10 TRANSFORMATION INTO RELATIVE AND CENTRE-OF-MASS CO-ORDINATES

In most of the calculations for evaluating matrix elements of the interaction potentials in nuclear shell theory e.g. [70], the co-ordinates $\mathbf{r}_1$, $\mathbf{r}_2$ of the two-particle wavefunctions in the

harmonic oscillator potential have been transformed into co-ordinates **r**, **R** corresponding to the relative and centre of mass motions respectively by making use of transformation brackets [71,72].

To achieve a sound understanding about such a transformation we start with as follows;

If we have a particle in a harmonic oscillator potential, its wavefunction is written as,

$$|nlm\rangle = R_{nl}(r)\, Y_{lm}(\theta,\phi) \qquad (3.3.a.10.1)$$

Where $R_{nl}(r)$ is its radial function and $Y_{lm}(\theta,\phi)$ is a spherical harmonic.

If r is taken in units of $\sqrt{\frac{\hbar}{mw}}$, the radial function is [71]

$$R_{nl}(r) = \sqrt{\frac{2\,n!}{\Gamma(n+l+\frac{3}{2})}}\; r^{l}\; e^{-\frac{r^2}{2}}\; L_n^{l+\frac{1}{2}}(r^2) \qquad (3.3.a.10.2)$$

where $L_n^{l+\frac{1}{2}}$ is a laguerre polynomial as defined in ref. [68,69].

Therefore the two-particle wavefunction with states coupled to total angular momentum Λ is then given by

$$|n_1 l_1,\, n_2 l_2;\, \Lambda\mu\rangle = \sum_{m_{l_1} m_{l_2}} [(l_1 m_{l_1},\, l_2 m_{l_2} | \Lambda\mu)\, R_{n_1 l_1}(r_1)\, Y_{l_1 m_{l_1}}(\theta_1,\phi_1)\, R_{n_2 l_2}(r_2)\, Y_{l_2 m_{l_2}}(\theta_2,\phi_2)$$

. . . . (3.3.a.10.3)

If we now introduce the relative and centre-of-mass co-ordinates by defining them,

$$\mathbf{r} = \frac{1}{\sqrt{2}}(\mathbf{r}_1 - \mathbf{r}_2) \quad \text{and} \quad \mathbf{R} = \frac{1}{\sqrt{2}}(\mathbf{r}_1 + \mathbf{r}_2), \qquad (3.3.a.10.4)$$

we can express the two-particle wavefunction with same angular momentum Λ in terms of relative and centre-of-mass co-ordinates

$$|nl,\, NL;\, \Lambda\mu\rangle = \sum_{m_l m_L} [(lm_l,\, Lm_L | \Lambda\mu)\, R_{nl}(r)\, Y_{lm_l}(\theta,\phi)\, R_{NL}(R)\, Y_{Lm_L}(\theta,\phi)$$

. . . . (3.3.a.10.5)

where $(l_1 m_{l_1}, l_2 m_{l_2} | \Lambda\mu)$ in (3.3.a.10.3) and $(lm_l, Lm_L | \Lambda\mu)$ in (3.3.a.10.5) are Clebsch-Gordan Coefficients. In (3.3.a.10.5) the quantum numbers nl,NL correspond to relative motion and centre-of-mass motion respectively.

A relation between the wavefunction for two particles in the harmonic oscillator potential with the wavefunction associated with the relative and centre-of-mass co-ordinates for the same two particles is given by;

$$|n_1 l_1, n_2 l_2; \Lambda\mu\rangle = \sum_{nlNL} |nl, NL; \Lambda\mu\rangle\langle nl,NL; \Lambda|n_1 l_1, n_2 l_2; \Lambda\rangle \quad \ldots . \quad (3.3.a.10.6)$$

Here the coefficients $\langle nl,NL;\Lambda|n_1 l_1, n_2 l_2;\Lambda\rangle$ are called Brody -Moshinsky transformation brackets [71,72].

Because of conservation of energy, both the kets in expression (3.3.a.10.6) correspond to the same energy and the values of nlNL are restricted to the positive integers such that

$$\rho = 2n_1+l_1 +2n_2+l_2 = 2n + l +2N + L \quad (3.3.a.10.7)$$

the quantity ρ is called the energy index of the two-particle system.

The transformation bracket will only be non-zero if it satisfies the energy condition (3.3.a.10.7) and also taking into account that

$$l_1+l_2 = \Lambda = l+L \quad (3.3.a.10.8)$$

The condition (3.3.a.10.7) guarantees also the validity of conservation of parity in the wavefunction as,

$$(-1)^{l_1+l_2} = (-1)^{l+L}$$

Making use of the transformation (3.3.a.10.6), we can express the matrix element (3.3.a.9.2) in terms of relative and centre -of-mass co-ordinates as,

$$<(n_1l_1),\ (n_2l_2);\ \Lambda\| \frac{r_{12}}{r^3} \| (n_3l_3),\ (n_4l_4);\ \Lambda>$$

$$= \sum_{\substack{nlNL \\ n'l'N'L'}} \Big[<nl,\ NL;\ \Lambda|n_1l_1,\ n_2l_2;\ \Lambda><n'l',\ N'L';\ \Lambda'\ |n_3l_3,\ n_4l_4;\ \Lambda'>$$

$$\times <nl,\ NL;\ \Lambda|| \frac{r_{12}}{r^3} || n'l',\ N'L';\ \Lambda'> \Big] \qquad (3.3.a.10.9)$$

There exist many symmetry relations between transformation brackets e.g [71],

$$<nl,NL;\ \Lambda|n_1l_1,\ n_2l_2;\ \Lambda> = (-1)^{L-\Lambda} <nl,\ N\ L;\ \Lambda|n_2l_2,\ n_1l_1;\ \Lambda>$$

$$= (-1)^{l_1-\Lambda} <NL,\ nl;\ \Lambda|\ n_1l_1,\ n_2l_2;\ \Lambda>$$

$$= (-1)^{l_1+l} <NL,\ nl;\ \Lambda|\ n_2l_2\ ,\ n_1l_1;\ \Lambda> \quad \text{etc.}$$

. . . . (3.3.a.10.10)

The values of transformation brackets have been tabulated in ref. [72] for all cases required in the calculations of shell model wavefunctions and the matrix elements of the nuclear shell theory. The transformation bracket will be zero for all combinations of its parameters n,l,N,L and n_1,l_1,n_2,l_2 which do not satisfy the energy condition (3.3.a.10.7) and the condition (3.3.a.10.8) for conservation of total angular momentum of the two body system.

3.3.a.11 EVALUATION OF $<nl,\ NL;\ \Lambda|| \frac{r_{12}}{r^3} || n'l',\ N'L';\ \Lambda>$

As we know that the interaction V(r) betwen two quarks depends only on the magnitudes of the relative co-ordinates, therefore the operator in (3.3.a.10.9) operates on part 1 in a coupled state $|nl,NL;\ \Lambda>$ and we have [65],

$$<nl,\ NL;\ \Lambda|| \frac{r_{12}}{r^3} || n'l',\ N'L';\ \Lambda'>= (-1)^{l+L+\Lambda'+1}[(2\Lambda+1)(2\Lambda'+1)]^{\frac{1}{2}} \begin{Bmatrix} l & \Lambda & L \\ \Lambda' & l' & 1 \end{Bmatrix}$$

$$\times \langle nl \,||\, \frac{r_{12}}{r^3} \,||\, n'l' \rangle \delta_{NN'} \, \delta_{LL'} \qquad (3.3.a.11.1)$$

r_{12} is a tensor operator of rank 1 and negative parity. Conservation of angular momentum requires l'= l+1, l or l-1 and conservation of parity does not allow l' = l. Here l'=l+1 or l-1 only.

The following reduced matrix element

$$\langle nl \,||\, \frac{r_{12}}{r^3} \,||\, n'l' \rangle \qquad (3.3.a.11.2)$$

can be evaluated for l'=l+1 by using equation (A.7.13) and for l'=l-1 it may be calculated by making use of expression (A.7.12) in appendix A.

In a similar way, we may compute the exchange term (i.e the 2nd term) in equation (3.3.a.4.4).

3.3.a.12 EVALUATION OF MATRIX ELEMENT M_1'' (3.3.a.1.9)

After having evaluated the matrix element M_1' (3.3.a.1.8), we calculate the matrix element M_1''(3.3.a.1.9) in the same way as the evaluation of M_1' has been done. The matrix element M_1'' (to be evaluated) is given by,

$$(\alpha_1, \alpha_2; JT| \, B \, | \alpha_3, \alpha_4; JT) = (\alpha_1, \alpha_2; JT| \, O_1'(\lambda_1 . \lambda_2) | \alpha_3, \alpha_4; JT)$$

. . . . (3.3.a.12.1)

where $O_1' = (H_1 - H_2)(\sigma_1 + \sigma_2) . \frac{r_{12}}{r^3}$.

For simplicity, first we separate the colour factor and then the intrinsic parity factor of the functions as discussed before. The evaluation of the matrix element of a colour operator and intrinsic parity operator is carried out according to the procedure as mentioned in sections (3.3.a.2) and (3.3.a.3) respectively.

Eliminating intrinsic parity as in section 3.3.a.3 we get the matrix element of O'_1.

$$(\beta'_1 g,\ \beta'_2 h;\ JT|O'_1|\beta'_3 h,\ \beta'_4 h;\ JT) = \frac{1}{\sqrt{2}}\{\beta'_1,\ \beta'_2;\ JT|O'_p|\beta'_3,\ \beta'_4;\ JT)$$

where $Op' = (\sigma_1 + \sigma_2).\frac{r_{12}}{r^3}$.

By definitions (3.3.a.4.1) and (3.3.a.4.2), we write

$$\{\beta'_1,\ \beta'_2;\ JT|\ Op'|\beta'_3,\ \beta'_4;\ JT) = \frac{1}{2}\Big[\Big\{(1+\delta_{\beta'_1\beta'_2})(1+\delta_{\beta'_3\beta'_4})\Big\}^{-\frac{1}{2}}\Big\{<\beta'_1,\ \beta'_2;\ JT|Op'|\beta'_3,\ \beta'_4;\ JT>$$
$$+\ (-1)^{j_3+j_4-J-T}<\beta'_1,\ \beta'_2;\ JT|\ Op'|\beta'_4,\ \beta'_3;\ JT>$$
$$-\ (-1)^{j_1+j_2-J-T}<\beta'_2\ \beta'_1;\ JT|\ Op'|\beta'_3,\ \beta'_4;\ JT>$$
$$-\ (-1)^{j_1+j_2+j_3+j_4}<\beta'_2,\ \beta'_1;\ JT|\ Op'|\beta'_4,\ \beta'_3;\ JT>\Big\}\Big] \quad \ldots\ (3.3.a.12.3)$$

Since the operator $Op' = (\sigma_1 + \sigma_2).\frac{r_{12}}{r^3}$ is an antisymmetric operator the signs of term 3 and term 4 get changed by the exchange of particle-labels $1 \leftrightarrow 2$ and we obtain

$$\{\beta'_1,\ \beta'_2;\ JT|\ Op'|\beta'_3,\ \beta'_4;\ JT) = \Big\{(1+\delta_{\beta'_1\beta'_2})(1+\delta_{\beta'_3\beta'_4})\Big\}^{-\frac{1}{2}}\Big[<\beta'_1,\ \beta'_2;\ JT|Op'|\beta'_3,\ \beta'_4;\ JT>$$
$$+\ (-1)^{j_3+j_4-J-T}<\beta'_1,\ \beta'_2;\ JT|\ Op'|\beta'_4,\ \beta'_3;\ JT>\Big] \quad \ldots\ (3.3.a.12.4)$$

We evaluate the direct term (1st term) and exchange term (2nd term) of (3.3.a.12.4) separately. Following the procedure that has been described earlier from section (3.3.a.5) to (3.3.a.9), we can obtain expression for a direct term like (3.3.a.9.1) as given below.

$$<(n_1 n_2),\ \{\Lambda\ S\};\ JM\Big|(\sigma_1+\sigma_2).\frac{r_{12}}{r^3}\Big|(n_3 n_4),\ \{\Lambda'\ S'\};\ JM>$$
$$= (-1)^{\Lambda'+S+J}\begin{Bmatrix} J & S & \Lambda \\ 1 & \Lambda' & S' \end{Bmatrix}<S\ ||(\sigma_1+\sigma_2)||\ S'>$$

$$\times \langle (n_1 n_2)\Lambda \,||\, \frac{r_{12}}{r^3} \,||\, (n_3 n_4)\Lambda' \rangle \qquad (3.3.a.12.5)$$

The reduced matrix element of $(\sigma_1 + \sigma_2)$ has been evaluated in Appendix B. The procedure of evaluating $\langle (n_1 n_2)\Lambda || \frac{r_{12}}{r^3} || (n_3 n_4)\Lambda' \rangle$ has been described from section (3.3.a.9) to section (3.3.a.11). Similarly we can evaluate the exchange term of (3.3.a.12.4) by the procedure as described for its direct term.

3.3.b EVALUATION OF MATRIX ELEMENT M_2

To evaluate the matrix element

$$M_2 = (\alpha_1, \alpha_2; JT|V_2(1,2)|\alpha_3, \alpha_4; JT), \qquad (3.3.b.1)$$

we will adopt the same procedure as has been already described in section 3.3.a.

3.3.b.1 THE OPERATOR AND ITS SYMMETRISATION

The operator V_2 as given in equation 3.3.5 is

$$V_2(1,2) = (\lambda_1 . \lambda_2)\left\{\frac{i}{2}(\sigma_1 \times \sigma_2).\frac{r_{12}}{r^3}\right\}.H_1 \qquad (3.3.b.1.1)$$

The given operator is not symmetric under the exchange of particle-labels. To make it symmetric with respect to an exchange of labels of the particles, we write

$$V = V_2(1,2) + V_2(2.1)$$

$$\text{i.e} \quad V = (\lambda_1 . \lambda_2)\left\{\frac{i}{2}(\sigma_1 \times \sigma_2).\frac{r_{12}}{r^3}\right\}.H_1 + (\lambda_2 . \lambda_1)\left\{\frac{i}{2}(\sigma_2 \times \sigma_1).\frac{r_{21}}{r^3}\right\}.H_2$$

$$= (\lambda_1 . \lambda_2)\left\{\frac{i}{2}(\sigma_1 \times \sigma_2).\frac{r_{12}}{r^3}\right\}.(H_1 + H_2) \qquad (3.3.b.1.2)$$

Therefore, we write the matrix element M_2 as,

$$M_2 = (\alpha_1, \alpha_2; JT|\, V \,|\alpha_3, \alpha_4; JT) \qquad (3.3.b.1.3)$$

For evaluating M_2, the same procedure will be followed as that has been explained in section (3.3.a).

3.3.b.2 PROCEDURE OF EVALUATION

Following the same procedure as mentioned in section (3.3.a), first we separate the colour using (3.3.a.2.2) and evaluate the matrix element of the colour operator $(\lambda_1.\lambda_2)$. Similarly we separate the intrinsic parity quantum number and evaluate the matrix element of the parity operator (H_1+H_2). Consequently, except for a constant factor, we get the matrix element of the following form.

$$(\beta'_1, \beta'_2; JT|\ Op''\ |\ \beta'_3, \beta'_4; JT) \qquad (3.3.b.2.1)$$

Here $Op'' = (\sigma_1 \times \sigma_2).\dfrac{\mathbf{r}_{12}}{r^3}$.

We shall write matrix element (3.3.b.2.1) with properly normalised and antisymmetrised wave-functions as,

$$(\beta'_1, \beta'_2; JT|Op''|\beta'_3, \beta'_4; JT)=\left\{(1+\delta_{\beta'_1\beta'_2})(1+\delta_{\beta'_3\beta'_4})\right\}^{-\frac{1}{2}}\Big[\langle\beta'_1, \beta'_2; JT|Op''|\beta'_3, \beta'_4; JT\rangle + (-1)^{j_3+j_4-J-T}\langle\beta'_1, \beta'_2; JT|\ Op''\ |\beta'_4, \beta'_3; JT\rangle\Big] \quad \ldots\ (3.3.b.2.2)$$

The direct term (i.e 1st term in (3.3.b.2.2) and the exchange term (i.e 2nd term in (3.3.b.2.2) would be evaluated separately as they have been evaluated in section (3.3.a).

Since the operator $Op'' = (\sigma_1 \times \sigma_2).\dfrac{\mathbf{r}_{12}}{r^3}$ is independent of isospin quantum number, we have the following matrix element correspond -ing to the direct term.

$$\langle n_1 l_1 j_1, n_2 l_2 j_2; JM\,|\,(\sigma_1 \times \sigma_2).\frac{\mathbf{r}_{12}}{r^3}\,|\,n_3 l_3 j_3, n_4 l_4 j_4; JM\rangle \qquad (3.3.b.2.3)$$

Using transformation (3.3.a..8.4), we get the above matrix element with LS-coupled states instead of jj-coupled states as,

$$\langle n_1 l_1 j_1,\ n_2 l_2 j_2;\ JM \mid (\sigma_1 \times \sigma_2).\frac{r_{12}}{r^3} \mid n_3 l_3 j_3,\ n_4 l_4 j_4;\ JM\rangle$$

$$= \sum_{\substack{\Lambda\ S \\ \Lambda'\ S'}} \Bigg[\Big[\{(2\Lambda'+1)(2S'+1)(2j_3+1)(2j_4+1)\}\{(2\Lambda+1)(2S+1)(2j_1+1)(2j_2+1)\} \Big]^{\frac{1}{2}}$$

$$\times \begin{Bmatrix} l_3 & l_4 & \Lambda' \\ s_3 & s_4 & S' \\ j_3 & j_4 & J \end{Bmatrix} \begin{Bmatrix} l_1 & l_2 & \Lambda \\ s_1 & s_2 & S \\ j_1 & j_2 & J \end{Bmatrix}$$

$$\times \langle (n_1 n_2), \{(l_1 l_2)\Lambda, (s_1 s_2)S\};\ JM \Big| (\sigma_1 \times \sigma_2).\frac{r_{12}}{r^3} \Big| (n_3 n_4), \{(l_3 l_4)\Lambda', (s_3 s_4)S'\};\ JM\rangle \Bigg]$$

. . . . (3.3.b.2.4)

Analogous to equation (3.3.a.9.1), we get

$$\langle (n_1 n_2), \{\Lambda\ S\};\ JM \Big| (\sigma_1 \times \sigma_2).\frac{r_{12}}{r^3} \Big| (n_3 n_4), \{\Lambda'\ S'\};\ JM\rangle$$

$$= (-1)^{\Lambda' + S + J} \begin{Bmatrix} J & S & \Lambda \\ 1 & \Lambda' & S' \end{Bmatrix} \langle S \| (\sigma_1 \times \sigma_2) \| S'\rangle$$

$$\times \langle (n_1 n_2)\Lambda \| \frac{r_{12}}{r^3} \| (n_3 n_4)\Lambda'\rangle \qquad (3.3.b.2.5)$$

where $\langle S \| (\sigma_1 \times \sigma_2) \| S'\rangle$ has been evaluated in appendix B. The evaluation of reduced matrix element of r_{12}/r^3 has been described from section (3.3.a.9) to section (3.3.a.11).

The procedure for evaluating the second term (i.e the exchange term) in (3.3.b.2.2) is the same as mentioned in section (3.3.a.12).

3.3.c EVALUATION OF MATRIX ELEMENT M_3

Finally, we evaluate the matrix element M_3 (the expression 3.3.9). The matrix element M_3 is

$$M_3 = (\alpha_1, \alpha_2;\ JT | V_3(1,2) |\ \alpha_3, \alpha_4;\ JT) \qquad (3.3.c.1)$$

Where the operator V_3 (as given in 3.3.6) is

$$V_3(1,2) = \sqrt{2}\, i \left\{ (\sigma_1 . \frac{\mathbf{p}_2}{r}).H_1 \right\} (\lambda_1 . \lambda_2)$$

3.3.c.1 SYMMETRISATION OF THE OPERATOR

Since the given operator is not symmetric with respect to interchange of particle-labels, therefore we have to symmetrise the operator. We write the operator in a symmetric form as,

$$V = V_3(1,2) + V_3(2,1)$$

$$= \sqrt{2}\, i \left\{ (\sigma_1 . \frac{\mathbf{p}_2}{r}).H_1 + (\sigma_2 . \frac{\mathbf{p}_1}{r}).H_2 \right\} (\lambda_1 . \lambda_2)$$

$$= \frac{i}{\sqrt{2}} \left\{ (H_1+H_2)(\sigma_1 . \frac{\mathbf{p}_2}{r} + \sigma_2 . \frac{\mathbf{p}_1}{r}) + (H_1-H_2)(\sigma_1 . \frac{\mathbf{p}_2}{r} - \sigma_2 . \frac{\mathbf{p}_1}{r}) \right\} (\lambda_1 . \lambda_2)$$

$$= \frac{i}{2\sqrt{2}} \left[(H_1+H_2) \left\{ (\sigma_1+\sigma_2)(\frac{\mathbf{p}_2+\mathbf{p}_1}{r}) + (\sigma_1 - \sigma_2)(\frac{\mathbf{p}_2-\mathbf{p}_1}{r}) \right\} \right.$$

$$\left. + (H_1-H_2) \left\{ (\sigma_1 - \sigma_2)(\frac{\mathbf{p}_2+\mathbf{p}_1}{r}) + (\sigma_1+\sigma_2)(\frac{\mathbf{p}_2-\mathbf{p}_1}{r}) \right\} \right] (\lambda_1 . \lambda_2)$$

. . . (3.3.c.1.1)

We transform the momenta $\mathbf{p}_1$ and $\mathbf{p}_2$ into the momenta $\mathbf{p}$ and $\mathbf{P}$ corresponding to the relative and centre-of-mass motions respectively by the following fundamental expressions.

$$\mathbf{P} = \frac{1}{\sqrt{2}} (\mathbf{p}_1 + \mathbf{p}_2) \qquad (3.3.c.1.2)$$

$$\mathbf{p} = \frac{1}{\sqrt{2}} (\mathbf{p}_1 - \mathbf{p}_2) \qquad (3.3.c.1.3)$$

Using definitions (3.3.c.1.2) and (3.3.c.1.3) in expression 3.3.c.1.1 and putting $\mathbf{p} = -i\hbar\nabla_{rel}$ and $\mathbf{P} = -i\hbar\nabla_{C.M}$, we have the operator V given by ,

$$V = \frac{1}{2} \left[(H_1+H_2) \left\{ (\sigma_1+\sigma_2).\frac{\nabla_{C.M}}{r} - (\sigma_1 - \sigma_2).\frac{\nabla_{rel}}{r} \right\} \right.$$

$$\left. + (H_1 - H_2) \left\{ (\sigma_1 - \sigma_2).\frac{\nabla_{C.M}}{r} - (\sigma_1+\sigma_2).\frac{\nabla_{rel}}{r} \right\} \right] (\lambda_1 . \lambda_2) \qquad (\hbar = 1)$$

. . . . (3.3.c.1.4)

Or $$V = \frac{1}{2}\left\{(H_1 + H_2)O_1 + (H_1 - H_2)O_2\right\}(\lambda_1 . \lambda_2) \qquad (3.3.c.1.5)$$

Here $$O_1 = (\sigma_1 + \sigma_2).\frac{\nabla_{c.m}}{r} - (\sigma_1 - \sigma_2).\frac{\nabla_{rel}}{r} \qquad (3.3.c.1.6)$$

$$O_2 = (\sigma_1 - \sigma_2).\frac{\nabla_{c.m}}{r} - (\sigma_1 + \sigma_2).\frac{\nabla_{rel}}{r} \qquad (3.3.c.1.7)$$

3.3.c.2 PROCEDURE OF EVALUATION

From expression (3.3.c.1.5), it is clear that it will be more convenient to evaluate M_3 if we first calculate the matrix elements

$$M_3' = (\alpha_1, \alpha_2; JT|(\lambda_1 . \lambda_2)(H_1 + H_2)O_1|\ \alpha_3, \alpha_4;\ JT) \qquad (3.3.c.2.1)$$

$$M_3'' = (\alpha_1, \alpha_2; JT|(\lambda_1 . \lambda_2)(H_1 - H_2)O_2|\ \alpha_3, \alpha_4;\ JT) \qquad (3.3.c.2.2)$$

separately as we have

$$M_3 = \frac{1}{2}(M_3' + M_3'') \qquad (3.3.c.2.3)$$

The various steps of the procedure have been described in detail in section 3.3.a. First of all we dissociate the colour factor by using expression (3.3.a.2.2) and calculate the matrix element of the colour operator $(\lambda_1 . \lambda_2)$ as discussed in section 3.3.a.2. After that we separate the intrinsic parity and compute the matrix element of the intrinsic parity operators $(H_1 + H_2)$ and $(H_1 - H_2)$ in the same way as mentioned in section 3.3.a.3.

After having separated the colour and intrinsic parity factors of the matrix elements we are left with the matrix elements of the following forms.

$$(\beta_1', \beta_2'; JT|\ O_1\ |\beta_3', \beta_4'; JT) \qquad (3.3.c.2.4)$$

and $$(\beta_1', \beta_2'; JT|\ O_2\ |\beta_3', \beta_4'; JT) \qquad (3.3.c.2.5)$$

where $\beta' = nljmt_3$.

Making use of expressions (3.3.a.4.1) and (3.3.a.4.2), we obtain the matrix elements 3.3.c.2.4 and 3.3.c.2.5 in a properly normalised and antisymmetrised forms as given below.

$$(\beta'_1, \beta'_2; JT|O_1|\beta'_3, \beta'_4; JT)=\left\{(1+\delta_{\beta'_1\beta'_2})(1+\delta_{\beta'_3\beta'_4})\right\}^{-\frac{1}{2}}\left[\langle\beta'_1, \beta'_2; JT|O_1|\beta'_3, \beta'_4; JT\rangle + (-1)^{j_3+j_4-J-T}\langle\beta'_1, \beta'_2; JT|O_1|\beta'_4, \beta'_3; JT\rangle\right] \quad \ldots\ (3.3.c.2.6)$$

$$(\beta'_1, \beta'_2; JT|O_2|\beta'_3, \beta'_4; JT)=\left\{(1+\delta_{\beta'_1\beta'_2})(1+\delta_{\beta'_3\beta'_4})\right\}^{-\frac{1}{2}}\left[\langle\beta'_1, \beta'_2; JT|O_2|\beta'_3, \beta'_4; JT\rangle + (-1)^{j_3+j_4-J-T}\langle\beta'_1, \beta'_2; JT|O_2|\beta'_4, \beta'_3; JT\rangle\right] \quad \ldots\ (3.3.c.2.7)$$

On the right side of each of the above two expressions, the two terms namely direct term and exchange term are computed separately. The procedure of their evaluation has been described in section (3.3.a). After having carried out some steps of the procedure of evaluation, we obtain the following matrix elements

$$\langle nl, NL; \Lambda|\frac{\nabla_{rel}}{r}|n'l', N'L'; \Lambda'\rangle \qquad (3.3.c.2.8)$$

$$\langle nl, NL; \Lambda|\frac{\nabla_{CM}}{r}|n'l', N'L'; \Lambda'\rangle \qquad (3.3.c.2.9)$$

alongwith reduced matrix elements of the spin operators $(\sigma_1+\sigma_2)$ and $(\sigma_1-\sigma_2)$ with some additional factors. The reduced matrix elements of the spin operators have been already evaluated in sections B.1 and B.2 of appendix B. In matrix element 3.3.c.2.8, the operator acts only on part 1 of the coupled state, therefore according to expression (3.3.a.11.1) we write (3.3.c.2.8) as,

$$\langle nl, NL; \Lambda|\frac{\nabla_{rel}}{r}|n'l', N'L'; \Lambda'\rangle = (-1)^{l+L+\Lambda'+1}\left[(2\Lambda+1)(2\Lambda'+1)\right]^{\frac{1}{2}}\begin{Bmatrix} l & \Lambda & L \\ \Lambda' & l' & 1 \end{Bmatrix}$$

$$\times \langle nl \,||\, \frac{\nabla_{rel}}{r} \,||\, n'l' \rangle \delta_{NN'} \cdot \delta_{LL'} \qquad (3.3.c.2.10)$$

But in (3.3.c.2.9) the operator acts only on part 2 and we have

$$\langle nl, NL; \Lambda | \frac{\nabla_{CM}}{r} | n'l', N'L'; \Lambda' \rangle = (-1)^{l+L+\Lambda+1} [(2\Lambda+1)(2\Lambda'+1)]^{\frac{1}{2}} \begin{Bmatrix} L & \Lambda & l \\ \Lambda' & L' & 1 \end{Bmatrix}$$

$$\times \langle NL || \frac{\nabla_{CM}}{r} || N'L' \rangle \delta_{nn'} \cdot \delta_{ll'} \qquad (3.3.c.2.11)$$

The reduced matrix elements on the right side of the above equations are calculated by using expressions A.6.18 and A.6.17 (of Appendix A) for $L'=L+1$, $l'=l+1$ and $L'=L-1$, $l'=l-1$ respectively.

After having computed the matrix elements M_1, M_2 and M_3 we can evaluate the matrix element M of a transition potential (3.1.1) by making use of expression (3.3.10).

CHAPTER 4

RESULTS AND DISCUSSION

Having incorporated the quark-antiquark excitations generated by the pair creation interaction into the model space, we have performed the calculations to determine the mass and the electromagnetic properties of the nucleon using three different sets of parameters given in table 4.2.

First we used the parameters set 1 and set 2 of table 4.2 but we did not obtain reasonable values of the nucleon's mass and N-Δ mass-splitting as will be discussed in section 4.1.2. We, therefore, then predicted the new values of the model parameters (shown as parameters set 3 in table 4.2) and performed the calculations to obtain the energy and electromagnetic properties of the nucleon.

The techniques used in the present calculations have been described in chapter 2. For more technical details of the computational methods, see reference [45]. For comparison, we have also performed similar calculations in terms of the 3q-model of the single nucleon. All the results of our calculations are given and discussed in this chapter.

4.1 PRE-CALCULATIONS

To compute the ground state energy of the nucleon we first performed the following calculations. Having calculated single particle energies of the shells and core energy with parameter set 1 and set 2, we used their calculated values as input data for energy calculations. Using this data we re-evaluated the numerical values of the model parameters as discussed in section 4.1.2. Using each set of parameters, to calculate the nucleon's energy we have to first compute the single particle energies of the shells and energy of the core.

4.1.1 SINGLE PARTICLE ENERGIES AND ENERGY OF THE CORE

To compute the ground state energy of the nucleon we must know the exact values 0f the single particle energies of the shells and the energy of the core. Since the presence of the core changes the single particle energies in the various shells, we would have to re-calculate the single-particle energies and energy of the core by taking into account the changes arising from the interactions between the valence particles and the core particles. In the present case we are dealing with a many-particle system comprising an assumed filled-shell core and three quarks in 0S valence shell. For such a system, it would be convenient to write the many-body Hamiltonian (2.5.1.1) in the following form

$$H = H^{C} + H^{V} + H^{V\text{-}C} \qquad (4.1.1.1)$$

where H^{C} includes the K.E and the two-body interactions of the

sea quarks making up the closed-shell core, H^V is an analogous quantity for the valence quarks and H^{V-C} represents the interactions between real quarks and ghost (sea) quarks. If we denote the determinantal wavefunction of a system by Ψ then any diagonal matrix element of the Hamiltonian H will be given by

$$< \Psi \mid H \mid \Psi > = \sum_{i}^{occ} < i \mid T \mid i > + \sum_{i<j}^{occ} (ij \mid V \mid ij) \qquad (4.1.1.2)$$

where the summations run over the occupied single-particle states in many-particle determinantal state Ψ and a matrix element in the second term of the equation (4.1.1.2) is an antisymmetrised matrix element of the two body interaction V_{ij} Distinguishing between the core particles (i.e the ghost quarks) and the valence particles (i.e the real quarks), one can decompose the two body interaction V_{ij} in the form [75]

$$\sum_{i<j} V_{ij} = \sum_{i<j \in C} V_{ij} + \sum_{\substack{i \in C \\ j \in V}} V_{ij} + \sum_{i<j \in V} V_{ij} \qquad (4.1.1.3)$$

C and v represent the filled-shell core and the valence shell respectively.

With the help of expressions (4.1.1.1), (4.1.1.2) and (4.1.1.3), we obtain

$$\begin{aligned} < \Psi \mid H \mid \Psi > = & \sum_{1=i \in C}^{48} < i \mid T \mid i > + \sum_{1=i<j \in C}^{48} (\bar{i}\bar{j} \mid V_{QQ} \mid \bar{i}\bar{j}) \\ & + \sum_{1=i \in V}^{3} < i \mid T \mid i > + \sum_{1=i<j \in V}^{3} (ij \mid V_{qq} \mid ij) \\ & + \sum_{1=i \in V}^{3} \sum_{1=j \in C}^{48} (i\bar{j} \mid V_{qQ} \mid i\bar{j}) \qquad (4.1.1.4) \end{aligned}$$

where Ψ is the wavefunction of a many-quark system comprised

of 3 quarks in valence shell v and 48 ghost quarks in filled-shell core c.

Fig. 4.1

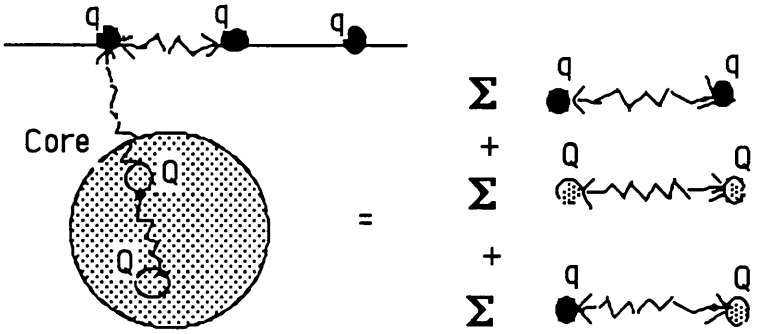

a) A system of 3 real quarks in a valence shell plus an assumed core of 48 ghost quarks below the Fermi-surface.

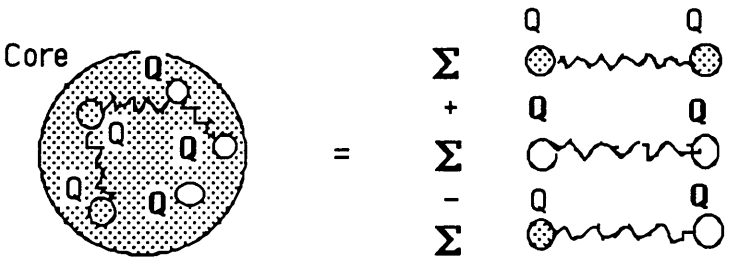

b) A system of three holes in an assumed core of 48 ghost quarks below the Fermi surface.

N.B: q, Q and **Q** represent a real quark, a ghost quark and a hole (i.e. anti-quark) respectively in a fig 4.1.

The interaction V_{qq} is given in table 4.3 while the other two-body interactions are obtained as

$$V_{qQ} = - V_{qq} \text{ and } V_{QQ} = V_{qq} \qquad (4.1.1.5)$$

In an expression (4.1.1.4), the 1st part is an eigenvalue E_c of the hamiltonian H^c which describes the energy of the filled core, i.e

$$E_c = \sum_{\bar{i} \in C}^{48} < \bar{i} \mid T \mid \bar{i} > + \sum_{\bar{i} < \bar{j} \in C}^{48} (\bar{i}\bar{j} \mid V_{QQ} \mid \bar{i}\bar{j}) \qquad (4.1.1.6)$$

and the second part gives the energy of the three quarks in a valence shell (on their own) without a core, i.e

$$E_{3q} = \sum_{i \in V}^{3} < i \mid T \mid i > + \sum_{i < j \in V}^{3} (ij \mid V_{qq} \mid ij) \qquad (4.1.1.7)$$

The third part of the equation (4.1.1.4) represents the effective interaction experienced by the 3 valence quarks due to the presence of an assumed filled-shell core occupying 48 ghost quarks which alters the single-particle energies of the various shells. If we denote the change in the single particle energy of a real shell by ε_{ic} then we write

$$3\varepsilon_{ic} = \sum_{i \in V}^{3} \sum_{\bar{j} \in C}^{48} (i\bar{j} \mid V_{qQ} \mid i\bar{j}) \qquad (4.1.1.8)$$

Keeping the expressions (4.1.1.6), (4.1.1.7) and (4.1.1.8) in view, we may re-write the expression (4.1.1.4) as

$$E_{3q+C} = E_C + E_{3q} + 3\,\varepsilon_{ic} \qquad (4.1.1.9)$$

In the second case we consider the core with three holes showing three quarks missing in the core. Similarly, with the same reasoning as described above one can finally arrive at the following expression

$$E_{C-3Q} = E_C + E_{3q} - 3\,\bar{\varepsilon}_{ic} \qquad (4.1.1.10)$$

where $\bar{\varepsilon}_{ic}$ represents the change in single-particle energy of a sea shell.

To work out the changes in the single-particle energies in the various shells, we performed calculations to evaluate i) E_C, the

energy of the assumed core with single-particle energy equal to the mass energy of the constituent quark 359.73 Mev in each shell, ii) E_{3q+C}, the energy of the 3 quarks in a real shell plus filled core, iii) E_{3q}, the energy of the 3 quark in a valence shell (on their own) without the assumed core and iv) E_{C-3Q}, the energy of the assumed core with 3 holes. Having evaluated the values of E_C, E_{3q+C}, E_{3q} and E_{C-3Q}, we worked out ε_{ic} and $\bar{\varepsilon}_{ic}$, the changes in single-particle energies of the various shells by making use of expressions (4.1.1.9) and (4.1.1.10) respectively. The exact single-particle energy of the shell is obtained by subtracting the change calculated for that particular shell from the mass energy of the quark $m_q c^2$=359.73 Mev. The corrected values of the single-particle energies of the shells are shown in the table 4.1.

In the present study, analogous to the Dirac vacuum with electrons occupying the negative energy states, we have imagined the fermion vacuum with quarks occupying the negative energy states below the Fermi energy level. The negative sign of the single-particle energy of the sea shell is due to the occupancy of the negative energy states. By summing over the single-particle energies of the sea shells, we obtain the energy of the core (i.e the energy of the vacuum).

TABLE 4.1

SINGLE-PARTICLE ENERGIES AND ENERGY OF THE CORE.

Set No:	Single-particle energies. ε_i (Mev)			$\bar{\varepsilon}_i$ (Mev)			Energy of the core E_c (Mev)
	Real shells			Sea shells			
	$0S_{1/2}$	$0P_{1/2}$	$0P_{3/2}$	$0\bar{S}_{1/2}$	$0\bar{P}_{1/2}$	$0\bar{P}_{3/2}$	
I	226.88	174.59	174.81	-1053.51	-1410.45	-1407.61	-36503.73
II	397.64	351.01	352.78	-1157.62	-1471.70	-1471.35	-22981.75
III	267.23	209.18	209.22	-1125.56	-2527.40	-2527.41	-57902.07

The energy possessed by the single quark in a harmonic oscillator potential is given [76] by

$$E_{n,l} = (2n+l+\frac{3}{2})\hbar w.$$

where l is the orbital angular momentum quantum number and n=0,1,2,3 . . .is the principal quantum number associated with the number of nodes in the radial wavefunction. Therefore the kinetic energy of the quark in a 0S shell and in a 0P shell will be as f.ollows;

$$(K.E)_{0S} = \frac{3}{4}\hbar w \quad \text{and} \quad (K.E)_{0P} = \frac{5}{4}\hbar w.$$

The values of $\hbar w$ for the sets of model parameters (mentioned in table 4.2) are given in table 4.3.

Including the kinetic energy term into the energy of the single quark, we obtain the 0S and 0P energy-levels which are shown diagrametically in a figure 4.2. From the energy-diagram shown in a fig. 4.2 it is clear that the energy difference between the $0P_{1/2}$

level and $0P_{3/2}$ level is extremely small and these are nearly degenerate levels because of the reason that the potential used in our calculations did not include the spin-orbit interaction term. Otherwise the order of the levels looks fine.

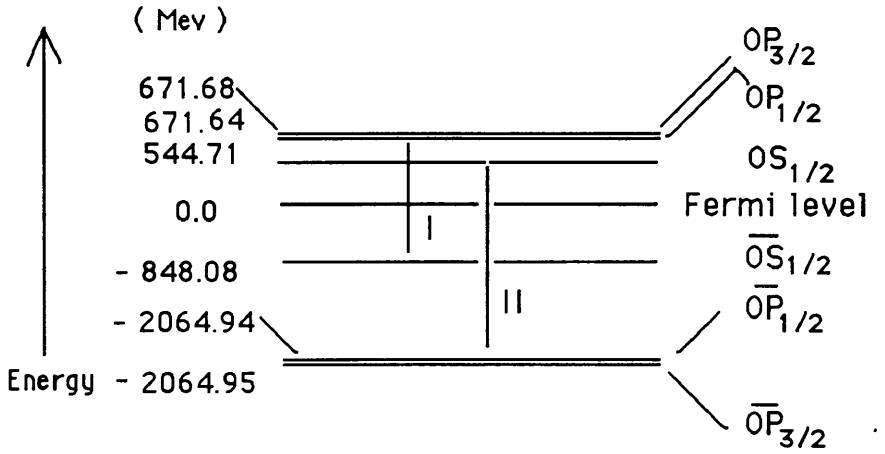

Fig 4.2 Single particle energy levels.

To define the Fermi level as zero of the energy scale, we subtracted off the core's energy from all the computed values of the energies.

4.1.2 CHOICE OF MODEL PARAMETERS

In order to specify the quark-quark interaction the following four essential parameters have been used in the quark potential models [21-30].

1) b,the oscillator length parameter of the quark spatial wave function, ii) m_q, the mass of the constituent quark, iii) α_s , the quark-gluon coupling constant,the QCD analog of the fine structure constant relevant to nuclear energies and iv) a_c, the confining

potential constant that describes the strength of the confinement interaction for the quarks.

The same model parameters b, m_q, α_s and a_c are contained in the interaction potentials of table 4.3 that have been used in the present calculations.

It is very important to select or determine the most suitable values of these parameters to develop an exact potential between the quarks. To obtain a good choice of model parameters, we proceeded as follows;

First we performed the calculation based on the 3q- model to obtain the energy, magnetic moment and root mean square radii of the nucleon using parameter set 1 of table 4.2 which have been already used in reference [30]. The results of the calculation are given in tables 4.8, 4.11 and 4.12. The calculated mass of the nucleon and isobar delta, M_N=938.09 Mev/c^2,M_Δ=1229.65 Mev/c^2 and their mass splitting, M_Δ-M_N=291.56 Mev/c^2 are in remarkably good agreement with the observed values [77]. Similarly the results of the electromagnetic properties of a nucleon are also quite satisfactory. We obtained exactly the same energy for the anti-nucleon as that of the nucleon i.e $E_{\bar{N}}$=938.12 Mev. This was a good check of our shell model computation. We are,therefore, confident that the code yields the correct results for the present study. But when the same calculations are repeated in terms of the present model, the computed energies (as shown in table 4..8) are found to be very low as compared with the experimental data. The nucleon's energy is lowered by 570.59 Mev/c^2 from the previous value to 367.50 Mev/c^2. The radii and magnetic moment are

improved by 2% and 6 % respectively. It shows that the model, with the given set of parameters, produces an exact energy of the nucleon and reasonable values of its electromagnetic properties if it is based on the 3q-structure of a nucleon but failed to give an exact nucleon's energy when based on the present $(3q+q^4\bar{q})$ -structure of the single nucleon.

Since the $(q^4\bar{q})$-components make significant contributions to the masses M_N, M_Δ and also to the electromagnetic properties of the nucleon,it is necessary to readjust the values of the model parameters b, m_q, α_s and a_c for the present model. Parameter set 2 shown in table 4.2 was predicted and used by Fujiwara and Hecht in the present-model study of the NN-interaction within a framework of the resonating group method [37].We,therefore, performed the same calculations based on the present model using these parameters b=0.524 fm, m_q=471.2 Mev/c^2,α_s=2.973 and a_c=335.7 Mev/fm^2 within the framework of the Glasgow shell-model programme.The results obtained from these calculations are shown in tables 4.8,4.11 and 4.12. The N and Δ–masses M_N=660.34 Mev/c^2,M_Δ=1022.01 Mev/c^2 and their mass-splitting M_Δ-M_N =361.67 Mev/c^2 are still not in good agreement with the observed values. The magnetic moment and radii were found to be round about 80 % of the observed values.

In fact, Fujiwara and Hecht did not aim to choose the parameters to obtain the exact energy (ground-state) of the nucleon as it was the philosophy of their study not to trust the property of the nucleon dependent on the confining potential constant a_c because of its phenomenological character. Anyhow

their predicted set of parameters may produce better results in the space smaller than ours.

To obtain other more suitable values of the parameters, we have checked the sensitivity of the nucleon's energy and N-Δ energy-splitting to the parameters, using the data obtained from the calculations with parameters set 2. We have examined the variation of the nucleon's energy by changing the value of the oscillator length parameter b and the value of the confining potential constant a_c(as shown in fig 4.3.a and 4.3.d respectively) while keeping the other three parameters constant. From the graph shown in fig 4.3.a, it is obvious that the stability condition $\delta(M_N)/\delta b = 0$ [35] is satisfied at b=0.524 fm and we get the minimum energy of the nucleon at b=0.524 fm as the nucleon's energy changes with respect to the variation of the size parameter b. It has been noticed from the results shown in fig 4.3.d that the energy of the nucleon increases on increasing the value of the confining potential constant a_c at the constant values of other three parameters m_q, b, and α_s.

Similarly we have also checked the variation of N-Δ energy-splitting by changing the quark-gluon coupling constant α_s at given values of other three parameters. The results are graphically presented in fig 4.3.c. The graph shows that the N-Δ mass-splitting is directly proportional to the coupling constant α_s.We have found (as it is obvious from the plots shown in fig 4.3) that the energy of the nucleon is more or less sensitive to all parameters but it depends mostly upon the confining potential

Fig. 4.3

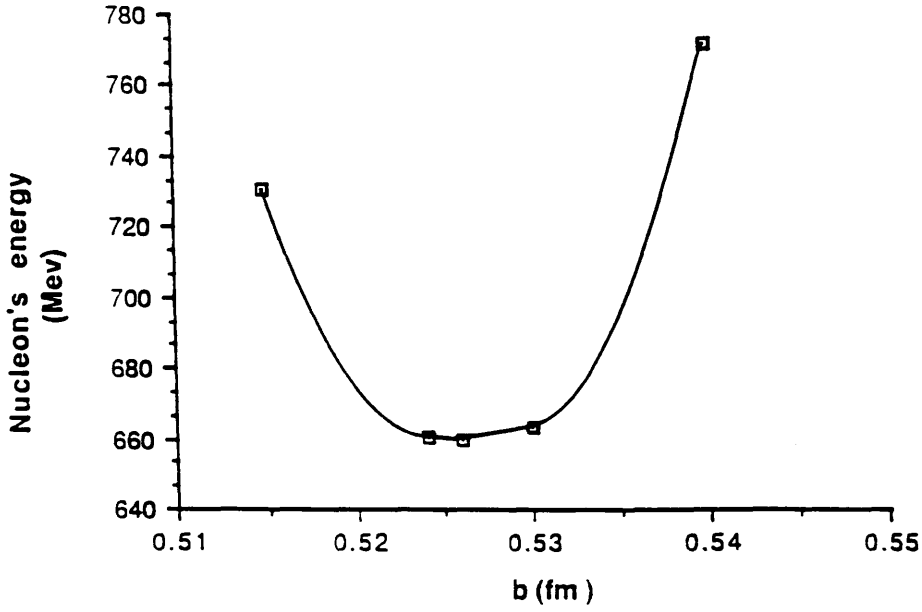

a) The variation of nucleon's energy by changing the oscillator length parameter b.

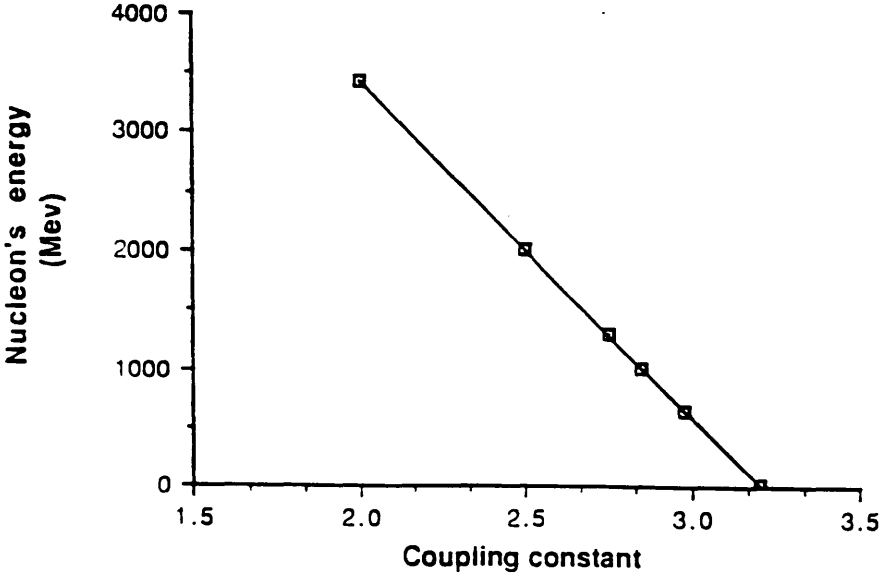

b) The nucleon's energy decreases on increasing the coupling constant α_s at constant b and a_c.

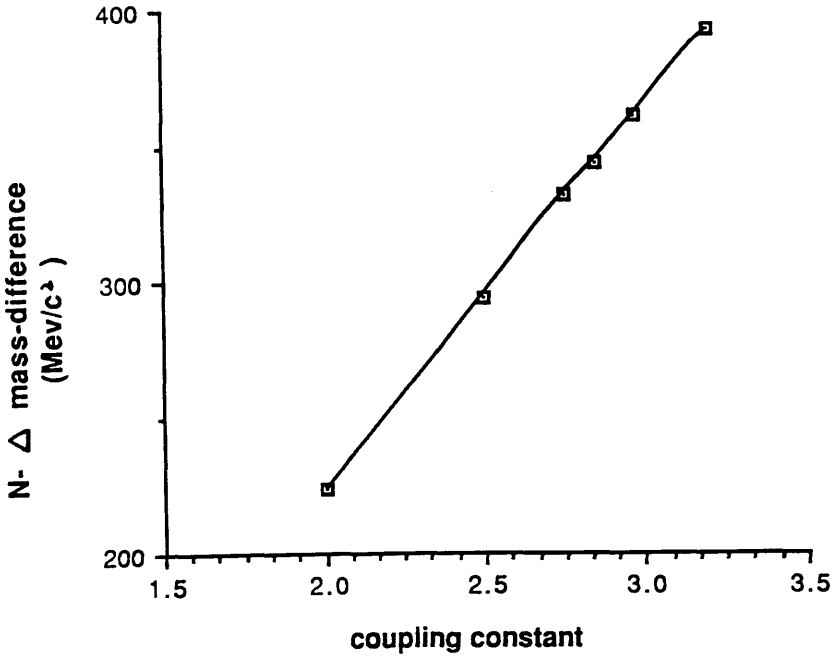

c) N-Δ mass-difference increases by increasing coupl. constant α_s at constant b and a_c.

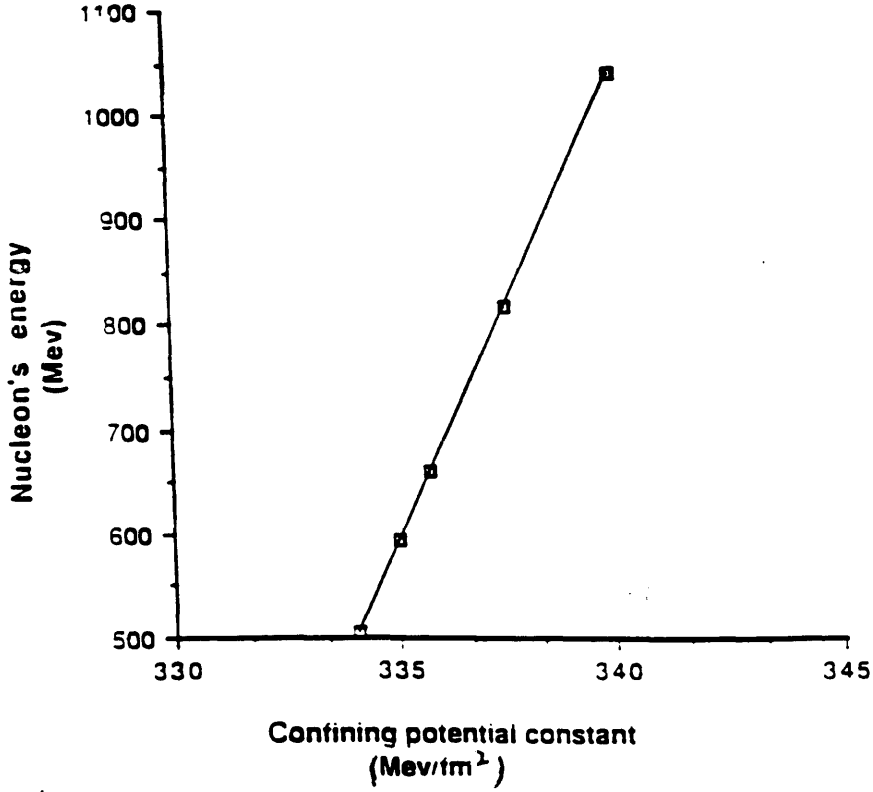

d) The nucleon's energy increases on increasing the confining potential constant a_c at constant b and α_s.

constant a_c i.e the strength of the confinement interaction for the quarks.

With the help of the plots shown in fig 4.3 and other relevant information obtained from the previous calculations with parameters set 2, we re-evaluated the parameters (3rd entry of table 4.2) for the present model to obtain better agreement with the measured mass and electromagnetic properties of the nucleon.

4.1.2.1 RE-EVALUATION OF THE MODEL PARAMETERS

We know that the numerical values of the oscillator length parameter b and mass of the quark m_q are strongly constrained by the size of the nucleon and its magnetic moment respectively. We, therefore, first chose suitable values of b and m_q to fit the mean square radius and the magnetic moment of the nucleon by making use of the qualitative information borrowed from the numerical results of the previous calculations with parameters set 1 and set 2 through the relations,

$$\langle r^2 \rangle \propto b^2 \quad \text{and} \quad \mu \propto \frac{1}{m_q} \qquad (4.1.2.1)$$

We have chosen m_q=359.73 Mev/c^2 and b=0.54 fm. The value of 'b' has been selected larger than the value given in parameter set 2 because of the fact that the smaller values of b would require larger masses of the quark. Having selected the specific values of b and m_q, initially we estimated α_s, the quark-gluon coupling constant, from the N–Δ mass splitting from the expression [24a],

TABAE 4.2

SETS OF MODEL PARAMETERS

Parameters set number	Oscillating length parameter, b (fm)	mass of the quark, m_q (Mev/c^2)	Coupling constant α_s	Conf: Potential constant, a_c (Mev/fm^2)
1	0.60	313	1.517	23.67
2	0.524	471.2	2.973	335.7
3	0.54	359.73	1.75	195.44

valid in the 3q-model

$$M_\Delta - M_N = \frac{2}{3}\sqrt{\frac{2}{\pi}}\,\frac{\alpha_s\,(hc)^3}{m_q^2\,b^3} \qquad (4.1.2.2)$$

to fit the observed mass difference of 293 Mev/c^2. The strength constant a_c of the quadratic confining potential was worked out from the expression [24a]

$$a_c = \left[\frac{(hc)^2}{16 m_q b^4}\right] F \qquad (4.1.2.3)$$

where the factor F is given by $F = 1 - \frac{1}{2}(\Delta m\, m_q b^2/c^2) - (\Delta m\, m_q b^4/c^4)$.

Using the value of α_s calculated from equation (4.1.2.2) and the value of a_c calculated from equation (4.1.2.3), we could not get reasonable values of the N-Δ mass-splitting and energy of the nucleon. This shows that the above expressions are valid only in the 3q-model but no longer valid in the present model. Although the proportionalities among the quantities given in the expressions (4.1.2.2) and (4.1.2.3) still remain the same (as

Fig. 4.4

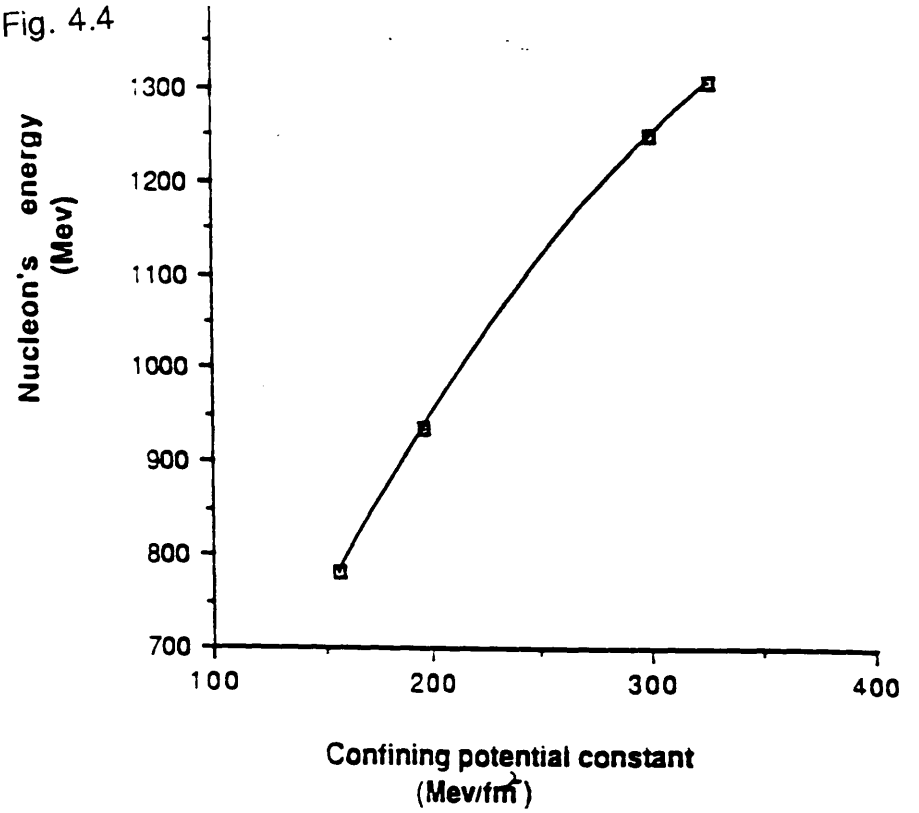

a) Nucleon's energy versus confining potential constant a_c for parameterset 3.

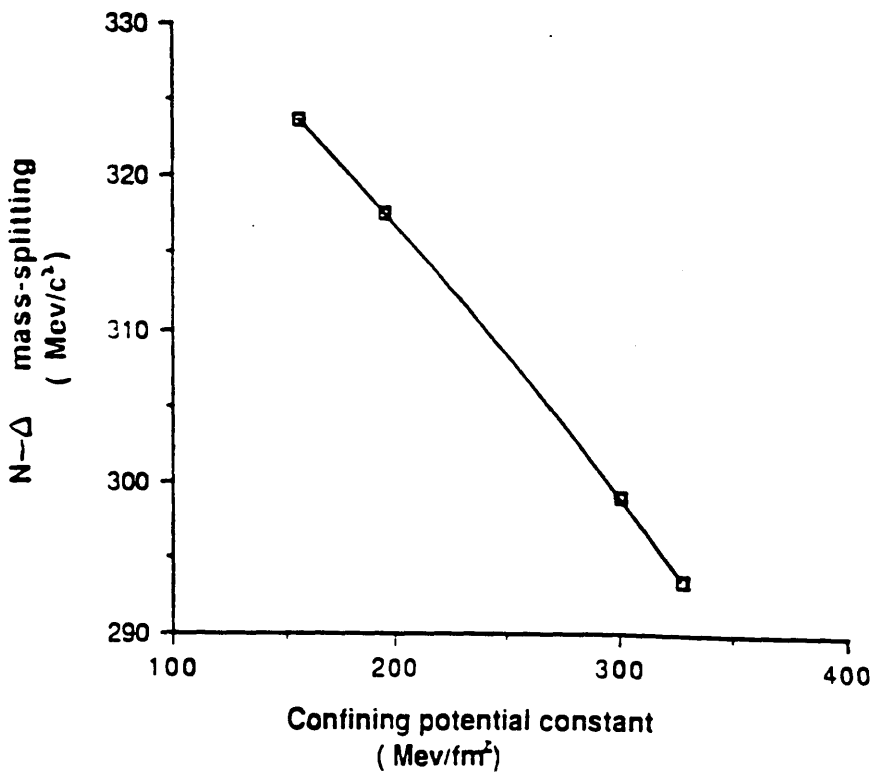

b) The N-Δ mass-splitting versus confining potential constant for parameter set 3.

obvious from the plots shown in fig 4.3) in the present model but the effect of the mesonic cloud might change the constant of proportionality in each relation. Anyhow the results obtained provided us a clue to attack the problem. Making use of the proportionalities between the quantities to be determined and the relevant parameters (as shown in the plots b and c of fig 4.3) and the quantitative information derived from these results,first we re-adjusted the value of α_s =1.75 to fit the observed value of N–Δ energy-splitting of 293 Mev.

Finally we acheived an exact fit of the nucleon's energy (ground state) E_N=938.231 Mev by a further adjustment of the confining potential constant a_c equal to 195.44 Mev/fm^2 as clear from the plot shown in fig 4.4.a. This re-adjustment of a_c=195.44 Mev/fm^2 shifted the value of N-Δ mass-splitting from 293 Mev/c^2 to 317.58 Mev/c^2 as it is obvious in a graph shown in fig 4.4.b.

In a way as mentioned above, having made the following consistency checks,

i) mass of the nucleon is 938.23 Mev/c^2,

ii) N-Δ mass splitting is 317.58 Mev/c^2 and

iii) the ratio μ_n/μ_p = -0.675

we have finalised the numerical values of the model parameters compatible to the present study of the nucleon's structure to be b=0.54 fm, m_q=359.73 Mev/c^2, α_s=1.75 and a_c= 195.44 Mev/fm^2. The final parameter sets are summarised in table 4.2.

TABLE 4.3

1. MODEL HAMILTONIAN.

$$H = \left(\sum_i T_i \right) - K_{C.M} + \sum_{i<j} V(ij)$$

with $T=(m_q)_i+\frac{\mathbf{P}_i^2}{2(m_q)_i}$ (for non-relativistic many-quark hamiltonian).

2. QUARK-QUARK INTERACTION.

$$V_{ij} = (\lambda_i \cdot \lambda_j)\left[\frac{A}{r_{ij}} - B\left\{\delta(\mathbf{r}_{ij})[1+ \frac{2}{3}(\sigma_i \cdot \sigma_j)]\right\}\right] - (\lambda_i \cdot \lambda_j)A_c r_{ij}^2$$

3. QUARK-ANTIQUARK PAIR CREATION INTERACTION.

$$V_{q\to qq\bar{q}}(1,2) = K(\lambda_1 \cdot \lambda_2)\left[(\sigma_1 \cdot \frac{\mathbf{r}_{12}}{r^3}) + \frac{i}{2}(\sigma_1 \times \sigma_2) \cdot \frac{\mathbf{r}_{12}}{r^3} + \frac{\sqrt{2}\,i}{r}(\sigma_1 \cdot \mathbf{p}_2)\right] H_1$$

4. STRENGTH-CONSTANTS OF THE POTENTIALS AND $\hbar w$.

Set No:	A (Mev.fm)	B (Mev.fm^3)	A_c (Mev/fm^2)	K (Mev.fm^2)	$\hbar w$ (Mev)
1	295.85	371.91	94.68	47.02	344.42
2	585.68	321.61	1342.28	61.22	299.96
3	344.75	324.81	781.76	47.20	369.97

4.2 WAVEFUNCTION AND ENERGY OF THE SYSTEM

In this section we describe the improved wavefunction of the nucleon and its ground state energy obtained from the present calculations.

4.2.1 WAVEFUNCTION OF THE SINGLE NUCLEON

In the present model, we have imagined a filled-shell core of 48 ghost quarks occupying $0\bar{S}_{1/2}$, $0\bar{P}_{1/2}$ and $0\bar{P}_{3/2}$ sea shells below the fermi level above which there are $0S_{1/2}$, $0P_{1/2}$ and $0P_{3/2}$ real shells with 3 valence quarks in the $0S_{1/2}$ shell. Analogously our assumed core of ghost quarks reflects the same physical picture as that of Dirac's vacuum assumed to be a sea of electrons.

In view of this model-picture based on the same foundation as that of Dirac's vacuum, in the present case one can create a 'hole' in the sea by exciting a quark from a negative energy state to one of the unoccupied positive energy state. The absence of a quark of charge $-e_q$ and of energy -E is interpreted as the presence of an antiquark of charge $+e_q$ and of energy +E. It means that the net effect of this excitation is the creation of a quark-antiquark pair.In the present model these quark-antiquark excitations are generated by applying the transition potential [42] in between a real quark and a ghost (sea) quark which excites a quark from a sea to the real shell in accordance with the parity conservation.

Based on this idea, by using the Glasgow shell-model techniques we have extended the simple 3q-quark model of the nucleon to include the mesonic contributions into the internal wavefunction of the single nucleon in addition to 3 quarks in the 0S valence

shell. The input occupancies of the real and sea shells were as follows;

TABLE 4.4

INPUT OCCUPANCIES OF THE SHELLS

Real shells	Number of particles Minimum	Maximum	Sea shells	Number of particles Minimum	Maximum
$0S_{1/2}$	3	4	$0\bar{S}_{1/2}$	11	12
$0P_{1/2}$	0	1	$0\bar{P}_{1/2}$	11	12
$0P_{3/2}$	0	1	$0\bar{P}_{3/2}$	23	24
Total quarks	3	4	Total quarks	47	48

The improved wavefunction (ground state) of the nucleon calculated on the basis of the present extended model is of the form

$$\Psi_0 = a_0 \Phi_0(3q) + \sum_{\alpha} a_\alpha \Phi_\alpha ((3q)(q\bar{q})) \qquad (4.2.1)$$

where α runs over the summation of all the components with $q\bar{q}$-excitations and a_0, a_α describe the contributions of the 3q-component and the $(3q+q\bar{q})$-components respectively.

we calculated the probabilities for the possible shell-occupancies using parameters set 3, given in table 4.5.

TABLE 4.5

Probabilities of the shell-occupancies

Probabilities	Occupancies of the shells	
	Real shells $0S_{1/2}$ $0P_{1/2}$ $0P_{3/2}$	Sea shells $0\bar{S}_{1/2}$ $0\bar{P}_{1/2}$ $0\bar{P}_{3/2}$
0.0134	4 0 0	12 12 23
0.0059	4 0 0	12 11 24
0.5486	3 0 0	12 12 24
0.1348	3 1 0	11 12 24
0.2973	3 0 1	11 12 24

It can be noted from table 4.5 that the probability of the shell occupancies corresponding to the configuration $(0S)^3(0P)(0\bar{S})$ shown diagrametically in fig 4.5.a is larger than the probability of the other mode of excitation (shown in fig 4.5.b) corresponding to the configuration $(0S)^4(0\bar{P})$.

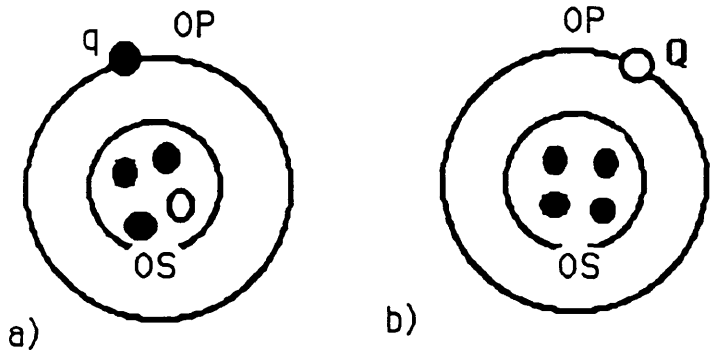

Fig. 4.5 a)1st mode of excitation in which 3 valence quarks and a hole are in $0\bar{S}$ shell and an excited quark in 0P shell. b) Second mode of excitation in which 3 valence quarks and an excited quark are in 0S and a hole in $0\bar{P}$ sea shell.

TABLE 4.6

QUANTUM NUMBER (EXCEPT COLOUR) OF THE SINGLE-PARTICLE STATES/ORBITS

S.P.Orbit	$\mathcal{N}$ (=2n+l)	l	2 j	2m	$2t_3$ *	p *
1	0	0	1	- 1	- 1	0
2	0	0	1	1	- 1	0
3	0	0	1	- 1	1	0
4	0	0	1	1	1	0
5	0	0	1	- 1	- 1	1
6	0	0	1	1	- 1	1
7	0	0	1	- 1	1	1
8	0	0	1	1	1	1
9	1	1	1	- 1	- 1	0
10	1	1	1	1	- 1	0
11	1	1	1	- 1	1	0
12	1	1	1	1	1	0
13	1	1	1	- 1	- 1	1
14	1	1	1	1	- 1	1
15	1	1	1	- 1	1	1
16	1	1	1	1	1	1
17	1	1	3	- 3	- 1	0
18	1	1	3	- 1	- 1	0
19	1	1	3	1	- 1	0
20	1	1	3	3	- 1	0
21	1	1	3	- 3	1	0
22	1	1	3	- 1	1	0
23	1	1	3	1	1	0
24	1	1	3	3	1	0
25	1	1	3	- 3	- 1	1
26	1	1	3	- 1	- 1	1
27	1	1	3	1	- 1	1
28	1	1	3	3	- 1	1
29	1	1	3	- 3	1	1
30	1	1	3	- 1	1	1
31	1	1	3	1	1	1
32	1	1	3	3	1	1

* u-quark and d-quark are represented by isospin quantum numbers 1 and -1 respectively and the parity quantum number 0 and 1 denote even and odd intrinsic parity respectively.

It is because of the fact that it is easier to excite a quark from a highest negative energy level in $0\bar{S}$ shell than to excite it from the deeper level in a $0\bar{P}$ sea shell as clear from the diagram shown in fig. 4.2. From the diagram shown in fig 4.2, it is clear that the gap between 0S and $0\bar{P}$ is larger than the gap between $0\bar{S}$ and 0P. Therefore 96% of the excitations takes place from the $0\bar{S}$ to 0P whereas only 4% takes place from $0\bar{P}$ to 0S in accordance with the parity conservation, because the former requires less energy for the excitations to take place than the latter. It can also be noticed that the probability of finding an excited quark in $0P_{3/2}$ is nearly double the probability of finding it in $0P_{1/2}$. The reason is that the $0P_{3/2}$ shell possesses a number of available single particle orbits two times greater than the number of single particle states available in $0P_{1/2}$ shell. From the predicted probabilities of the shell occupancies given in a table 4.5, one can learn how much contribution is made by the various components of the wavefunction.

The component-contributions of the nucleon's and of the isobar delta's wavefunctions with their proportions in percentage are given in a table 4.7.

The contribution made by the 3q-component is greater than the contribution of the $(q^4\bar{q})$-components, even though the contribution of $(q^4\bar{q})$-components is found to be quite significant. It contributes 45% in the nucleon's wavefunction and 47% in the wavefunction of the isobar delta.

TABLE 4.7

COMPONENT-CONTRIBUTIONS IN NUCLEON'S WAVEFUNCTION.

Set No:	State	3q-component	$q^4\bar{q}$-components	
		$(0S)^3$ %	$(0S)^4(0\bar{P})$ (%)	$(0S)^3(0P)(0\bar{S})$ (%)
1	N	76.18	1.4	22.42
	Δ^+	75.28	0.84	23.88
2	N	48.67	17.67	33.66
	Δ^+	46.23	18.17	35.60
3	N	54.86	1.93	43.21
	Δ^+	53.01	1.33	45.66

The contribution of the $(q^4\bar{q})$-components in a nucleon's wavefunction or in an isobar-delta's wavefunction depends upon the strength of the transition potential $V_{q\text{-}qq\bar{q}}$.

If we compare the contributions of the $(q^4\bar{q})$-components of the nucleon's and the isobar delta's wavefunctions in three cases with given different sets of the model parameters, we find different contributions (as shown in table 4.7) corresponding to different values of K, the strength of the transition potential in the three cases as shown in table 4.3. The greater the value of K, the larger will be the contribution of the $(3q+q\bar{q})$-components in the wavefunction.

We obtained 312 states (in total) of positive parity with z-component of the angular momentum, M=1/2. The lowest eigenstate is the ground state of the nucleon. All the low energy

states are non-spurious and colourless. The spuriosity and colouredness of the states have been avoided to make the system physical by subtracting the kinetic energy due to the motion of centre-of-mass of the system from the total kinetic energy of the system and using the constraint R≤G≤B, where R, G, B denote the codes for red, green and blue quarks respectively. These problems have been already discussed in section 2.5.2 and section 2.5.3.

4.2.2 MASS OF THE NUCLEON AND N-Δ MASS-SPLITTING

The wavefunction of the nucleon has been improved by adding $(3q+q\bar{q})$-components to its 3q-component in the present extended quark model of the nucleon as discussed in section 4.2.1. The ground state wavefunction of the nucleon is shown in equation (4.2.1). The ground state energy (referred as mass) of the nucleon is obtained by computing the energy of the lowest state in the energy spectrum of the system defined for a nucleon in the present model.

The many-body Hamiltonian used in the present study is of the form given in table 4.3. The values of the pre-calculated two body matrix elements along with other requisite data like the oscillator length parameter b, the strength-constants of the potentials used and the value of $\hbar w$ (given in table 4.3),the energy of the core E_c and the single-particle energies of the shells (given in table 4.1) were provided as input data to the program. We performed the energy calculation with three different sets of model parameters given in table 4.2.

Since we were mainly interested in ground state energy of the nucleon, we computed the energies of a few lowest eigenstates of the system. The values of J , T, parity and the expectation value of the colour operator $(\Sigma \lambda)^2$ calculated for the states obtained show that these are good physical states. The first two lowest colourless eigenstates with positive parity having J=1/2,T=1/2 and J=3/2,T=3/2 represent the nucleon and isobar Δ^+ particles respectively. With model parameters set 3, their energies have been calculated and found, E_N=938.23 Mev and E_Δ =1255.81 Mev which gives the N-Δ energy-splitting equal to 317.58 Mev. Our theoretically predicted mass of the nucleon M_N=938.23 Mev/c^2 is in good agreement with the observed nucleon's mass [77]. The N-Δ mass-splitting is also close to the experimental value. It is only 8 % greater than the experimental value.

TABLE 4.8
Results of Nucleon's energy.

Set No:	3q - model			(3q + $q^4\bar{q}$)- model		
	E_N (Mev)	E_Δ (Mev)	$E_N - E_\Delta$ (Mev)	E_N (Mev)	E_Δ (Mev)	$E_N - E_\Delta$ (Mev)
1	938.09	1229.65	291.56	367.50	649.99	282.49
2	2391.16	2769.36	378.21	660.34	1022.01	361.67
3	2070.53	2419.58	349.05	938.23	1255.81	317.58

If we compare the results of the energy obtained from calculations performed in the simple 3q-quark model and the

present $(3q+q^4\bar{q})$-quark model of the single nucleon using three different sets of parameters, we obtain the energies of the nucleon and isobar delta in the 3q-model greater than their energies obtained in the present extended quark model. The energy-splitting of the nucleon and isobar delta, i.e their mass difference has also been found smaller in the present model. The reason is that when we extend the model space the smaller eigenvalues get further lowered while the greater energy eigenvalues move higher in energy.

A general comments about the N-Δ mass-splitting is that the colour magnetic interaction is largely responsible for the energy splitting. Since the two quarks couple their spins either to S=0 or S=1, the 51 (u and d) quarks in the present system will couple their spins and orbital angular momenta either to give J=1/2 or J=3/2 giving rise to a N-state or a Δ–state respectively. The colour-magnetic interaction splits the qq-pairs with spin S=1 or S=0 in such a way as to move the triplet up and the singlet down. The splitting depends upon the strength of the colour-magnetic interaction and it is proportional to the ratio $\alpha_s/(m_q)^2b^3$ [24a] which is constrained by the suitable choice of the numerical values of the size parameter b, the constituent quark mass m_q and the coupling constant α_s.

4.3 ELECTROMAGNETIC PROPERTIES OF THE NUCLEON

In the present shell-model study based on the extended quark model of the nucleon, we have considered the one-particle contributions to evaluate the electromagnetic properties of the nucleon (which has been supposed to be a many-quark system).

To evaluate the magnetic moment, in addition to the contributions made by the 4 quarks in real shells we have also included the contributions made by the 47 occupied single-particle states within the core. But while calculating the radii and charge densities instead of including the additional contributions made by the whole core containing 47 occupied single-particle states we included the equivalent contribution made by the 'hole state' in a core. The values of the electromagnetic properties of the nucleon were obtained using three different sets of parameters. The results of the magnetic moments and radii are given in table 4.11 and table 4.12 respectively whereas the calculated charge densities of the proton and a neutron are presented graphically in figures 4.8 and 4.9 respectively. The electromagnetic properties of the nucleon are affected quite significantly by the inclusion of the quark-antiquark excitations in the quark model of the single nucleon.

TABLE 4.9
SINGLE-PARTICLE DENSITY MATRIX ELEMENTS

S.P.STATES		FOR PROTON			FOR NEUTRON		
i	j	set 1	set 2	set 3	set 1	set 2	set 3
1	1	0.6835	0.7264	0.7046	0.3632	0.4471	0.3844
2	2	0.3602	0.4168	0.3812	1.6071	1.5863	1.5491
3	3	0.3632	0.4471	0.3844	0.6835	0.7264	0.7046
4	4	1.6071	1.5863	1.5491	0.3602	0.4168	0.3812
5	5	2.9514	2.9250	2.9077	2.9374	2.9043	2.8815
6	6	2.9426	2.9175	2.8867	2.9434	2.9158	2.8913
7	7	2.9374	2.9043	2.8815	2.9514	2.9250	2.9078
8	8	2.9434	2.9158	2.8912	2.9426	2.9175	2.8868
9	9	0.0065	0.0164	0.0167	0.0273	0.0635	0.0608
9	18	0.0027	0.0052	0.0060	-0.0172	-0.0287	-0.0344
10	10	0.0070	0.0211	0.0200	0.0157	0.0384	0.0373
10	19	0.0027	0.0052	0.0060	-0.0172	-0.0287	-0.0344
11	11	0.0273	0.0635	0.0608	0.0065	0.0164	0.0167
11	22	-0.0172	-0.0287	-0.0344	0.0027	0.0052	0.0060
12	12	0.0157	0.0384	0.0373	0.0070	0.0211	0.0200
12	23	-0.0172	-0.0287	-0.0344	0.0027	0.0052	0.0060
13	13	2.9986	2.9910	2.9988	2.9976	2.9824	2.9979
13	26	-0.0001	-0.0050	-0.0005	-0.0006	-0.0079	-0.0009
14	14	2.9989	2.9907	2.9988	2.9981	2.9820	2.9979
14	27	-0.0001	-0.0005	-0.0005	-0.0006	-0.0079	-0.0009
15	15	2.9976	2.9824	2.9978	2.9986	2.9910	2.9989
15	30	-0.0006	-0.0079	-0.0009	-0.0001	-0.0050	-0.0005
16	16	2.9981	2.9820	2.9978	2.9989	2.9907	2.9989
16	31	-0.0006	-0.0079	-0.0009	-0.0001	-0.0050	-0.0005
17	17	0.0190	0.0202	0.0310	0.0095	0.0101	0.0156
18	9	0.0027	0.0052	0.0060	-0.0172	-0.0287	-0.0344
18	18	0.0154	0.0168	0.0255	0.0221	0.0262	0.0395
19	10	0.0027	0.0052	0.0060	-0.0172	-0.0287	-0.0344
19	19	0.0118	0.0135	0.0201	0.0347	0.0422	0.0635
20	20	0.0082	0.0101	0.0146	0.0473	0.0583	0.0875
21	21	0.0095	0.0101	0.0156	0.0190	0.0202	0.0310
22	11	-0.0172	-0.0287	-0.0344	0.0027	0.0052	0.0060
22	22	0.0221	0.0262	0.0395	0.0154	0.0168	0.0255
23	12	-0.0172	-0.0287	-0.0344	0.0027	0.0052	0.0060
23	23	0.0347	0.0422	0.0635	0.0118	0.0135	0.0201
24	24	0.0473	0.0583	0.0875	0.0082	0.0101	0.0146
25	25	2.9985	2.9739	2.9974	2.9988	2.9856	2.9982
26	13	-0.0001	-0.0050	-0.0005	-0.0006	-0.0079	-0.0009
26	26	2.9987	2.9801	2.9979	2.9988	2.9855	2.9981
27	14	-0.0001	-0.0050	-0.0005	-0.0006	-0.0079	-0.0009
27	27	2.9990	2.9863	2.9984	2.9987	2.9853	2.9981
28	28	2.9993	2.9925	2.9989	2.9987	2.9852	2.9981
29	29	2.9988	2.9856	2.9981	2.9985	2.9739	2.9975
30	15	-0.0006	-0.0079	-0.0009	-0.0001	-0.0050	-0.0005
30	30	2.9988	2.9855	2.9981	2.9987	2.9801	2.9980
31	16	-0.0006	-0.0079	-0.0009	-0.0001	-0.0050	-0.0005
31	31	2.9987	2.9853	2.9980	2.9990	2.9863	2.9985
32	32	2.9987	2.9852	2.9980	2.9993	2.9925	2.9990

4.3.1 MAGNETIC MOMENT OF THE NUCLEON

Results of the nucleon's magnetic moment obtained from the calculations based on the present model and the 3q-model using the given sets of parameters (table 4.2) are presented in table 4.11. The procedure adopted in this calculation has already been described in section 2.7.1.

Comparing the results of the nucleon's magnetic moment obtained in the present model and the values of the magnetic moment of the nucleon obtained in the 3q-model given for each set of parameters in a table 4.11, we can see that the predictions of the present model are better than the values predicted by the 3q-model. From the above comparison, the contributions of the $q^4\bar{q}$-components to the magnetic moment of the nucleon can also be found.

These results obtained with parameters set 3 show that the $q^4\bar{q}$-components of the nucleon's wavefunction do carry 13-14 % contributions of the magnetic moment of the nucleon. This is a quite significant part of the total magnetic moment of the nucleon. Similarly the results of the proton's and a neutron's magnetic moment for the other two sets of parameters show that the part of the magnetic moment contributed by the $q^4\bar{q}$-components is 7-9 % of the predicted magnetic moment of the proton and 5-8 % of the predicted magnetic moment of the neutron.

TABLE 4.10

MATRIX ELEMENTS OF l_z AND s_z.

Single-particle Orbits				Orb: M.Elements	Spin M.Elements
u-quarks		d-quarks			
initial	final	initial	final	$\langle l_z \rangle_{ij}$	$\langle s_z \rangle_{ij}$
i	j	$\bar{i}$	$\bar{j}$		
3	3	1	1	0.000000000	-0.499999999
4	4	2	2	0.000000000	+0.499999999
7	7	5	5	0.000000000	-0.499999999
8	8	6	6	0.000000000	+0.499999999
11	11	9	9	-0.666666667	+0.166666666
12	12	10	10	+0.666666667	-0.166666666
15	15	13	13	-0.666666667	+0.166666667
16	16	14	14	+0.666666667	-0.166666667
21	21	17	17	-1.000000000	-0.500000012
22	22	18	18	-0.333333333	-0.166666667
23	23	19	19	+0.333333333	+0.166666667
24	24	20	20	+1.000000000	+0.500000000
29	29	25	25	-1.000000000	-0.500000000
30	30	26	26	-0.333333333	-0.166666667
31	31	27	27	+0.333333333	+0.166666667
32	32	28	28	+1.000000000	+0.500000000
11	22	9	18	+0.471404521	-0.942809042
12	23	10	19	+0.471404521	-0.942809042
15	30	13	26	+0.471404521	-0.942809042
16	31	14	27	+0.471404521	-0.942809042
22	11	18	9	+0.471404521	-0.942809042
23	12	19	10	+0.471404521	-0.942809042
30	15	26	13	+0.471404521	-0.942809042
31	16	27	14	+0.471404521	-0.942809042

TABLE 4.11

NUCLEON'S MAGNETIC MOMENTS

Set No:	Model	μ_p (n.m)	μ_n (n.m)	μ_n / μ_p
I	3q-model	2.997	- 1.998	- 0.667
	$(3q + q^4\bar{q})$ -model	3.219	- 2.154	- 0.676
II	3q-model	1.99	- 1.33	- 0. 668
	$(3q + q^4\bar{q})$ -model	2.18	- 1.40	- 0.642
III	3q-model	2.61	- 1.74	- 0.667
	$(3q + q^4\bar{q})$ -model	3.007	- 2.031	- 0.675

* n.m denotes nuclear magneton.

If we compare the results of the nucleon's magnetic moment obtained from the calculations based on the present model with the given three different sets of parameters (table 4.2), we see that the values of the magnetic moment of the proton and a neutron predicted with parameters set 3 are more reasonable than the values obtained for the other two sets of parameters.

The values of the proton's and the neutron's magnetic moments obtained for the parameters set 3 are shown in the 3rd main row of the table 4.11. The results of the 3q-model and the present model are given in the 1st and 2nd entries of the row respectively. The values of the magnetic moments of a proton and a neutron predicted in the present model are 3.007 n.m and -2.031 n.m

respectively. These values seem to be quite reasonable because these are close to the experimental values . Our calculated magnetic moments of the neutron and the proton are 6-8 % greater than the observed values. Their ratio μ_n/μ_p=-0.675 is in impressive agreement with the experimental value of -0.685 [77].

The magnetic moments of a proton and a neutron obtained in 3q-model for the parameters set 3 are 2.61 n.m and -1.74 n.m respectively. We obtained their ratio μ_p/μ_n=-1.5 that is also a good prediction of the present calculations.

The 3q-model's predictions [7,79] of μ_p/μ_n ratio is generally to be -1.5 which is considered to be in good agreement with the observed value. Our predicted value of the ratio μ_p/μ_n =-1.48 in the present quark model is,therefore, in quite good agreement with the experimental value of -1.46 [77]. Our predicted values of the magnetic moment of the proton and a neutron in the present model are either better than or consistent with their values obtained from the previous calculations like bag-model's calculations [14b,82] and the skyrme model's investigation [83].

Previously With the same model approach, quite reasonable results for the nucleon's magnetic moment have been obtained by using the resonating group method [37,38].

For parameter set 3, we have predicted that the magnetic moments contributed by the u-quarks and d-quarks in a proton's magnetic moment are 2.657 n.m and 0.351 n.m respectively. The parts of the neutron's magnetic moment carried by the u-quarks and d-quarks are -0.702 n.m and -1.328 n.m respectively. These differences can be explained as follows. In a proton the 0S

valence-shell may contains 3 or 4 total quarks, but at least 2 are u-quarks and 1 is a d-quark. In a neutron, at least 2 d-quarks and 1 u-quark are contained in the 0S valence-shell. The u-quark possesses positive charge two times greater than the negative charge possessed by a d-quark. Therefore the proton, having greater positive charge in the single-particle states (of the 0S valence-shell in the present case) with greater values of the density matrix elements, will get magnetic moment contributed by the u-quarks more than the part of the magnetic moment contributed by the d-quarks. For the neutron the contributions made by the u-quarks and d-quarks are the other way round which can be understood in a similar way.

We have also noticed that the contribution made by the orbital angular momentum in the magnetic moment is negligibly small as compared to the contribution made by the spin angular momentum. The reason is that since we have considered the quark as pointlike spin 1/2 charged fermion, according to Dirac's theory its magnetic moment due to the spin should have gyromagnetic ratio g (that comes as relativistic correction due to its charge and magnetic field interaction) equal to 2. We have taken the g-factor (g=2) in a magnetic moment due to spin angular momentum becuase of the fact that having a light quark, one can not obtain a reasonable value for μ_p with non-relativistic considerations. The second reason is that the magnetic moment due to the orbital angular momentum is contributed by only the p-shells (with l=1) states as the s.p.states with l=0 contribute nothing at all whereas the magnetic moment due to spin is contributed by all the given

s.p.states including s.p.states of the 0S shell which have got comparatively greater values of their density matrix elements than the 0P states in the present case.

4.3.2 MASS AND CHARGE R.M.S RADII OF THE NUCLEON

The root mean square mass and charge radii of the proton and the neutron have been worked out, using three given sets of parameters, by the procedures mentioned in sections 2.7.2 and 2.7.3 respectively. The results of the nucleon's radii obtained from the calculations based on the 3q-model and the present quark model are given in the table 4.12. Comparing the 1st and 2nd entries of the results for each set of parameters, we find that the values of the radii predicted in our present model are better than the values calculated in the 3q-model. The mesonic contribution to the mass and the charge r.m.s radius of the nucleon is 3-5% of the total radius which is a good contribution to be considered. This may be increased by including the q^2q^{-2} and other possible higher excitations.

If we compare the values of the mass and charge r.m.s radii of the proton and a neutron obtained from the calculations performed within the framework of the present $(3q+q^4\bar{q})$-quark model using the given three different sets of parameters, we find the values of the nucleon's radii obtained with parameters set 3 better than the values of the radii obtained for the other two sets of model parameters.

TABLE 4.12

Nucleon's root mean squared mass and charge radii.

Set No:	Model	Mass radius	Charge radius		
		$\langle r^2 \rangle^{\frac{1}{2}}$ (fm)	$\langle r^2_{ch} \rangle^{\frac{1}{2}}_p$ (fm)	$\langle r^2_{ch} \rangle_n$ (fm)	$\lvert \langle r^2_{ch} \rangle \rvert^{\frac{1}{2}}_n$ (fm)
1	3q-model	0.73	0.73	$+5.476 \times 10^{-7}$	0.00074
	$(3q+q^4 \bar{q})$ - model	0.752	0.754	-0.00323	0.0568
2	3q-model	0.64	0.64	$+4.10 \times 10^{-7}$	0.00064
	$(3q+q^4 \bar{q})$ - model	0.668	0.661	-0.01096	0.1047
3	3q-model	0.66	0.66	$+4.356 \times 10^{-7}$	0.00066
	$(3q+q^4 \bar{q})$ -model	0.687	0.695	-0.00545	0.0738
Experimental[84] values		0.836 fm		$-0.12\ fm^2$	0.34 fm

The r.m.s mass and charge radii of the proton and the neutron predicted theoretically by our present model of an isolated nucleon (with model parameters set 3) are

$$\langle r^2 \rangle^{\frac{1}{2}}_p = 0.687 \text{ fm}, \quad \langle r^2 \rangle^{\frac{1}{2}}_n = 0.687 \text{ fm}, \quad \langle r^2_{ch} \rangle^{\frac{1}{2}}_p = 0.695 \text{ fm}$$

and $\langle r^2_{ch} \rangle_n = -0.00545\ fm^2$ i.e $\lvert \langle r^2_{ch} \rangle_n \rvert^{\frac{1}{2}} = 0.0738$ fm

Apparently, these values are not very close to the observed values [84] but are quite reasonable.The agreement with the experimental values is found to be within about 84-86% except for the neutron's charge mean square radius which is smaller than the observed

value of -0.12 fm^2. Our results of the nucleon's r.m.s radii do agree with the results obtained from the calculations based on the same model approach [37]. Y.Fujiwara and K.T.Hecht [37] included relativistic corrections in the radii whereas our consideration was purely non-relativistic. Basically their work presented in reference [37] is based on the same principle as that of ours but they performed their calculation in a smaller space with parameters set 2 by making use of the resonating group method.

In the present model, we predicted the mean square radius of the neutron to be non-zero with a negative sign which is favoured by the experimental data [85]. The value of the neutron's charge root mean square radius is smaller than the experimental value but it is in good agreement with the value predicted in a similar study [37] . Our predicted proton's charge r.m.s radius seems to be smaller than its generally accepted value of 0.81 fm [88] but is quite reasonable as it has got a fair consistency with the value obtained from the previous investigation [37] based on the same extended quark model of the single nucleon. It is also consistent with the proton's charge radius obtained in the bag model study of the nucleon [14b].

We expected the values of the nucleon's radii to be smaller in the present investigation because of the reason that we have not included the all possible quark-antiquark excitations except $q\bar{q}$-excitations. q^2q^{-2} and other higher excitations have been ignored because it is then too hard to handle the calculations with all possible $q\bar{q}$-excitations at present. The gap between our theoretically predicted values and the observed values of the

nucleon's radii may be either removed or minimised by introducing the q^2q^{-2} and the other higher possible excitations into the model space when it could be managed to do big calculations with the availability of more sophisticated computing machines in future.

Introducing the higher quark-antiquark excitations into the model space, the numerical values of the model parameters will have to be re-adjusted. The new value of the size parameter b will change the single quark contributions to the mean square radius and hence the root mean square mass and charge radius of the single nucleon gets changed.

A simple 3q-model of the single nucleon indicates that the charge density should be zero everwhere inside the neutron and therefore it suggests the neutron's charge mean square radius to be zero as well. Our calculated values (in 3q-model) of the charge mean square radius of the neutron for the three different sets of parameters shown in the table 4.12 are also zero because the given negligibly small values are due to the rounding error in the computation. It is not easy to predict the charge mean square of the neutron to be non-zero with negative sign in the simple versions [90] of the quark model of an isolated nucleon.

The mass and charge radii of the proton in 3q-model are found to be equal but there is a small difference between the mass radius and the charge radius in the present model. This difference may be due to the re-distribution of the charge inside the nucleon caused by the inclusion of the mesonic contributions into the nucleon's wavefunction.

Since the hyperfine interactions between the quarks with the same flavour are repulsive and the hyperfine interactions between the quarks with different flavour are attractive [89], the uu quarks or dd quarks get further apart from one another and ud quarks get closer to each other. Because of this fact the u-quarks and the d-quarks intermix with each other.

In our present model the inclusion of a mesonic contributions, of parameter set 3, in an internal wavefunction of the nucleon has increased the nucleon's radii by 4.1-5.3% and made a small difference between the charge and mass radii of the proton. Our model could not give the experimental value of the neutron's charge mean square radius. Its predicted value is too small as compared to the observed value but the model predicted the sign of the mean square radius of the neutron to be negative as reported by the experimental literature [84,85].

The negative sign of the mean square charge radius of the neutron is attained due to the inhomogeneous distribution of the charge caused by the spin-dependent interactions between the quarks in accordance with the symmetry requirement of the spin-isospin wavefunction of the neutron as argued in reference [86]. The inhomogeneity of the charge distribution seems to appear consistently in many quark systems where the resultant overall force is of a repulsive nature [89].

In a neutron, therefore,the repulsive forces between the pairs of the d-quarks (which are greater in number than the uu-pairs) in spin 1 state will consequently move the negative charge (i.e d-quarks) farther from the centre of mass than the positive charge

(i.e u-quarks). This indicates that the neutron's charge mean square radius should be negative. This is confirmed by examining the charge distribution for the neutron shown in figure 4.7, where we see that the negative charge (d-quarks) exists farther from the centre of mass of the neutron than the positive charge (u-quarks).

4.3.3 CHARGE DENSITY OF THE NUCLEON

Following the procedure mentioned in section (2.7.4), we have calculated the charge density of a nucleon using the three different sets of parameters (shown in table 4.2).

We obtained the proton's charge density as a function of radial distance r for the three sets of model parameters given by

$$\{\rho_{ch}(r)\}_1^p = (0.766 + 0.12\, r^2)\, e^{-(2.78)\, r^2} \qquad (4.3.3.1)$$

$$\{\rho_{ch}(r)\}_2^p = (1.132 + 0.28\, r^2)\, e^{-(3.64)\, r^2} \qquad (4.3.3.2)$$

$$\{\rho_{ch}(r)\}_3^p = (0.963 + 0.41\, r^2)\, e^{-(3.43)\, r^2} \qquad (4.3.3.3)$$

The neutron's charge density (as a function of r) calculated for the given sets of parameters is as follows;

$$\{\rho_{ch}(r)\}_1^n = (0.682 - 0.013\, r^2)\, e^{-(2.78)\, r^2} \qquad (4.3.3.4)$$

$$\{\rho_{ch}(r)\}_2^n = (0.492 - 0.12\, r^2)\, e^{-(3.64)\, r^2} \qquad (4.3.3.5)$$

$$\{\rho_{ch}(r)\}_3^n = (0.021 - 0.048\, r^2)\, e^{-(3.43)\, r^2} \qquad (4.3.3.6)$$

In the above expressions (4.3.3), p and n used on the top right of

TABLE 4.13(a)

PROBABILITY DENSITY OF THE S.P.ORBITS

REAL SINGLE PARTICLE ORBITS

S.P.Orbit number i	Square of the modulus of the single-particle wavefunction. $\lvert \Phi_i \rvert^2$		
	Set 1	Set 2	Set 3
*			
1	1.14050 F_1	1.24819 F_1	0.83142 F_1
2	1.14050 F_1	1.24819 F_1	0.83142 F_1
3	1.14050 F_1	1.24819 F_1	0.83142 F_1
4	1.14050 F_1	1.24819 F_1	0.83142 F_1
9	2.60744 F_2	3.03059 F_2	1.53967 F_2
10	2.60744 F_2	3.03059 F_2	1.53967 F_2
11	2.60744 F_2	3.03059 F_2	1.53967 F_2
12	2.60744 F_2	3.03059 F_2	1.53967 F_2
17	3.91117 F_3	4.54589 F_3	2.30951 F_3
18	1.30972 F_4	1.51530 F_4	0.76984 F_4
19	1.30972 F_4	1.51530 F_4	0.76984 F_4
20	3.91117 F_3	4.54589 F_3	2.30951 F_3
21	3.91117 F_3	4.54589 F_3	2.30951 F_3
22	1.30972 F_4	1.51530 F_4	0.76984 F_4
23	1.30972 F_4	1.51530 F_4	0.76984 F_4
24	3.91117 F_3	4.54589 F_3	2.30951 F_3

* $F_1 = e^{-\frac{r^2}{b^2}}$, $F_2 = r^2 e^{-\frac{r^2}{b^2}}$

$F_3 = (r^2 - z^2) e^{-\frac{r^2}{b^2}}$ and $F_4 = (r^2 + 3z^2) e^{-\frac{r^2}{b^2}}$

TABLE 4.13(b)

PROBABILITY DENSITY OF S.P.ORBITS

S.P Orbit number	SEA SINGLE-PARTICLE ORBITS Square of the modulus of the S.P.wavefunction $\lvert \Phi_i \rvert^2$		
i	Set 1	Set 2	Set 3
*			
5	1.14050 F_1	1.24819 F_1	0.83142 F_1
6	1.14050 F_1	1.24819 F_1	0.83142 F_1
7	1.14050 F_1	1.24819 F_1	0.83142 F_1
8	1.14050 F_1	1.24819 F_1	0.83142 F_1
13	2.60744 F_2	3.03059 F_2	1.53967 F_2
14	2.60744 F_2	3.03059 F_2	1.53967 F_2
15	2.60744 F_2	3.03059 F_2	1.53967 F_2
16	2.60744 F_2	3.03059 F_2	1.53967 F_2
25	3.91117 F_3	4.54589 F_3	2.30951 F_3
26	1.30972 F_4	1.51530 F_4	0.76984 F_4
27	1.30972 F_4	1.51530 F_4	0.76984 F_4
28	3.91117 F_3	4.54589 F_3	2.30951 F_3
29	3.91117 F_3	4.54589 F_3	2.30951 F_3
30	1.30972 F_4	1.51530 F_4	0.76984 F_4
31	1.30972 F_4	1.51530 F_4	0.76984 F_4
32	3.91117 F_3	4.54589 F_3	2.30951 F_3

* $F_1 = e^{-\frac{r^2}{b^2}}$, $F_2 = r^2 e^{-\frac{r^2}{b^2}}$

$F_3 = (r^2 - z^2) e^{-\frac{r^2}{b^2}}$ and $F_4 = (r^2 + 3z^2) e^{-\frac{r^2}{b^2}}$

the curly brackets represent the proton and the neutron respectively. The indices 1,2 and 3 have been used for the model parameters set 1, set 2 and set 3 respectively.

The above expressions show that the charge density of the nucleon is a function of the radial distance r only and therefore the charge distribution is spherically symmetric. From table 4.13, it is clear that the single-particle states in $0P_{3/2}$ shell have got z-dependent term in their probability density values. But when we add up the charge density contributions carried by the single-particle states, the coefficient of the term containing z becomes zero and that is why we obtain the total charge density of the nucleon free of z-dependent term.

The results of the charge density of the proton and a neutron (for parameters set 3) are graphically represented by the plots shown in the figures 4.6 and 4.7 respectively. From the plot shown in figure 4.6, it is clear that the charge density of the proton is roughly uniform very near to the centre and then falls relatively slow through some distance with the increase of radial distance to a certain point r = 0.66 fm (the r.m.s charge radius of the proton obtained with parameters set 3 in a 3q-model) beyond which the charge density drops exponentially to the negligibly small values at the larger distances. The shape of the distribution of charge in the neutron appears to be the same (as that of a proton) upto the radial distance r = 0.66 fm. But after that the charge density of the neutron changes sign and shows the parabolic variations in its magnitude with increasing r. At large values of a radial distance r, the neutron's charge density also approaches negligible small

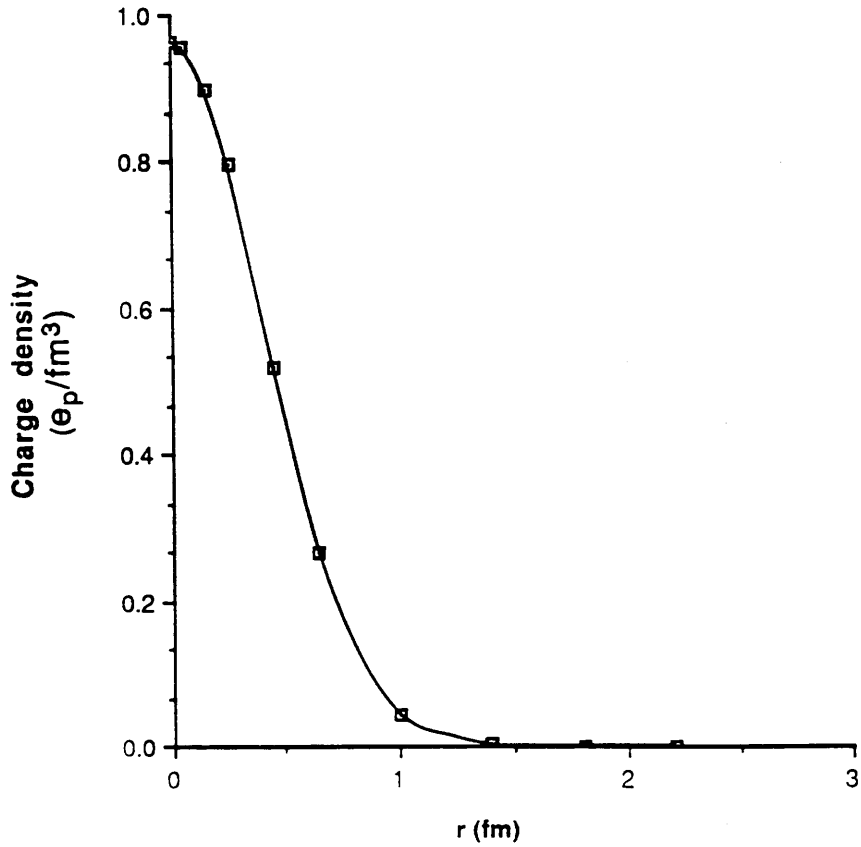

Fig: 4.6 Proton's charge density versus radial distance r for parameters set 3.

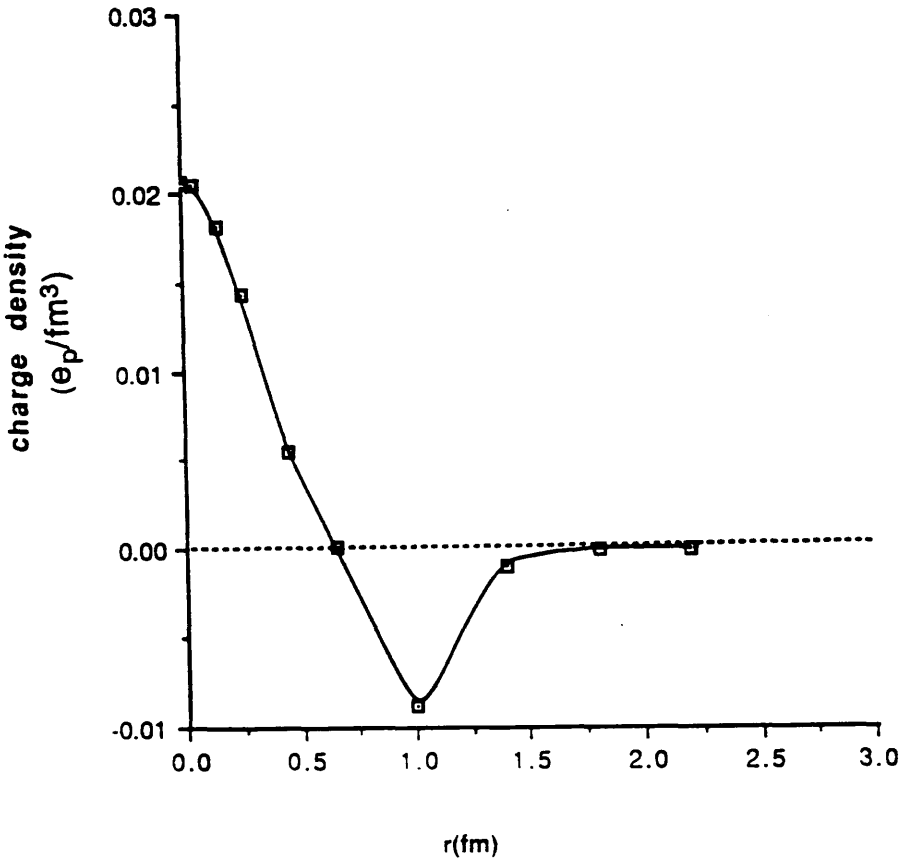

Fig: 4.7

Neutron's charge density versus radial distance r for the parameter set 3. Below 0-line the charge density has been taken 10 times greater than the actual value.

values. Comparing the values of the protons and a neutron's charge density at any radial distance r, It can be noted that the value of the neutron's charge density is very small as compared to the value of the proton's charge density. The charge density curve of the proton shows that as the proton possesses more positive charge (carried by the u-quarks) than the negative charge (carried by the d-quarks), its charge density has got only positive sign though it has negative contributions due to its negative charge carriers. It seems that the negative charge extending beyond the positive charge (nearer to the centre of the proton) gets neutralised due to intermixing of u and d quarks (near the region of the negative charge) caused by the hyperfine interactions between quarks with unlike flavours mentioned in section 4.3.2. Consequently the proton's charge density becomes smaller and smaller at large values of r but it never becomes negative.

On the other hand if we re-examine the charge density of the neutron we see that it is partly positive and partly negative. The negative part starts at the radial distance r roughly greater than 0.66 fm. The negative part of the neutron's charge density curve goes on increasing in the negative side for r>0.66 fm and reaches a maximum negative value at r=1.0 fm and then beyond that it starts decreasing as the radial distance goes on increasing. At the distance (roughly speaking) r>1.5 fm the neutron's charge density goes on decreasing to negligibly small values. The charge density curve of the neutron shows that the positive charge (i.e u-quarks) dominates in the vicinity of the neutron's centre of mass and the negative charge (i.e d-quarks) extends beyond the positive charge

to greater distances. The charge segregation in the neutron is caused by the net repulsive quark-spin-dependent interactions as discussed in section 4.3.2. Due to this inhomogeneity of charge observed in a neutron,the mean square radius of the neutron should be negative [86] which is in agreement with the experimental information [84,85].

According to the simple quark model [7,79-81] the charge density of the neutron should be everywhere zero because of the fact that a u-quark carry as much positive charge as the total negative charge carried by the two d-quarks. Actually the neutron's charge density is not exactly zero because if it were zero then the neutron's mean square radius should not be non-zero in contrast to the experimental evidences [84,85].

Our theoretically predicted value of the neutron's charge mean square radius is non-zero with negative sign as also reported in references [37,82,87].

The plots shown in figures 4.8 and 4.9 represent the charge density of a proton and a neutron respectively obtained from the calculations based on the present model using the three given sets of parameters.The part of the curves beyond r= 0.66 fm is very interesting because it corresponds to the mesonic contributions of the nucleon. The differences between the values of the charge density of different sets of parameters for any particular radial distance r are very small as compared to their total values. The neutron's charge density curves (shown in fig 4.9) for the three different sets of parameters appear to have unduly large differences. This arises from re-scaling, as the negative values of

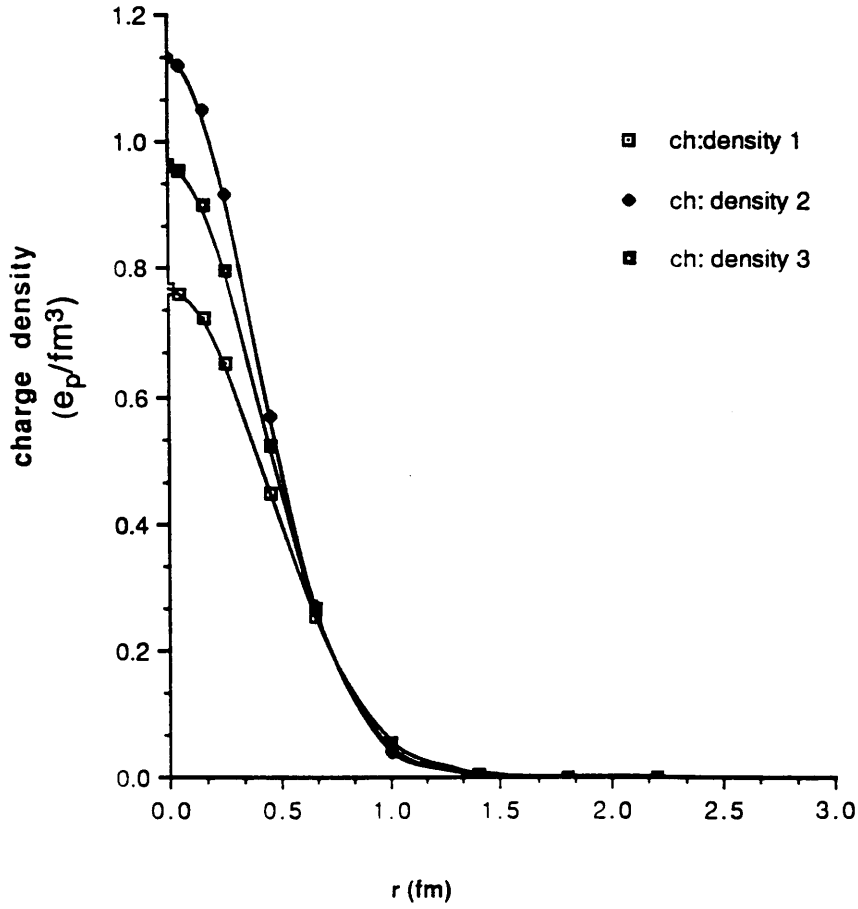

Fig 4.8

Proton's charge density versus radial distance r
for three different sets of parameters.

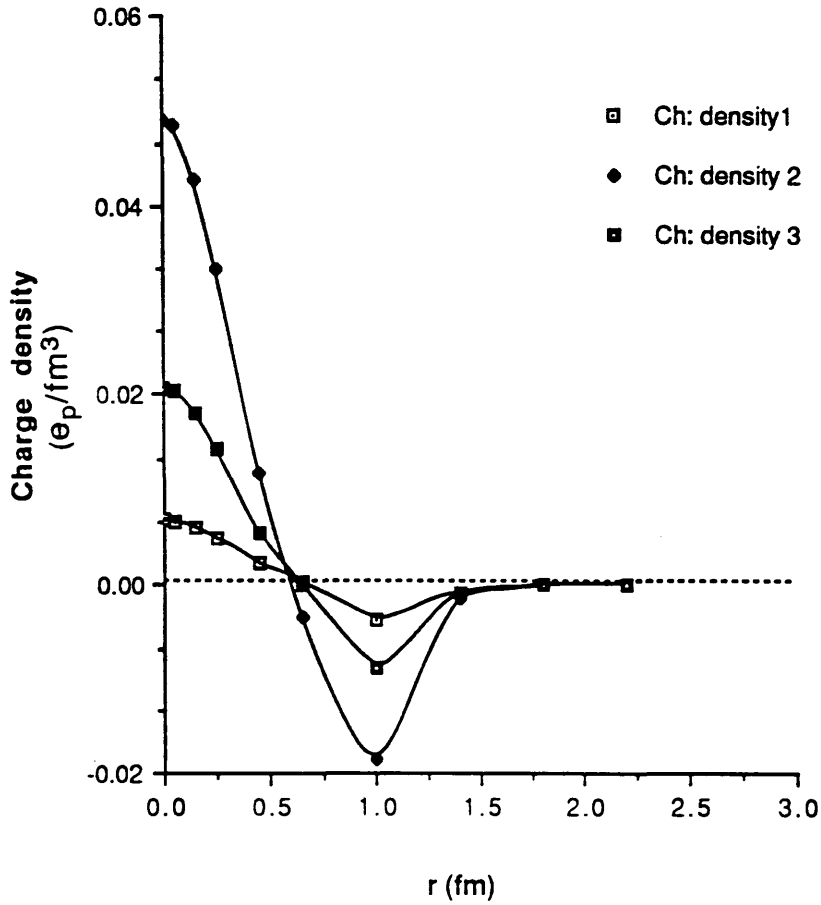

Fig: 4.9

Neutron's charge density versus radial distance r for three different sets of parameters. Below 0-line the charge density has been taken 10 times greater than the actual value.

the charge density have been taken 10 times greater than their actual values. The charge density curves of the proton and neutron for the different sets of parameters show differences in their maximum or greatest positive values (also the negative values in case of neutron). This different quantitative distribution of charge for the three sets of model parameters happens due to the spin-spin perturbative force which depends upon the numerical values of the parameters. Quantitatively however,the shape and the general appearance of the charge distribution within the nucleon does not look very sensitive to the model parameters.

Our predicted electric charge distribution of the proton and of the neutron looks the same as that obtained previously [83,91] showing a significant mesonic contribution.

In fact the inclusion of the mesonic contributions into the internal wavefunction of the nucleon does affect the charge density of the nucleon. No doubt it is not easy to understand the actual mechanism of the distribution of the charge inside the nucleon described by the present model. In spite of that, the effects of the inclusion of the $q\bar{q}$-excitations into the nucleon's wavefunction are quite important.

Since we have obtained quite significant effects on the electromagnetic properties of the nucleon due to the inclusion of quark-antiquark excitations, these may provide a basis for a proper understanding of the internal features of the nucleon's structure and a satisfactory understanding of the nucleon-nucleon interaction.

CHAPTER 5

CONCLUSION

Our aim of the present investigations was to study the effects of introducing quark-antiquark excitations into the internal wavefunction of the single nucleon. We have considered the ground state energy (i.e. mass) of the nucleon and its electromagnetic properties within the framework of the shell model.

We introduced a new technique into the framework of the Glasgow shell model method, namely, colour code representation for storing basis states which is more compact and effective than the bit-mapped representation previously used. This technique when used in computational manipulations, makes the Glasgow shell model programme more useful for many quark calculations. If the colour codes are constrained by the condition that $R \leq G \leq B$, then automatically the space is truncated by removing nearly all unphysical coloured states.

Using the Glasgow shell model computational techniques [45], we incorporated the quark-antiquark excitations into a quark model of the nucleon which have been generated by the $(q\bar{q})$-pair creation interaction (1.3) as discussed in chapter 1. We first performed calculations to calculate the ground state energy of a nucleon with parameters set 1 and set 2 of table 4.2 in terms of the simple 3-quark model and then the same calculations were repeated with the same set of parameters in the present model.

The ground state energy of the nucleon computed in the present model is much smaller than the energy calculated in the simple 3q-model. Since we were interested in reproducing the observed mass of the nucleon on the basis of the present model, we re-evaluated the numerical values of the parameters (given as parameters set 3 in table 4.2) as described in section 4.1.2.1. To choose suitable values of the parameters, we performed a number of calculations with parameters set 2 to check the sensitivity of the nucleon energy to the numerical values of the parameters. By changing the value of one of the parameters with constant values of the others, we calculated the energy of the nucleon. The variations in nucleon energy by changing one of the parameters b, α_s and a_c while keeping the others constant, has been shown by the plots given in fig. 4.3. It is clear from fig. 4.3 that the nucleon energy is sensitive more or less to all the four parameters but is strongly dependent of the a_c, the strength of the phenomenological confining potential. The expressions (4.1.2.2) and (4.1.2.3) usually used to derive the values of the coupling constant α_s and confining potential constant a_c respectively, could not give the correct values of α_s and a_c to produce the nucleon energy closer to the observed mass of a nucleon. Having re-adjusted the numerical values of the parameters with the help of the data obtained, we chose the values of the parameters compatible with the present model in reproducing the observed mass of the proton. It has been noticed that the expressions (4.1.2.2) and (4.1.2.3) may be valid in the extended quark model with different proportionality constants.

As we described earlier, the energy of the nucleon calculated in the present extended quark model of the nucleon is less than the

nucleon energy calculated in the simple 3-quark model with the same parameters.

The computed probabilities of the shell occupancies in the present model suggests that 45% of total contributions are carried by the $(3q)(q\bar{q})$-components (as shown in table 4.7) of the improved wavefunction of the single nucleon, which is a quite significant part of the wavefunction. The $(3q)(q\bar{q})$-components with the configuration $(0S)^3(0P)(0\bar{S})$ make dominant contribution to the wavefunction as compared to the configuration $(0S)^4(0\bar{P})$.

The model predictions show that the $(3q)(q\bar{q})$ -components do not contribute in the same ratio to the electromagnetic properties of the nucleon, but even then their contributions are quite significant. The components of the wavefunction arising from the inclusion of $q\bar{q}$-excitations in the quark model of the single nucleon contribute nearly 5% and 13-14% to the root mean square radii and the magnetic moment of the single nucleon respectively. The present model predicts that the mean square charge radius of the neutron is negative whereas the simple 3q-model fails to predict this experimental fact.

Generally, the values of the r.m.s radii of the nucleon obtained in the present model are smaller than their observed values. This we expected because relativistic effects are not included in the model. If it becomes possible (as may be expected in the future) to perform calculations with greater number of $q\bar{q}$-excitations using more efficient computing machines, one may obtain improved values of the radii, with re-adjusted numerical values of the parameters. It is also hoped that our calculated magnetic moment of the nucleon which is slightly greater than the

experimental value may be brought closer to the observed value if the numerical value of m_q can be re-adjusted a little more than our suggested value m_q = 359.73 Mev/c^2.

The present extended quark model of the single nucleon describes the charge density of a nucleon quite successfully. Specially, in the simple 3-quark model it is quite difficult to produce the charge density of the neutron to be non-zero but the present model predicts that the charge density of the neutron is non-zero and its explicit negative part of the curve (as shown in fig 4.7 and fig 4.9) appears due to the inclusion of mesonic contributions into the internal wavefunction of the neutron. The r.m.s. mass radius of the neutron calculated with parameters set 3 is 0.66 fm in the simple 3-quark model whereas in the present model it has been computed equal to 0.687 fm. From fig 4.7, it is clear that the negative part of the curve starts just after the 0.66 fm which is predicted by the present model. Because of this fact it can be concluded that the present model predicts that the positive charge (i.e. u-quarks) dominates near the centre of mass of the neutron and the negative charge (i.e. d-quarks) extends beyond the positive charge to the outer radial distances.It is also clear that the charge distribution beyond 0.66 fm (shown in fig. 4.6) arises from the inclusion of mesonic components into the wavefunction of the proton. The distribution of the charge beyond 0.66 fm is very important for the description of the medium range and long range of the nuclear force usually explained by the one pion exchange potentials.

As we mentioned earlier the inclusion of $(q\bar{q})$-excitations is low energy effect, it may be expected that probably the mesonic

contributions are mostly displayed by the pionic effects.

Since we did not include all the possible quark-antiquark excitations (which could not be managed at present), we did not expect our calculated values of the electromagnetic properties to be exactly equal to the experimental values.

Apart from this one can think of several ways in which the calculations could be improved. We suggest and recommend that the following things be taken into account as these may help to further improve the results obtained in the present extended quark model.

1. The model space can be extended to include q^2q^{-2} -excitations and as many other higher excitations as one can possibly manage.
2. The part of the transition potential involving the terms of order $1/c^2$ (which has been ignored in the present work because of its unimportance) can be introduced as it makes some contribution to the results [42].
3. In quark-quark interaction potential, one can also include the spin -orbit and tensor terms (which were also ignored because their contributions are not very important), but we suggest that it may improve the results as in the present shell model study the p-energy sub levels appeared degenerate.

The disadvantage of this approach is that very large number of particles (51 quarks in 96 orbits) makes the calculation simple in principle but very time consuming. Another approach is to regard antiquark as a new type of particle. The number of particles (quarks and antiquarks) is then no longer constant, which is serious but soluble problem, but they are only 3 or 5 in number. This approach is much more complex in principle and leads to more

involved computer programmes which do however require much less time. This means that more complex physical systems may be accessible to the investigation by this method. This work is in progress at the moment.

Finally we conclude that the extended quark model of the single nucleon in conjunction with Glasgow shell model presents a unified model which describes the hadron spectroscopy quite successfully. Hopefully, the present work extended in the light of the above recommendations will make a very important study and future work of this nature will be very interesting.

APPENDIX A

A.1 GAMMA FUNCTION

A.1.1 DEFINITION

The gamma function is defined [69]by

$$\Gamma(x) = \int_0^\infty e^{-t}\, t^{x-1}\, dt \qquad (x > 0) \qquad \text{(A.1.1.1)}$$

A.1.2 PROPERTIES AND SPECIAL VALUES.

$$\Gamma(x+1) = x! \qquad (\text{For } x \geq 0) \qquad \text{(A.1.2.1)}$$

$$\Gamma(x+1) = x\,\Gamma(x) \qquad (\text{for } x > 0) \qquad \text{(A.1.2.2)}$$

Using definition and the above properties of gamma function, we get some special values; e.g

$$\Gamma(1) = \Gamma(2) = 1$$

$$\Gamma(\tfrac{1}{2}) = \sqrt{\pi}$$

$\Gamma(x)$ has a simple pole at x=0 or a negative integer

A.2 BINOMIAL EXPANSION AND BINOMIAL COEFFICIENT

A.2.1 BINOMIAL THEOREM.

The binomial theorem states that for n > 0, we have

$$(a+b)^n = a^n + c_1^n\, a^{n-1}b + c_2^n\, a^{n-2}\, b^2 + \ldots\ldots + c_{n-1}^n\, a\, b^{n-1} + c_n^n\, b^n \qquad \ldots\ldots \text{(A.2.1.1)}$$

where $c^n{}_r$; r= 0,1,2,3 . . . . n are called binomial coefficients.

A.2.2 BINOMIAL COEFFICIENT.

The binomial coefficient is defined as

$$C_r^n = \frac{n!}{(n-r)!\ r!} \qquad \text{(A.2.2.1)}$$

By definition we can get

$$c_0^n = c_n^n = 1 \qquad \text{(A.2.2.2)}$$

$$c_r^n = c_{n-r}^n = \frac{n(n-1)\ .\ .\ .\ (n-r+1)}{r!} \qquad \text{(A.2.2.3)}$$

$$c_r^{n+1} = c_r^n + c_{r-1}^n \qquad \text{(A.2.2.4)}$$

The binomial coefficient can also be denoted by $\binom{n}{r}$.

A.2.3 INFINITE BINOMIAL EXPANSION

According to the binomial theorem, we can have the expansion (for $\alpha > 0$),

$$(1+x)^{\alpha} = 1 + \alpha x + \frac{\alpha(\alpha-1)}{2!}x^2 + \frac{\alpha(\alpha-1)(\alpha-2)}{3!}x^3 + \ .\ . \qquad \text{(A.2.3.1)}$$

The above expansion may be described by a generating function as

$$(1+x)^{\alpha} = \sum_{r=0}^{\infty} \binom{\alpha}{r} x^r$$

$$= \sum_{r=0}^{\alpha} \frac{\alpha!}{(\alpha-r)!\ r!} x^r$$

i.e $$(1+x)^{\alpha} = \sum_{r=0}^{\infty} \frac{\Gamma(\alpha+1)}{\Gamma(\alpha-r+1)\ r!} x^r \qquad \text{(A.2.3.2)}$$

Similarly we have (for $\alpha > 0$)

$$(1+x)^{-\alpha} = 1 - \alpha x + \frac{(-\alpha)(-\alpha-1)}{2!}x^2 + \frac{(-\alpha)(-\alpha-1)(-\alpha-2)}{3!}x^3 + \ .\ .\ .\ .$$

$$= \sum_{r=0}^{\infty} (-1)^r \frac{\Gamma(\alpha+r)}{\Gamma(\alpha)r!} x^r \qquad \text{(A.2.3.3)}$$

A.3 ASSOCIATED LAGUERRE POLYNOMIAL

A.3.1 DEFINITION.

The associated laguerre polynomial is defined by [69]

$$L_n^k(x) = \sum_{r=0}^{n} (-1)^r \frac{(n+k)!}{(n-r)!\ (k+r)!\ r!} x^r \qquad \text{(A.3.1.1)}$$

A.3.2 PROPERTIES.

a) Generating Function.

$$\frac{\exp\left\{\frac{-xt}{(1-t)}\right\}}{(1-t)^{k+1}} = \sum_{n=0}^{\infty} L_n^k(x)t^n \qquad \text{(A.3.2.1)}$$

b) Recurrence Relations.

i) $$L_{n-1}^k(x) + L_n^{k-1}(x) = L_n^k(x) \qquad \text{(A.3.2.b.1)}$$

ii) $$(n+1)\,L_{n+1}^k(x) = (2n+k+1-x)\,L_n^k(x) - (n+k)\,L_{n-1}^k(x) \qquad \text{(A.3.2.b.2)}$$

iii) $$x\,L_n^{k'}(x) = n\,L_n^k(x) - (n+k)\,L_{n-1}^k(x) \qquad \text{(A.3.2.b.3)}$$

iv) $$L_n^{k'}(x) = -\sum_{r=0}^{n-1} L_r^k(x) \qquad \text{(A.3.2.b.4)}$$

v) $$L_n^{k'}(x) = -\,L_{n-1}^{k+1}(x) \qquad \text{(A.3.2.b.5)}$$

A.4 RADIAL WAVEFUNCTION

For a particle in the harmonic oscillator potential the radial wavefunction is defined [73] by the following expression;

$$|n,l\rangle = R_{nl}(r) = \sqrt{\frac{2n!}{b^{2(l+\frac{3}{2})}\Gamma(n+l+\frac{3}{2})}}\; r^l\; L_n^{l+\frac{1}{2}}\left(\frac{r^2}{b^2}\right)\; e^{-\frac{r^2}{2b^2}} \qquad \text{(A.4.1)}$$

A.5 EVALUATION OF $\langle n'l' \mid r^{\lambda} \mid n\,l \rangle$

Using expression (A.4.1), we write

$$\langle n'l' \mid r^{-\lambda} \mid n\,l\rangle = \sqrt{\frac{4\,n!\,n'!}{b^{2(l+l'+3)}\Gamma(n+l+\frac{3}{2})\Gamma(n'+l'+\frac{3}{2})}} \int r^{l+l'-\lambda+2}\; e^{-\frac{r^2}{b^2}}$$

$$\times\, L_{n'}^{l'+\frac{1}{2}}\left(\frac{r^2}{b^2}\right) L_n^{l+\frac{1}{2}}\left(\frac{r^2}{b^2}\right) dr \qquad \text{(A.5.1)}$$

If we make use of the generating function (A.3.2.a.1), then the intergral in (A.5.1) equals the coefficient of $u^{n'}v^{n}$ in

$$\int r^{l'+l-\lambda+2}\, e^{-\frac{r^2}{b^2}}\, e^{-\frac{r^2}{b^2}\left\{\frac{u}{1-u}+\frac{v}{1-v}\right\}} \frac{1}{(1-u)^{l'+\frac{3}{2}}} \frac{1}{(1-v)^{l+\frac{3}{2}}}\, dr \qquad \text{(A.5.2)}$$

Therefore by putting $\frac{r^2}{b^2}\left\{\frac{1-uv}{(1-u)(1-v)}\right\} = x$, we get

$$I = \frac{1}{2}\,(1-u)^{\frac{1}{2}(l-l'-\lambda)}\,(1-v)^{\frac{1}{2}(l'-l-\lambda)}\,\frac{b^{2\left\{\frac{1}{2}(l+l'-\lambda+3)\right\}}}{(1-uv)^{\frac{1}{2}(l+l'-\lambda+3)}}\int_0^{\infty} x^{\frac{1}{2}(l+l'-\lambda+1)}\, e^{-x}\, dx$$

. . . (A.5.3)

We must consider several special cases depending on the values of l, l' and λ since the expression of $(1-u)^m$ depends on whether m is positive or negative.

Let $l' \geq l+\lambda \geq l$

Therefore we have

$$I = \frac{1}{2}\,\frac{1}{(1-u)^{\mu}}\,(1-v)^{\mu'}\,\frac{b^{2(t+1)}}{(1-uv)^{t+1}}\,\Gamma(t+1) \qquad \text{(A.5.4)}$$

where $t = \frac{1}{2}(l+l'-\lambda+1)$

$\mu = \frac{1}{2}(l'-l+\lambda) \geq 0$

$\mu' = \frac{1}{2}(l'-l-\lambda) \geq 0$

With the help of the generating functions (A.2.3.2) and (A.2.3.3), we obtain (A.5.4) in the following form,

$$I = \frac{b^{2(t+1)}\Gamma(t+1)}{2} \cdot \sum_{ijk}\left\{\frac{\Gamma(\mu+i)}{\Gamma(\mu)\,i!}\,u^i \times \frac{\Gamma(\mu'+1)}{\Gamma(\mu'-j+1)j!}\,(-v)^j\,\frac{\Gamma(t+1+k)}{\Gamma(t+1)k!}\,(uv)^k\right\}$$

$$= \frac{b^{2(t+1)}\Gamma(t+1)}{2} \cdot \frac{\Gamma(\mu'+1)}{\Gamma(\mu)\Gamma(t+1)} \sum_{ijk} \frac{\Gamma(\mu+i)}{i!}\,u^i\,\frac{1}{\Gamma(\mu'-j+1)j!}\,(-v)^j \times \frac{\Gamma(t+1+k)}{k!}\,(uv)^k \qquad \text{(A.5.5)}$$

To obtain the term in $u^{n'}v^{n}$; we must have $i=n'-k$ and $j=n-k$ and we get

$$I=\left\{\frac{(-1)^n b^{2(t+1)}}{2}\,\frac{\Gamma(\mu'+1)}{\Gamma(\mu)}\sum_k \frac{\Gamma(\mu+n'-k)\Gamma(t+1+k)(-1)^k}{\Gamma(\mu'-n+k+1)(n'-k)!\ (n-k)!\ k!}\right\}u^{n'}v^{n}$$

. . . . . (A.5.6)

From (A.5.6) it is clear that the coefficient of $u^{n'}v^{n}$ is

$$\frac{(-1)^n b^{2(t+1)}}{2}\,\frac{\Gamma(\mu'+1)}{\Gamma(\mu)}\sum_k \frac{\Gamma(\mu+n'-k)\Gamma(t+1+k)(-1)^k}{\Gamma(\mu'-n+k+1)(n'-k)!\ (n-k)!\ k!}$$

Therefore we obtain

$$\langle n'l' \mid r^{-\lambda} \mid nl\rangle = \sqrt{\frac{4\,n'!\,n!}{b^{2(l+l'+3)}\Gamma(n'+l'+\frac{3}{2})\Gamma(n+l+\frac{3}{2})}}\ \frac{(-1)^n b^{2(t+1)}}{2}\,\frac{\Gamma(\mu'+1)}{\Gamma(\mu)}$$

$$\times\sum_k \frac{\Gamma(\mu+n'-k)\Gamma(t+1+k)(-1)^k}{\Gamma(\mu'-n+k+1)(n'-k)!\ (n-k)!\ k!}$$

$$\langle n'l' \mid r^{-\lambda} \mid nl\rangle = (-1)^n b^{-\lambda}\,\frac{\Gamma(\mu'+1)}{\Gamma(\mu)}\sqrt{\frac{n'!\,n!}{\Gamma(n'+l'+\frac{3}{2})\Gamma(n+l+\frac{3}{2})}}$$

$$\times\sum_k \frac{(-1)^k\Gamma(\mu+n'-k)\Gamma(t+1+k)}{\Gamma(\mu'-n+k+1)(n'-k)!(n-k)!k!} \qquad \text{(A.5.7)}$$

where $\mu=\frac{1}{2}(l'-l+\lambda) \geq 0$,

$\mu'=\frac{1}{2}(l'-l-\lambda) \geq 0$

and $t=\frac{1}{2}(l+l'-\lambda+1)$

If we take $l'=l+\lambda$ i.e $\lambda=l'-l$, $\mu'=0$, $\mu=\lambda$ and $k=n$ we get

$$\langle n'l' \mid r^{-\lambda} \mid nl\rangle = b^{-\lambda}\,\frac{\Gamma(\lambda+n'-n)}{\Gamma(\lambda)\Gamma(n'-n)!n!}\sqrt{\frac{n'!\,n!\,\Gamma(n+l+\frac{3}{2})}{\Gamma(n'+l'+\frac{3}{2})}} \qquad \text{(A.5.8)}$$

But if we have $l+\lambda \geq l' \geq l$ then (A.5.3) will have the following form

$$I=\frac{1}{2}\,\frac{1}{(1-u)^{\mu}(1-v)^{\mu'}}\cdot\frac{b^{2(t+1)}}{(1-uv)^{t+1}}\Gamma(t+1) \qquad \text{(A.5.9)}$$

where $\mu=\frac{1}{2}(l'-l+\lambda) \geq 0$

$\mu'=\frac{1}{2}(l-l'+\lambda) \geq 0$

Or

$$I=\frac{b^{2(t+1)}}{2}\frac{\Gamma(t+1)}{}\sum_{ijk}\frac{\Gamma(\mu+i)}{\Gamma(\mu)i!}u^i\frac{\Gamma(\mu'+j)}{\Gamma(\mu')j!}v^j\frac{\Gamma(t+1+k)}{\Gamma(t+1)k!}(uv)^k \qquad \text{(A.5.10)}$$

By putting $i=n'-k$, $j=n-k$ we get

$$I=\frac{b^{2(t+1)}}{2}\cdot\frac{1}{\Gamma(\mu)\Gamma(\mu')}\sum_{k}\frac{\Gamma(\mu+n'-k)\Gamma(\mu'+n-k)\Gamma(t+1+k)}{(n'-k)!(n-k)!\ k!}u^{n'}v^n$$

Therefore we have

$$\langle n'l'|r^{-\lambda}|nl\rangle=\frac{b^{-\lambda}}{\Gamma(\mu)\Gamma(\mu')}\sqrt{\frac{n'!\ n!}{\Gamma(n+l+\frac{3}{2})\Gamma(n'+l'+\frac{3}{2})}}$$
$$\times\sum_{k}\frac{\Gamma(\mu+n'-k)\Gamma(\mu'+n-k)\Gamma(t+1+k)}{(n'-k)!(n-k)!k!} \qquad \text{(A.5.11)}$$

If we have $k=n$, we obtain

$$\langle n'l'|r^{-\lambda}|nl\rangle=\frac{b^{-\lambda}}{\Gamma(\mu)}\sqrt{\frac{n'!\ n!}{\Gamma(n+l+\frac{3}{2})\ \Gamma(n'+l'+\frac{3}{2})}}\times\frac{\Gamma(\mu+n'-n)\ \Gamma(t+1+n)}{(n'-n)!\ n!}$$

. . . . (A.5.12)

A.6 EVALUATION OF $\langle n'l'||\frac{\nabla}{r^{\lambda}}||nl\rangle$

With the help of gradient formula [65], one can evaluate the matrix element of the type

$$\langle l'0|\nabla_0|l\,0\rangle \quad \text{where}$$

$$\nabla_0=\frac{\delta}{\delta z}=\cos\theta\frac{\delta}{\delta r}-\frac{\sin\theta}{r}\frac{\delta}{\delta\theta} \qquad \text{(A.6.1)}$$

The only non-zero matrix element of the above type can be written [65] as

$$\langle n'\,l+1\,0|\nabla_0|n\,l\,0\rangle=\frac{l+1}{[(2l+1)(2l+3)]^{\frac{1}{2}}}\int R_{n'l+1}(r)\left(\frac{\delta}{\delta r}-\frac{l}{r}\right)R_{nl}(r)\,r^2\,dr$$

. . . . (A.6.2)

and

$$\langle n'\,l-1\,0|\nabla_0|n\,l\,0\rangle=\frac{l}{[(2l-1)(2l+1)]^{\frac{1}{2}}}\int R_{n'l-1}(r)\left(\frac{\delta}{\delta r}+\frac{l+1}{r}\right)R_{nl}(r)\,r^2\,dr$$

. . . . (A.6.3)

Since we have

$$R_{nl}(r) = \eta_{nl}\, r^{l} L_n^{l+\frac{1}{2}}\left(\frac{r^2}{b^2}\right) e^{-\frac{r^2}{2b^2}} \qquad \text{(A.6.4)}$$

where η_{nl}, the normalization constant is given by

$$\eta_{nl} = \sqrt{\frac{2\, n!}{b^{2(l+\frac{3}{2})}\,\Gamma(n+l+\frac{3}{2})}}$$

We can write

$$\left(\frac{\delta}{\delta r} - \frac{l}{r}\right)R_{nl}(r) = \eta_{nl}\left[r^{l}\left\{ L_n^{l+\frac{1}{2}}\left(\frac{r^2}{b^2}\right)\frac{\delta}{\delta r}\left(e^{-\frac{r^2}{2b^2}}\right) + e^{-\frac{r^2}{2b^2}}\frac{\delta}{\delta r}\left(L_n^{l+\frac{1}{2}}\left(\frac{r^2}{b^2}\right)\right)\right\}\right]$$

Making use of recurrence relation (A.3.2.b.5), we obtain ..(A.6.5)

$$= \eta_{nl}\, r^{l+1}\left\{ -\frac{1}{b^2} L_n^{l+\frac{1}{2}}\left(\frac{r^2}{b^2}\right) - \frac{2}{b^2} L_{n-1}^{l+1+\frac{1}{2}}\left(\frac{r^2}{b^2}\right)\right\} e^{-\frac{r^2}{2b^2}} \qquad \text{..(A.6.6)}$$

Making use of recurrence relation (A.3.2.b.1), we obtain

$$= \eta_{nl}\, r^{l+1}\left\{ -\frac{1}{b^2} L_n^{l+1+\frac{1}{2}}\left(\frac{r^2}{b^2}\right) - \frac{1}{b^2} L_{n-1}^{l+1+\frac{1}{2}}\left(\frac{r^2}{b^2}\right)\right\} e^{-\frac{r^2}{2b^2}}$$

$$= -\frac{\sqrt{n}}{b}\sqrt{\frac{2\,(n-1)!}{b^{2(l+1+\frac{3}{2})}\,\Gamma(n-1+l+1+\frac{3}{2})}}\; r^{l+1} L_{n-1}^{l+1+\frac{1}{2}}\left(\frac{r^2}{b^2}\right) e^{-\frac{r}{2b^2}}$$

$$-\frac{\sqrt{n+l+\frac{3}{2}}}{b}\sqrt{\frac{2\, n!}{b^{2(l+1+\frac{3}{2})}\,\Gamma(n+1+l+\frac{3}{2})}}\; r^{l+1} L_n^{l+1+\frac{1}{2}}\left(\frac{r^2}{b^2}\right) e^{-\frac{r^2}{2b^2}}$$

i.e

$$\left(\frac{\delta}{\delta r} - \frac{l}{r}\right)R_{nl}(r) = \frac{1}{b}\left\{ -\sqrt{n}\, R_{n-1,l+1}(r) - \sqrt{n+l+\frac{3}{2}}\, R_{n,l+1}(r)\right\} \qquad \text{(A.6.7)}$$

Similarly we start with

$$\left(\frac{\delta}{\delta r} + \frac{l+1}{r}\right)R_{nl}(r) = \left(\frac{\delta}{\delta r} + \frac{l+1}{r}\right)\left\{ \eta_{nl}\, r^{l} L_n^{l+\frac{1}{2}}\left(\frac{r^2}{b^2}\right) e^{-\frac{r^2}{2b^2}}\right\} \qquad \text{(A.6.8)}$$

and obtain

$$\left(\frac{\delta}{\delta r}+\frac{l+1}{r}\right)R_{nl}(r)= n_{nl}\ (2l+1)\ r^{l-1}\ L_n^{l+\frac{1}{2}}\left(\frac{r^2}{b^2}\right)+2\ r^{l-1}\left\{-\frac{r^2}{b^2}L_{n-1}^{l+\frac{1}{2}+1}\left(\frac{r^2}{b^2}\right)\right\}$$

$$-\frac{r}{b^2}r^l\ L_n^{l+\frac{1}{2}}\left(\frac{r^2}{b^2}\right)\ .\ e^{-\frac{r^2}{2b^2}}$$

By making use of recurrence relations (A.3.2.b), the above expression can be reduced to

$$\left(\frac{\delta}{\delta r}+\frac{l+1}{r}\right)R_{nl}(r)=\frac{\sqrt{n+1}}{b}\sqrt{\frac{2(n+1)!}{b^{2(l-1+\frac{3}{2})}\Gamma(n+1+l-1+\frac{3}{2})}}\ r^{l-1}L_{n+1}^{l-1+\frac{1}{2}}\left(\frac{r^2}{b^2}\right)e^{-\frac{r^2}{2b^2}}$$

$$+\frac{\sqrt{n+l+\frac{1}{2}}}{b}\sqrt{\frac{2\ n!}{b^{2(l-1+\frac{3}{2})}\Gamma(n+l-1+\frac{3}{2})}}\ r^{l-1}L_n^{l-1+\frac{1}{2}}\left(\frac{r^2}{b^2}\right)e^{-\frac{r^2}{2b^2}}$$

. . . . (A.6.9)

The expression (A.6.9) can be rewritten as

$$\left(\frac{\delta}{\delta r}+\frac{l+1}{r}\right)R_{nl}(r)=\frac{1}{b}\left\{\sqrt{n+1}\ R_{n+1,l-1}(r)+\sqrt{n+l+\frac{1}{2}}\ R_{n,l-1}(r)\right\} \qquad (A.6.10)$$

From expressions (A.6.2) and (A.6.7), we have

$$\langle n'\ l+1\ 0|\ \frac{\nabla}{r^\lambda}\ |n\ l\ 0\rangle=\frac{(l+1)}{[(2l+1)(2l+3)]^{\frac{1}{2}}}\left[\frac{1}{b}\left\{-\sqrt{n}\ \langle n'\ l+1|\frac{1}{r^\lambda}\ |n-1\ l+1\rangle\right.\right.$$

$$\left.\left.-\sqrt{n+l+\frac{3}{2}}\ \langle n'\ l+1|\frac{1}{r^\lambda}\ |\ n\ l+1\rangle\right\}\right] \qquad (A.6.11)$$

Therefore we obtain

$$\langle n'\ l+1\ ||\ \frac{\nabla}{r^\lambda}\ ||\ n\ l\rangle=\frac{(l+1)}{[(2l+1)(2l+3)]^{\frac{1}{2}}}\cdot\frac{1}{(-1)^{l+1}\begin{pmatrix} l+1 & 1 & l \\ 0 & 0 & 0\end{pmatrix}}$$

$$\times\frac{1}{b}\left\{-\sqrt{n}\ \langle n'\ l+1\ |\ \frac{1}{r^\lambda}\ |\ n-1\ l+1\ \rangle-\sqrt{n+l+\frac{3}{2}}\right.$$

$$\left.\times\langle n'\ l+1\ |\ \frac{1}{r^\lambda}\ |\ n\ l+1\rangle\right\}$$

i.e

$$< n' l+1 \,||\, \frac{\nabla}{r^{\lambda}} \,||\, n\, l > = \frac{\sqrt{l+1}}{b}\left\{ -\sqrt{n}\ <n' l+1 \,|\, \frac{1}{r^{\lambda}} \,|\, n-1\ l+1> - \sqrt{n+l+\frac{3}{2}} \right.$$

$$\left. \times <n' l+1 \,|\, \frac{1}{r^{\lambda}} \,|\, n\ l+1> \right\}$$

. . . . (A.6.12)

Similarly with the help of (A.6.3) and (A.6.10), we can obtain

$$<n'\ l-1\ 0 \,|\, \frac{\nabla_0}{r^{\lambda}} \,|\, n\ l\ 0> = \frac{1}{b\left[(2l+1)(2l-1)\right]^{\frac{1}{2}}} \left\{ \sqrt{n+1} <n' l-1| \frac{1}{r^{\lambda}} |n+1, l-1> \right.$$

$$\left. + \sqrt{n+l+\frac{1}{2}} <n'\ l-1| \frac{1}{r^{\lambda}} |n\ l-1> \right\}$$

. . . . (A.6.13)

which gives

$$<n'\ l-1 \,||\, \frac{\nabla}{r^{\lambda}} \,||\, n\ l> = \frac{1}{\left[(2l+1)(2l-1)\right]^{\frac{1}{2}}} \cdot \frac{1}{(-1)^{l-1}\begin{pmatrix} l-1 & 1 & l \\ 0 & 0 & 0 \end{pmatrix}}$$

$$\times \left[\frac{1}{b} \left\{ \sqrt{n+1} <n' l-1| \frac{1}{r^{\lambda}} |n+1, l-1> + \sqrt{n+l+\frac{1}{2}} \right.\right.$$

$$\left.\left. \times <n' l-1 \,|\, \frac{1}{r^{\lambda}} \,|\, n\ l-1> \right\} \right]$$

or

$$<n'\ l-1 \,||\, \frac{\nabla}{r^{\lambda}} \,||\, n\ l> = -\frac{\sqrt{l}}{b}\left\{ \sqrt{n+1} <n' l-1| \frac{1}{r^{\lambda}} |n+1\ l-1> + \sqrt{n+l+\frac{1}{2}} \right.$$

$$\left. \times <n' l-1 \,|\, \frac{1}{r^{\lambda}} \,|\, n\ l-1> \right\} \qquad \text{(A.6.14)}$$

The values of matrix elements of $(\frac{1}{r^{\lambda}})$ can be determined either by expression (A.5.7) or expression (A.5.11) subject to the conditions satisfied.

We know that

$<n' l' m' \,|\, \nabla_0 \,|\, n\ l\ m> = 0$ unless we have

$l' = l \pm 1$

$m' = m \pm 1, m$

and $\Delta E = \hbar w \Rightarrow 2n' + l'$

i.e $\Delta E = 2n + l \pm 1$

Therefore for non-zero matrix element of above type, the following conditions must be satisfied.

i) If $l' = l + 1$ n' must be either n-1 or n, ... (A.6.15)

ii) if $l' = l-1$ n' must be either n+1 or n. . . . . (A.6.16)

The expressions (A.6.12) and (A.6.14) satisfy the conditions (A.6.15) and (A.6.16) respectively.

Special cases.

i) $$\langle n' l+1 \| \frac{\nabla}{r} \| n\, l\rangle = -\frac{\sqrt{l+1}}{b}\left\{\sqrt{n}\,\langle n' l+1|\frac{1}{r}|n-1,l+1\rangle + \sqrt{n+l+\frac{3}{2}} \times \langle n' l+1 | \frac{1}{r} | n\, l+1\rangle\right\} \quad (A.6.17)$$

ii) $$\langle n' l-1 \| \frac{\nabla}{r} \| n\, l\rangle = -\frac{\sqrt{l}}{b}\left\{\sqrt{n+1}\,\langle n' l-1|\frac{1}{r}|n+1\, l-1\rangle + \sqrt{n+l+\frac{1}{2}} \times \langle n' l-1 | \frac{1}{r} | n\, l-1\rangle\right\} \quad (A.6.18)$$

iii) $$\langle n' l+1 \| \nabla \| n\, l\rangle = -\frac{1}{b}\sqrt{n(l+1)}\ \delta_{n',n-1} \quad (A.6.19)$$

or $$= -\frac{1}{b}\sqrt{(l+1)(n+l+\frac{3}{2})}\ \delta_{n',n} \quad (A.6.20)$$

iv) $$\langle n' l-1 \| \nabla \| n\, l\rangle = -\frac{1}{b}\sqrt{l(n+1)}\ \delta_{n',n+1} \quad (A.6.21)$$

or $$= -\frac{1}{b}\sqrt{l\,(n+l+\frac{1}{2})}\ \delta_{n',n} \quad (A.6.22)$$

The evaluation of matrix element of $(\frac{1}{r^{\lambda}})$; $\lambda \geq 0$ has been described in section (A.5).

A.7 EVALUATION OF $\langle n' l' \| \frac{r}{r^3} \| n\, l\rangle$

We have

$$z|nl0\rangle = r\, R_{nl}(r)\, \cos\theta\, Y_{l0}(\theta,\phi) \quad (A.7.1)$$

By the properties of the Legendre function one can finds [65],

$$\cos\theta\, Y_{l0}(\theta,\phi) = \frac{(l+1)}{[(2l+1)(2l+3)]^{\frac{1}{2}}}\, Y_{l+1\,0} + \frac{l}{[(2l+1)(2l-1)]^{\frac{1}{2}}}\, Y_{l-1\,0} \quad . . . . (A.7.2)$$

$$z|nl0\rangle = \frac{(l+1)}{[(2l+1)(2l+3)]^{\frac{1}{2}}} \cdot rR_{nl}Y_{l+1\,0} + \frac{l}{[(2l+1)(2l-1)]^{\frac{1}{2}}} rR_{nl}Y_{l-1\,0}$$

. . . . (A.7.3)

Since

$$R_{nl}(r) = \eta_{nl}\, r^{l}\; L_n^{l+\frac{1}{2}}\left(\frac{r^2}{b^2}\right)\; e^{-\frac{r^2}{2b^2}}$$

where η_{nl} is a normalisation constant,

we have

$$r\,R_{nl}(r) = \eta_{nl}\, r^{l+1}\; L_n^{l+\frac{1}{2}}\left(\frac{r^2}{b^2}\right)\; e^{-\frac{r^2}{2b^2}} \qquad (A.7.4)$$

Making use of recurrence relation (A.3.2.b.1), we obtain

$$rR_{nl}(r) = \eta_{nl}\, r^{l+1}\left\{L_n^{l+1+\frac{1}{2}}\left(\frac{r^2}{b^2}\right) - L_{n-1}^{l+1+\frac{1}{2}}\left(\frac{r^2}{b^2}\right)\right\} e^{-\frac{r^2}{2b^2}}$$

$$= b\sqrt{n+l+\frac{3}{2}}\sqrt{\frac{2\,n!}{b^{2(l+1+\frac{3}{2})}\,\Gamma(n+l+1+\frac{3}{2})}}\; r^{l+1} L_n^{l+1+\frac{1}{2}}\left(\frac{r^2}{b^2}\right) e^{-\frac{r^2}{2b^2}}$$

$$- b\sqrt{n}\sqrt{\frac{2\,(n-1)!}{b^{2(l+1+\frac{3}{2})}\,\Gamma(n-1+l+1+\frac{3}{2})}}\; r^{l+1}\; L_{n-1}^{l+1+\frac{1}{2}}\left(\frac{r^2}{b^2}\right) e^{-\frac{r^2}{2b^2}}$$

Using equation (A.4.1) we can write the above expression as

$$r\,R_{nl} = b\left[\sqrt{n+l+\frac{3}{2}}\; R_{n,l+1} - \sqrt{n}\; R_{n-1,l+1}\right] \qquad (A.7.5)$$

Employing the recurrence relation (A.3.2.b.1), the expression (A.7.4) may also be expressed as

$$rR_{nl}(r) = \eta_{nl} b^2\, r^{l-1}\left\{(2n+l+\frac{1}{2}+1)L_n^{l+\frac{1}{2}}\left(\frac{r^2}{b^2}\right) - (n+1)L_{n+1}^{l+\frac{1}{2}}\left(\frac{r^2}{b^2}\right)\right.$$

$$\left. -(n+l+\frac{1}{2})L_{n-1}^{l+\frac{1}{2}}\left(\frac{r^2}{b^2}\right)\right\} e^{-\frac{r^2}{2b^2}} \qquad (A.7.6)$$

or

$$= b\sqrt{n+l+\frac{1}{2}} \sqrt{\frac{2\,n!}{b^{2(l-1+\frac{3}{2})}\,\Gamma(n+l-1+\frac{3}{2})}}\; r^{l-1}\; L_n^{l-1+\frac{1}{2}}\left(\frac{r^2}{b^2}\right) e^{-\frac{r^2}{2b^2}}$$

$$- b\sqrt{n+1} \sqrt{\frac{2\,(n+1)!}{b^{2(l-1+\frac{3}{2})}\,\Gamma(n+1+l-1+\frac{3}{2})}}\; r^{l-1}\; L_{n+1}^{l-1+\frac{1}{2}}\left(\frac{r^2}{b^2}\right) e^{-\frac{r^2}{2b^2}}$$

Therefore we have

$$r\,R_{nl}(r) = b\left[\sqrt{n+l+\tfrac{1}{2}}\;R_{n,l-1} \;-\; \sqrt{n+1}\;R_{n+1,l-1}\right] \qquad \text{(A.7.8)}$$

Putting the values of rR_{nl} (given in (A.7.6) and (A.7.8) in the expression (A.7.3) on proper places, we obtain

$$z|nl0\rangle = \frac{b(l+1)}{\left[(2l+1)(2l+3)\right]^{\frac{1}{2}}}\left\{\sqrt{n+l+\tfrac{3}{2}}\;R_{n\;l+1\;0} - \sqrt{n}\;R_{n-1\;l+1\;0}\right\}$$

$$+\frac{b\,l}{\left[(2l+1)(2l-1\;\;)\right]^{\frac{1}{2}}}\left\{\sqrt{n+l+\tfrac{1}{2}}\;R_{n\;l-1\;0} - \sqrt{n+1}\;R_{n+1\;l-1\;0}\right\}$$

. . . (A.7.9)

$$\therefore\ \langle n'\;l+1\;0\,|\,\frac{r}{r^3}\,|\,n\;l\;0\rangle = \frac{b(l+1)}{\left[(2l+1)(2l+3)\right]^{\frac{1}{2}}}\left\{\sqrt{n+l+\tfrac{3}{2}}\;\langle n'\;l+1|\,\frac{1}{r^3}\,|n\;l+1\rangle\right.$$

$$\left.-\sqrt{n}\;\langle n'\;l+1|\,\frac{1}{r^3}\,|n-1\;\;l+1\rangle\right\} \qquad \text{(A.7.10)}$$

and

$$\langle n'\;l-1\;0\,|\,\frac{r}{r^3}\,|n\;l\;o\rangle = \frac{b\;l}{\left[(2l+1)(2l-1)\right]^{\frac{1}{2}}}\left\{\sqrt{n+l+\tfrac{1}{2}}\;\langle n'\;l-1|\,\frac{1}{r^3}\,|n\;l-1\rangle\right.$$

$$\left.-\sqrt{n+1}\;\langle n'\;l-1|\,\frac{1}{r^3}\,|n+1\;\;l-1\rangle\right\} \qquad \text{(A.7.11)}$$

Hence we obtain

$$< n' \; l+1 \; || \; \frac{r}{r^3} \; || \; n \; l > = \frac{b(l+1)}{\left[(2l+1)(2l+3)\right]^{\frac{1}{2}}} \cdot \frac{1}{(-1)^{l+1}\begin{pmatrix} l+1 & 1 & l \\ 0 & 0 & 0 \end{pmatrix}} \left\{ \sqrt{n+l+\frac{3}{2}} \right.$$

$$\left. x < n' \; l+1 \; | \; \frac{1}{r^3} \; | \; n \; l+1 > - \sqrt{n} \; < n' \; l+1 \; | \; \frac{1}{r^3} \; | \; n-1 \; l+1 > \right\}$$

Therefore we have

$$< n' \; l+1 \; || \; \frac{r}{r^3} \; || \; n \; l > = b\sqrt{l+1} \; \left\{ \sqrt{n+l+\frac{3}{2}} < n' \; l+1 \; | \; \frac{1}{r^3} \; | \; n \; l+1 > \right.$$

$$\left. - \sqrt{n} \; < n' \; l+1 \; | \; \frac{1}{r^3} \; | \; n-1 \; l+1 > \right\} \qquad \text{(A.7.12)}$$

Similarly we obtain

$$< n' \; l-1 \; || \; \frac{r}{r^3} \; || \; n \; l > = -b \sqrt{l} \; \left\{ \sqrt{n+l+\frac{1}{2}} < n' \; l-1 \; | \; \frac{1}{r^3} \; | \; n \; l-1 > \right.$$

$$\left. - \sqrt{n+1} \; < n' \; l-1 \; | \; \frac{1}{r^3} \; | \; n+1 \; l-1 > \right\} \qquad \text{(A.7.13)}$$

The values of matrix elements of $1/r^{\lambda}$ can be determined by either (A.5.7) or (A.5.11) subject to the condition satisfied.

APPENDIX B

B.1 EVALUATION $\langle S \| (\sigma_1 - \sigma_2) \| S' \rangle$

Since the operator $(\sigma_1 - \sigma_2)$ is an antisymmetric operator, we can have the non-zero matrix elements only for the values S'=1, S=0 and S'=0, S=1. We define the spin operator σ in terms of Pauli matrices

$$\sigma_x = \begin{pmatrix} 0 & 1 \\ 1 & 0 \end{pmatrix}, \quad \sigma_y = \begin{pmatrix} 0 & -i \\ i & 0 \end{pmatrix} \quad \text{and} \quad \sigma_z = \begin{pmatrix} 1 & 0 \\ 0 & -1 \end{pmatrix} \qquad \text{(B.1.1)}$$

as $$\sigma = \sigma_x \mathbf{i} + \sigma_y \mathbf{j} + \sigma_z \mathbf{k} \qquad \text{(B.1.2)}$$

where σ_x, σ_y and σ_z are the components of a σ and **i**, **j** and **k** are the unit vectors along x-axix, y-axix and z-axix respectively. We also define the raising and lowering spin operators as,

$$\sigma_+ = \frac{1}{\sqrt{2}} (\sigma_x + i\sigma_y)$$

and $$\sigma_- = \frac{1}{\sqrt{2}} (\sigma_x - i\sigma_y) \qquad \text{(B.1.3)}$$

Therfore we can write,

$$\sigma_x = \frac{1}{\sqrt{2}} (\sigma_+ + \sigma_-)$$

and $$\sigma_y = -\frac{i}{\sqrt{2}} (\sigma_+ - \sigma_-) \qquad \text{(B.1.4)}$$

From (B.1.2) and (B.1.4) we obtain,

$$\sigma = \frac{1}{\sqrt{2}} \{(\sigma_+ + \sigma_-)\mathbf{i} - i(\sigma_+ - \sigma_-)\mathbf{j}\} + \sigma_z \mathbf{k} \qquad \text{(B.1.5)}$$

But as we know that the spherical unit vectors are defined [65] as

$$e_{+1} = -\frac{1}{\sqrt{2}}(\mathbf{i} + \mathbf{ij})$$
$$e_0 = \mathbf{k} \qquad \text{(B.1.6)}$$
$$e_{-1} = \frac{1}{\sqrt{2}}(\mathbf{i} - \mathbf{ij})$$

Therefore using expression (B.1.5), We get

$$(\sigma_1 - \sigma_2) = (\sigma_{1+} - \sigma_{2+})e_{-1} - (\sigma_{1-} - \sigma_{2-})e_{+1} + (\sigma_{1z} - \sigma_{2z})e_0 \qquad \text{(B.1.7)}$$

where e_{-1}, e_{+1} and e_0 are spherical unit vectors defined in (B.1.6). If the operator $(\sigma_1 - \sigma_2)$ operates on a spin wavefunction $|S'=0, m_{s'} = 0\rangle$ then making use of expression (B.1.7) we have

$$(\sigma_1 - \sigma_2)|S'=0, m_{s'}=0\rangle = \left\{(\sigma_{1+} - \sigma_{2+})e_{-1} - (\sigma_{1-} - \sigma_{2-})e_{+1} + (\sigma_{1z} - \sigma_{2z})e_0\right\}|S'=0, m_{s'}=0\rangle$$
. . . . (B.1.8)

By definitions (B.1.1) and (B.1.3), it can be found, since

$$\sigma_+ = \sqrt{2}\begin{pmatrix} 0 & 1 \\ 0 & 0 \end{pmatrix} \quad \text{and} \quad \sigma_- = \sqrt{2}\begin{pmatrix} 0 & 0 \\ 0 & 1 \end{pmatrix}, \qquad \text{(B.1.9a)}$$

$$\sigma_+(\alpha) = 0\,, \quad \sigma_+(\beta) = \sqrt{2}\,\alpha$$

and $$\sigma_-(\alpha) = \sqrt{2}\,\beta\,, \quad \sigma_-(\beta) = 0 \qquad \text{(B.1.9b)}$$

Here α and β have been used to denote up-spin $\begin{pmatrix} 1 \\ 0 \end{pmatrix}$ and down-spin $\begin{pmatrix} 0 \\ 1 \end{pmatrix}$ respectively.

By using the information given in eqns. (B.1.9), we rewrite the expression (B.1.8) as

$$(\sigma_1 - \sigma_2)|S'=0, m_{s'}=0\rangle = \left\{(\sigma_{1+} - \sigma_{2+})e_{-1} - (\sigma_{1-} - \sigma_{2-})e_{+1} + (\sigma_{1z} - \sigma_{2z})e_0\right\} \times \left|\frac{1}{\sqrt{2}}\{\alpha(1)\beta(2) - \beta(1)\alpha(2)\}\right\rangle .$$

$$= \frac{1}{\sqrt{2}}\Big[\Big|\sqrt{2}\{-\alpha(1)\alpha(2)-\alpha(1)\alpha(2)\}e_{-1}-\sqrt{2}\{\beta(1)\beta(2)+\beta(1)\beta(2)\}e_{+1}$$

$$+2\{\alpha(1)\beta(2)+\beta(1)\alpha(2)\}e_0\Big>\Big] \qquad \text{(B.1.10)}$$

Or $(\sigma_1 - \sigma_2)|S'=0, m_{S'}=0> = -2|11>e_{-1} - 2|1-1>e_{+1} + 2|10>e_0$ (B.1.11)

We know that a vector quantity V can be expressed in terms of its spherical components $V_q(q=0, \pm1)$ [65] as given below.

$$V = \sum_q (-e)^q V_q\, e_{-q} \qquad \text{(B.1.12)}$$

Therefore an operator $(\sigma_1 - \sigma_2)$ being a vector (i.e a tensor of rank 1) can be written as

$$(\sigma_1 - \sigma_2)^1 = -(\sigma_1 - \sigma_2)^1_{+1} e_{-1} - (\sigma_1 - \sigma_2)^1_{-1} e_{+1} + (\sigma_1 - \sigma_2)^1_0 e_0 \qquad \text{(B.1.13)}$$

With the help of expressions (B.1.12) and (B.1.13), we obtain

$$<S=1, m_S=+1|(\sigma_1-\sigma_2)|S'=0, m_{S'}=0> = <S=1, m_S=+1|(\sigma_1-\sigma_2)^1_{+1}|S'=0, m_{S'}=0> = 2$$

$$<S=1, m_S=0|(\sigma_1-\sigma_2)|S'=0, m_{S'}=0> = <S=1, m_S=0|(\sigma_1-\sigma_2)^1_0|S'=0, m_{S'}=0> = 2$$

$$<S=1, m_S=-1|(\sigma_1-\sigma_2)|S'=0, m_{S'}=0> = <S=1, m_S=-1|(\sigma_1-\sigma_2)^1_{-1}|S'=0, m_{S'}=0> = 2$$

. . . . (B.1.14)

Using the Wigner Eckart Theorem [67] we get

$$<S=1||(\sigma_1 - \sigma_2)||S'=0> = \frac{<S=1, m_S=0|(\sigma_1 - \sigma_2)^1_0|S'=0, m_{S'}=0>}{(-1)\begin{pmatrix} 1 & 1 & 0 \\ 0 & 0 & 0 \end{pmatrix}}$$

$$= \frac{2}{(-1)(-\frac{1}{\sqrt{3}})} = 2\sqrt{3} \qquad \text{(B.1.15)}$$

The values of Wigner's coefficients (called 3j-symbols) have been tabulated in ref. [52].

Similarly we can obtain the same result by taking the left-hand spin wavefunction with other two possible values of $m_s=+1,-1$. Therefore the value of the reduced matrix element is given by

$$\langle S=1||(\sigma_1 - \sigma_2)||S'=0\rangle = 2\sqrt{3} \qquad \text{(B.1.16)}$$

By following the same procedure as mentioned above, we can evaluate the other possible non-zero matrix elements of the operator $(\sigma_1 - \sigma_2)$ and hence calculate their reduced matrix elements.

B.2 EVALUATION OF $\langle S||(\sigma_1+\sigma_2)||S'\rangle$

The matrix element of an operator $(\sigma_1+\sigma_2)$ can be different from zero only for $S'=S=1$, i.e. We have to calculate only the following reduced matrix element;

$$\langle S=1||(\sigma_1+\sigma_2)||S'=1\rangle \qquad \text{(B.2.1)}$$

We Know that S and σ are related by an expression

$$\mathbf{S} = \frac{1}{2}\sigma,$$

therefore replacing $(\sigma_1+\sigma_2)$ by $2\mathbf{S}$, we obtain

$$\langle S=1||(\sigma_1+\sigma_2)||S'=1\rangle = 2\langle S=1||\mathbf{S}||S'=1\rangle$$

i.e. $$\langle S=1||(\sigma_1+\sigma_2)||S'=1\rangle = 2\sqrt{6} \qquad \text{(B.2.2)}$$

B.3 EVALUATION OF $\langle S \| (\sigma_1 \times \sigma_2) \| S' \rangle$

As we know that the matrix element of an operator $(\sigma_1 \times \sigma_2)$ shall be different from zero only for $S'=0, S=1$ or $S'=1, S=0$, therefore we have to evaluate the following matrix elements;

$$\langle S=1 \| (\sigma_1 \times \sigma_2) \| S'=0 \rangle \qquad \text{(B.3.1)}$$

$$\langle S=0 \| (\sigma_1 \times \sigma_2) \| S'=1 \rangle \qquad \text{(B.3.2)}$$

B.3.1 REPRESENTATION OF $(\sigma_1 \times \sigma_2)$ AS A TENSOR OPERATOR.

The operator $(\sigma_1 \times \sigma_2)$ is a cross-product of two vectors σ_1 and σ_2. Since it is a vector , it may be expressed as a tensor of rank one. Using definition (B.1.2), we have

$$(\sigma_1 \times \sigma_2) = (\sigma_{1x}\mathbf{i} + \sigma_{1y}\mathbf{j} + \sigma_{1z}\mathbf{k}) \times (\sigma_{2x}\mathbf{i} + \sigma_{2y}\mathbf{j} + \sigma_{2z}\mathbf{k}) \qquad \text{. . . . (B.3.1.1)}$$

We define the spherical components of a vector as,

$$\sigma_{\pm 1} = \mp \frac{1}{\sqrt{2}} (\sigma_x \pm i\sigma_y) \qquad \text{(B.3.1.2)}$$

$$\text{i.e} \quad \sigma_x = \frac{1}{\sqrt{2}} (\sigma_{-1} - \sigma_{+1}) \quad ; \quad \sigma_y = \frac{i}{\sqrt{2}} (\sigma_{-1} + \sigma_{+1}) \qquad \text{(B.3.1.3)}$$

We re-write expression (B.3.1.1) as

$$(\sigma_1 \times \sigma_2) = (\sigma_{1y}\sigma_{2z} - \sigma_{1z}\sigma_{2y})\mathbf{i} + (\sigma_{1z}\sigma_{2x} - \sigma_{1x}\sigma_{2z})\mathbf{j} + (\sigma_{1x}\sigma_{2y} - \sigma_{1y}\sigma_{2x})\mathbf{k}$$

Making use of (B.3.1.3) and (B.1.6), we replace cartesian components by spherical components as follows;

$$(\sigma_1 \times \sigma_2) = \frac{i}{\sqrt{2}} (i - ij)\,(\sigma_{1+}\sigma_{20} - \sigma_{2+}\sigma_{10}) + \frac{i}{\sqrt{2}} (i + ij)\,(\sigma_{1-}\sigma_{20} - \sigma_{2-}\sigma_{10})$$
$$- (i)\mathbf{k}\,(\sigma_{1+}\sigma_{2-} - \sigma_{2+}\sigma_{1-})$$

$$= (-i)\left\{\frac{1}{\sqrt{2}} (i - ij)\right\} - \sigma_{1+}\sigma_{20} + \sigma_{10}\sigma_{2+}) + (-i)\left\{\frac{-1}{\sqrt{2}} (i + ij)\right\}$$
$$\times (\sigma_{1-}\sigma_{20} - \sigma_{2-}\sigma_{10}) + (-i)\mathbf{k}\,(\sigma_{1+}\sigma_{2-} - \sigma_{1-}\sigma_{2+})$$

$$= (-i)\{e_{-1}\}(-\sigma_{1+}\sigma_{20} + \sigma_{10}\sigma_{2+}) + (-i)\{e_{+1}\}(\sigma_{1-}\sigma_{20} - \sigma_{10}\sigma_{2-})$$
$$+ (-i)\{e_0\}(\sigma_{1+}\sigma_{2-} - \sigma_{1-}\sigma_{2+}) \qquad \text{(B.3.1.4)}$$

Here signs "±"and "0" with sigmas have been used for spherical components (i.e for q= ±1, 0). This convention differs from that of section B.1) and B.2).

We can express the components of a product vector (a tensor of rank 1) in terms of components of the vectors [65] as given below.

$$T(1q) = \sum_{q_1 q_2} X_{q_1} Y_{q_2} (1q_1 1q_2 | 111q) \qquad \text{(B.3.1.5)}$$

where $q, q_1, q_2 = 0, \pm 1$.

Equation (B.3.1.5) implies that

$$[\sigma_1\sigma_2]^1_{-1} = \frac{1}{\sqrt{2}} (-\sigma_{1-}\sigma_{20} + \sigma_{10}\sigma_{2-}) \qquad \text{(B.3.1.6a)}$$

$$[\sigma_1\sigma_2]^1_{0} = \frac{1}{\sqrt{2}} (-\sigma_{1-}\sigma_{2+} + \sigma_{1+}\sigma_{2-}) \qquad \text{(B.3.1.6b)}$$

$$\left[\sigma_1\sigma_2\right]^1_{+1} = \frac{1}{\sqrt{2}}\left(-\sigma_{10}\sigma_{2+} + \sigma_{1+}\sigma_{20}\right) \qquad \text{(B.3.1.6c)}$$

The Clebsch-Gordan coefficients have been evaluated by using formulae given in ref. [65].

Comparing equation (B.3.1.4) and expressions (B.3.1.6), we get

$$(\sigma_1 \times \sigma_2) = (-i)\{e_{-1}\}\left[-\sqrt{2}\left[\sigma_1\sigma_2\right]^1_{+1}\right]$$

$$+ (-i)\{e_{+1}\}\left[-\sqrt{2}\left[\sigma_1\sigma_2\right]^1_{-1}\right]$$

$$+ (-i)\{e_0\}\left[+\sqrt{2}\left[\sigma_1\sigma_2\right]^1_0\right] \qquad \text{(B.3.1.7)}$$

$$\text{Or} \qquad (\sigma_1 \times \sigma_2) = -i\sqrt{2}\left[\sum_q (-1)^q e_{-q}\left[\sigma_1\sigma_2\right]^1_q\right] \qquad \text{(B.3.1.8)}$$

where $q=0,\pm1$.

The expression in bracket corresponds to definition (B.1.12) therefore we express the operator $(\sigma_1 \times \sigma_2)$ as

$$(\sigma_1 \times \sigma_2) = -i\sqrt{2}\left[\sigma_1\sigma_2\right]^1 \qquad \text{(B.3.1.9)}$$

B.3.2 EVALUATION OF $\langle S=1 \,||(\sigma_1 \times \sigma_2)||\, S'=0\rangle$

We have the reduced matrix element of $(\sigma_1 \times \sigma_2)$ given by

$$\langle S=1 \,||(\sigma_1 \times \sigma_2)||\, S'=0\rangle = -i\sqrt{2}\,\langle(\tfrac{1}{2}\,\tfrac{1}{2})S=1 \,||\left[\sigma_1\sigma_2\right]^1||(\tfrac{1}{2}\,\tfrac{1}{2})S'=0$$

. . . . (B.3.2.1)

we can express the above reduced matrix element of a cross product of two vectors σ_1 and σ_2 in terms of their reduced

matrix elements [65] involving 9j-symbol as,

$$\langle S \,||(\sigma_1 \times \sigma_2)||\, S' \rangle = -i\sqrt{2}\,[(2S+1)(2S'+1)(2K+1)]^{\frac{1}{2}} \begin{Bmatrix} \frac{1}{2} & \frac{1}{2} & k_1 \\ \frac{1}{2} & \frac{1}{2} & k_2 \\ S & S' & K \end{Bmatrix} \times \langle \tfrac{1}{2} || \sigma_1^{k_1} || \tfrac{1}{2} \rangle \langle \tfrac{1}{2} || \sigma_2^{k_2} || \tfrac{1}{2} \rangle \qquad \text{(B.3.2.2)}$$

Since we have [52],

$$\langle j \,||\, J \,||\, j \rangle = \sqrt{j(j+1)(2j+1)} \qquad \text{(B.3.2.3)}$$

Therefore for spin-1/ 2 operator(S) we derive

$$\langle \tfrac{1}{2} || \, S \, || \tfrac{1}{2} \rangle = \sqrt{\frac{3}{2}} \quad \text{or} \quad \langle \tfrac{1}{2} || \, \sigma \, || \tfrac{1}{2} \rangle = \sqrt{6} \qquad \text{(B.3.2.4)}$$

Putting the values of reduced matrix elements of sigmas from eqn. (B.3.2.4) in expression (B.3.2.2), we get

$$\langle S=1 \,||(\sigma_1 \times \sigma_2)||\, S'=0 \rangle = -i\sqrt{2}\,[3(2\times 1+1)(2\times 0+1)]^{\frac{1}{2}} \begin{Bmatrix} \frac{1}{2} & \frac{1}{2} & 1 \\ \frac{1}{2} & \frac{1}{2} & 1 \\ 1 & 0 & 1 \end{Bmatrix} \times 6 \qquad \text{. . . . (B.3.2.5)}$$

Having evaluated 9j-symbol in (B.3.2.5), we obtain

$$\langle S=1 \,||(\sigma_1 \times \sigma_2)||\, S'=0 \rangle = -2\sqrt{3}\, i \qquad \text{(B.3.2.6)}$$

B.3.3 EVALUATION OF $\langle S=0 \,||(\sigma_1 \times \sigma_2)||\, S'=1 \rangle$

We write the given reduced matrix element as,

$$\langle S=0 \,||(\sigma_1 \times \sigma_2)||\, S'=1 \rangle = -i\sqrt{2}\, \langle (\tfrac{1}{2}\tfrac{1}{2})S=0 || [\sigma_1 \sigma_2]^1 || (\tfrac{1}{2}\tfrac{1}{2})S'=1 \rangle \qquad \text{. . . . (B.3.3.1)}$$

According to expression (B.3.2.2), we obtain

$$\langle(\tfrac{1}{2}\,\tfrac{1}{2})S=0\|(\sigma_1\times\sigma_2)\|(\tfrac{1}{2}\,\tfrac{1}{2})S'=1\rangle=-\sqrt{2}\,i\,[3(2\times0+1)(2\times1+1)]^{\frac{1}{2}}\begin{Bmatrix}\frac{1}{2}&\frac{1}{2}&1\\ \frac{1}{2}&\frac{1}{2}&1\\ 0&1&1\end{Bmatrix}$$

$$\times\langle\tfrac{1}{2}\|\sigma_1\|\tfrac{1}{2}\rangle\langle\tfrac{1}{2}\|\sigma_2\|\tfrac{1}{2}\rangle \qquad \text{(B.3.3.2)}$$

Therefore, using (B.3.2.4) and having evaluated 9j-symbol, we obtain

$$\langle S=0\,\|(\sigma_1\times\sigma_2)\|\,S'=1\rangle=-2\sqrt{3}\,i \qquad \text{(B.3.3.3)}$$

REFERENCES

[1] E. Rutherford, Proc. Roy. Soc. London A 123, (1929) 373.

[2] J. Chadwick Proc. Roy. Soc. A136, (1932) 692.

[3] A. De Shalit and H. Feshbach, " Theoretical Nuclear physics Vol.1, Nuclear structure, John Wiley & Sons Inc. (1974).

[4] H. Yukawa, Proc. Phys. Math. Soc. Jap. 17(1935)48.

[5] C.M.G Lattes, H.Muirhead, G.P.S.Occhialini and C.F.Powell, Nature 159 (1947)694.

[6] M. Gell-Mann, Phys. Lett. 8 (1964)214.

[7] a) F. E. Close, " introduction to Quarks and Partons" Academic Press New York, London (1979).
b) F. Halzen, A.D. Martin, "Quarks andLeptons"An Introductory Course in Modern Particle Physics. John Wiley &Sons Inc. New York 1984.

[8] J. D. Bjorken and E. A. Paschos, Phys. Rev 185 No. 5 (1969) 1975.

[9] Anthony W. Thomas, Prog. Theor. Phys.Suplt: No. 91(1987) 204.

[10] J. V. Noble, Phys. Rev. Lett. 46(1981)412; F. E. Close, R.G. Roberts and G. G. Rose, Phys. Lett. 129B(1983)346; J. J. Avbert Phys. Lett. 123B(1983)275.

[11] M. Marciano and H. Pagels, Phys. Reports (Phys. Lett. Sec C) 36, No. 3 (1978)137.

[12] F. Mandl and G. Shaw, "Quantum field theory", John Wiley & Sons,1986.

[13] A. De Rujula, H.Georgi and S. L. Glashow, Phys. Rev. D12 (1975)147; N. Isgur and G. Karl, Phys. Rev. D18(1978)4187; D19 (1979) 2653.

[14] a) A. Chodos, R. L. Jaffe, K. Johnson,C. B. Thorn and V.F.Weisskopf, Phys. Rev. D9 (1974)3471.

b) T. De Grand, R. L. Jaffe, K. Johnson and J. Kiskis Phys. Rev. D12 No: 7 (1975)2060.

[15] R. Goldfalm and L. Wilets, Phys. Rev. D25 (1982)1951; S.Kahana, G. Ripka and Y. Soni, Nucl. Phys. A415(1984) 351; Th.Koppel and M. Harvey, Phys. Rev. D31(1985)171; R. Freidberg and T. D. Lee, Phys. Rev. D18(1978)2623.

[16] a) G. A. Miller, A. W. Thomas and S. Theberge, Phys. Lett. 91B (1980)192; A.W. Thomas, S. Theberge and G. A. Miller, Phys. Rev. D24(1981)216; S. Theberge, A. W.Thomas and G.A.Miller, Phys. Rev. D22 (1980) 2838.

b) G.E. Brown, M. Rho, Phys. Lett. 82B(1979)177; V. Vento, M. Rho, E.M. Nymann, G. H. Gun and G. E. Brown, Nucl. Phys. A345 (1980)413; A.Chodos, C. B. Thorn, Phys. Rev. D12 (1975) 2733; F.Myhrer, G.E.Brown and Z. Xu, Nucl. Phys. A362 (1981) 317; R. Freidberg and T. D. Lee, Phys. Rev. D15 (1977) 1694,T. D. Lee, Phys. Rev. D19(1979)1802; I.Duck, Phys. Rev. D34 (1986)1493.

[17] T. H. R. Skyrme, Proc. Roy. Soc. London A260(1961)127; G.S.Adkins,C. R.Nappi and E.Witten,Nucl. Phys. B223 (1983) 433.

[18] T.Fujiwara, Y.Igarashi, A. Kobayashi, H. Otsu, T.Sato and S.Sawada, Prog. Theor. Phys. 74 (1985)128; G. S. Adkins, Phys. Rev.D33 (1986)193.

[19] Rajat K. Bhaduri, "Models of the Nucleon". From Quarks to Soliton, Addison-Wesley Publishing Company Inc, New York, 1988

[20] W. Weise, Int. Rev. Nucl. Phys. Vol.1 "Quarks and NUclei" World Scientific Publishing Co. Pte. Ltd. Sinapore, Philadelphia (U.S.A)1984.

[21] C.De Tar Phys. Rev. D17(1978)323.

[22] D. A. Liberman, Phys. Rev. D16(1977)1542.

[23] M. Oka and K. Yazaki, Phys. Lett. 90B(1980)41; Prog. Theor. Phys. 66(1981)556,572; Nucl. Phys. A402 (1983)477.

[24] A. Faessler, F. Fernandez, G. Lubeck and K. Shimizu, Phys. Lett. 112B(1982)201; Nucl. Phys. A402(1983)555.

[25] M. Harvey, Nucl. Phys. A352(1981)301,326.

[26] Y. Suzuki and K. T. Hecht, Phys. Rev. C27(1983)299.

[27] Y. Suzuki and K. T. Hecht, Nucl. Phys. A420(1984)525.

[28] O. Morimatsu, S. Ohta, K. Shimizu and K. Yazaki, Nucl. Phys. A420(1984)573.

[29] Y. Suzuki, Nucl. Phys. A430(1984)539.

[30] Y. Suzuki, Nucl. Phys. A444(1985)637.

[31] K. Maltman and N. Isgur, Phys. Rev. Lett. 50(1983)1827; Phys. Rev. D29(1984)952.

[32] K. Holinde, Nucl. Phys. A415(1984)477.

[33] J. Burger and H. M. Hafmann, Phys. Lett. 148B (1984)25.

[34] D. Robson, Prog. Part. Nucl. Phys. Vol.8 (Proc. Int. Sch. Nuc. Phys. Erice, 1981) Edited by Wilkinson Pergamon Press Ltd. Oxford (1982)257.

[35] S. Ohta, M. Oka, A. Arima and K. Yazaki,Phys. Lett. 119B (1982) 35.

[36] M. H. Storm, A. Watt, Nucl. Phys. A408 (1983)397.

[37] Y. Fujiwara and K. T. Hecht, Nucl. Phys. A444 (1985)541.

[38] Yoshikazu Fujiwara, Prog. Theor. Phys. Suplt. No. 91 (1987)160.

[39] a) Y. Fujiwara and K. T. Hecht, Phys. Lett. 171B (1) 1986,17.
b) K. T. Hecht and Y. Fujiwara, Nucl. Phys. A463(1987) 255c.

[40] Y. Fujiwara and K. T. Hecht, Nucl. Phys. A456(1986)669; Nucl. Phys. A451(1986)625; Nucl. Phys. A462(1987)621.

[41] Yu You-Wen and Zhang Zong-Ye, Nucl. Phys. A426 (1984)557.

[42] Zong-Ye Zhang and You-Wen Yu, Prog. Theor. Phys. Suplt: No. 91 (1987) 193

[43] Nuclear Physics Conference, March 1988 at Manchester.

[44] R. R. Whitehead, Nucl. Phys. A182(1972)290.

[45] R. R. Whitehead, A. Watt, B. J. Cole, I. Morrison, " Advances in Nuclear Physics" Vol: 9 Edited by Michel Baranger and Erich Vogt Plenum Press, 1977, Page 123.

[46] E. Feenberg and E. P. Wigner, Phys. Rev. 51(1937)95.

[47] G. Racah, Phys. Rev. 63(1943)367; G. Racah, Phys. Rev. 76 (1949)1352.

[48] A. S. Householder, " The theory of matrices in numerical analysis", Blaisdill, New York(1964).

[49] J. H. Wilkinson, " The algebraic eigenvalue problem" , (Oxford (1965) p-388.

[50] R. R. Whitehead, A. Watt, Phys. Lett. 41B(1972)7.

[51] B. J. Cole, A. Watt and R. R. Whitehead, Phys. Lett 45B(1973) 429; J. Phys. A Math. Nucl. Gen. 7(1974)134; J. Phys. G Nucl. Phys. 1 (1975)303; Phys. Lett. 57B(1975)24.

[52] P. J. Brussaard and P.W. M. Glaudemans, " Shell-model applications in nuclear spectroscopy" , North Holland publishing company, Oxford (1977).

[53] J. C. Slater, Phys. Rev. 34 (1929)1293.

[54] Peter Ring, Peter Schuck, " The nuclear many body problem" Springer Verlag New York Inc. ,1980.

[55] Silvan S. Schweber, " An introduction to relativistic quantum field theory". Harper & Row New York, London and John Weatherhill Inc. Tokyo 1964.

[56] M.G. Mayer & J.H.D. Jensen "Elementary Theory of Nuclear Shell Structure" John Willey & Sons Lande Chapman & Hall Ltd. New York (1955).

[57] L. Susskind, " Fundamentals of quark models" SUSSP (1976) Edited by I. M. Barbour and A. T. Davies.

[58] J. P. Elliott, T. H. R. Skyrme, Proc. Roy. Soc. A232(1955)561.

[59] R. J. Philpott and P.P. Szydlik, Phys. Rev. 153(196701039.

[60] J. B. Mc Grory and B. H. Wildenthal, Phys. Lett. 60B(1975)5.

[61] P.K. Rath, A. Faessler and A. Watt, " A practical Solution to the Problem of Spurious States in Shell Model Calculations" Unpublished.

[62] T. Sebe and J. Nachamkin, Ann. of Phys. 51 (1969)100.

[63] M. K. Pal, "Theory of Nuclear structure" Scientific and academic editions (1983).

[64] Donald H. Perkin, "Introduction to High Energy Physics", Addison-Wesley Publishing Company,Inc., London (1982).

[65] A. R. Edmonds," Angular Momentum in Quantum Mechanics", Princeton University Press, London (1957).

[66] R. D. Lawson, "Theory of the Nuclear Shell Model", Claredon Press, Oxford (1980). p-423.

[67] L.C. Biedenharn and J.D Louck, "Angular Momentum in quantum physics (Theory and Applications) Encyclopedia of Mathematics & its applications", Vol. 8 Addison-Wesley Publishing company, London (1981).

[68] W Magnus & F. Uberhettinger, "Special functionns of mathematical physics",Chelsea publishing company new york (1949).

[69] W.W. Bell, "Special functions for Scientists and Engineers", D. Van Nostrand Company Ltd, London 1968.

[70] T.A.Brody, G. Jacob and M. Moshinsky, Nuclear physics 17 (1960), 16.

[71] M. Moshinsky, Nuclear physics 13 (1959), 104.

[72] T.A. Brody and M. Moshinsky, " Tables of transformation brackets for Nuclear shell model calculations" Monografias Del Instituto de Fisica Mexico, (1960) Gordon and Breach New York.

[73] A. De- Shalit and Igal Talmi, "Nuclear shell theory" Academic Press Inc. London (1963).

[74] Koichi Yazaki, Prog. Theo. Phys. Suppltt. No: 91(1987) 146.

[75] J.M.G Gomez and C.Prieto Nuc. phy. A452(1986)466.

[76] David Faiman and Archibald W. Hendry, Phys. Rew. vol.173 No. 5 (1968) 337.

[77] M.Aginlar Beniliz et al. Phys. letts. 111B(1982)7.

[78] H.R. Rubinstein and F.Scheck, Pys. Rev. Vol. 154 No:5 (1967) 1608.

[79] F. J.Gilman, " Hadron Spectroscopy" Proceeding of Summer institute on particle physics,1977; Quark Spectroscopy and Hadron Dynamics, SLAC Report No: 204 Edited by Martha Zipf Stanford,California.

[80] A.W.Hendry and D.B.Litchenberg, Reports on Prog. Phys. Vol. 41 (1978)1707.

[81] a) R.Horgan and R.H. Calitz, Nuc. Phys. B66(1973)135.

b) R.Horgan,Nuc. Phys. B71(1974) 514.

[82] G. A. Miller, " Hadron Substructure in Nuclear Physics" (Indiana University,1983) AIP Conference Proceedings No.110 page 38, Edited by W.Y.P.Hwang and M.H.Macfarlane, American Institute of Physics New York (1984).

[83] G.S.Adkins, C.R.Nappi and E. Witten Nuc. Phys. B228 (1983)552.

[84] M.M. Nagels et al. Nuc. Phys. B147 (1979)189.

[85] a) V.E.Krohn and G.R.Ringo, phys. Rev. D8 (1973)1305.

b) R.W.Berard et al., Phys. letts. B47 (1973)355.

[86] R.D.Carlitz and S.D.Ellis, Phys. letts. B 68 (1977) 443.

[87] J.L. Dethier and L. Wilets, Phys. Rew. D34 No. 1 (1986)207.

[88] a) J.J.Murphy, Y.M.shin and D.M.Skopie Phys. Rev. C9 No. 6 (1974) 2125.

b) L.N. Hand, D.G.Millar and R. Wilson, Rev. Mod. Phys. 35 (1963) 335.

[89] Harry J. Lipkin, Phys. letts. 198 B (1987)131.

[90] a) L.M.Sehgal, Phys. Letts. 53B (1974)106.

b) D.Parashar and R.S.Kaushal, Phys. Rev. D13(1976).

[91] U.G.Meissner,N.Kaiser and W.Weise,Nuc. phys. A466(1987)685.